JCI The Journal of Clinical Investigation

Reducing CXCR4-mediated nociceptor hyperexcitability reverses painful diabetic neuropathy

Nirupa D. Jayaraj, … , Richard J. Miller, Daniela M. Menichella

J Clin Invest. 2018. https://doi.org/10.1172/JCI92117.

Research Article In-Press Preview Neuroscience

Painful diabetic neuropathy (PDN) is an intractable complication of diabetes that affects 25% of patients. PDN is characterized by neuropathic pain and small-fiber degeneration, accompanied by dorsal root ganglion (DRG) nociceptor hyperexcitability and loss of their axons within the skin. The molecular mechanisms underlying DRG nociceptor hyperexcitability and small-fiber degeneration in PDN are unknown. We hypothesize that chemokine CXCL12/CXCR4 signaling is central to this mechanism, as we have shown that CXCL12/CXCR4 signaling is necessary for the development of mechanical allodynia, a pain hypersensitivity behavior common in PDN. Focusing on DRG neurons expressing the sodium channel Nav1.8, we applied transgenic, electrophysiological, imaging, and chemogenetic techniques to test this hypothesis. In the high-fat diet mouse model of PDN, we were able to prevent and reverse mechanical allodynia and small-fiber degeneration by limiting CXCR4 signaling or neuronal excitability. This study reveals that excitatory CXCR4/CXCL12 signaling in $Na_v1.8$-positive DRG neurons plays a critical role in the pathogenesis of mechanical allodynia and small-fiber degeneration in a mouse model of PDN. Hence, we propose that targeting CXCR4-mediated DRG nociceptor hyperexcitability is a promising therapeutic approach for disease-modifying treatments for this currently intractable and widespread affliction.

Reducing CXCR4-mediated Nociceptor Hyperexcitability Reverses Painful Diabetic Neuropathy

Authors: Nirupa D. Jayaraj[1]*, Bula J. Bhattacharyya[1]*, Abdelhak A. Belmadani[2]*, Dongjun Ren[2], Craig A. Rathwell[2], Sandra Hackelberg[1], Brittany E. Hopkins[2], Herschel R. Gupta[2], Richard J. Miller[2], and Daniela M. Menichella[1,2^]. `

Author affiliation: [1] Department of Neurology, [2] Department of Pharmacology, Feinberg School of Medicine, Northwestern University, Chicago, IL, USA,

* These authors contributed equally to this work

^ **Corresponding author**: Daniela Maria Menichella

Daniela Maria Menichella, MD., PhD.

Department of Neurology and Pharmacology

Feinberg School of Medicine, Northwestern University

Lurie 8-123, 303 E. Superior St, Chicago, IL 60611, USA

Email: d-menichella@northwestern.edu

Conflict of interest statement: The authors have declared that no conflict of interest exists.

ABSTRACT

Painful diabetic neuropathy (PDN) is an intractable complication of diabetes that affects 25% of patients. PDN is characterized by neuropathic pain and small-fiber degeneration, accompanied by dorsal root ganglion (DRG) nociceptor hyperexcitability and loss of their axons within the skin. The molecular mechanisms underlying DRG nociceptor hyperexcitability and small-fiber degeneration in PDN are unknown. We hypothesize that chemokine CXCL12/CXCR4 signaling is central to this mechanism, as we have shown that CXCL12/CXCR4 signaling is necessary for the development of mechanical allodynia, a pain hypersensitivity behavior common in PDN. Focusing on DRG neurons expressing the sodium channel $Na_v1.8$, we applied transgenic, electrophysiological, imaging, and chemogenetic techniques to test this hypothesis. In the high-fat diet mouse model of PDN, we were able to prevent and reverse mechanical allodynia and small-fiber degeneration by limiting CXCR4 signaling or neuronal excitability. This study reveals that excitatory CXCR4/CXCL12 signaling in $Na_v1.8$-positive DRG neurons plays a critical role in the pathogenesis of mechanical allodynia and small-fiber degeneration in a mouse model of PDN. Hence, we propose that targeting CXCR4-mediated DRG nociceptor hyperexcitability is a promising therapeutic approach for disease-modifying treatments for this currently intractable and widespread affliction.

45 **INTRODUCTION**

46 PDN is one of the most common and intractable complications of diabetes,
47 affecting 25% of diabetic patients(1, 2). Given the increasing prevalence of type II
48 diabetes mellitus(3), the incidence of PDN is expected to rise(4). Neuropathic pain
49 associated with PDN substantially affects patients' quality of life and health care
50 costs(5) and is difficult to treat. Opiates are mostly ineffective for treating neuropathic
51 pain and problematic for chronic use(2). Gabapentinoids and antidepressants produce
52 limited relief in some patients, but have many side effects and a low response rate for
53 PDN(6-9). Thus, safer and more effective therapies based on mechanistic targets
54 specific to PDN are urgently required.

55 The hallmarks of PDN are neuropathic pain and small-fiber degeneration (10,
56 11), particularly a "dying back" axonopathy that affects the smallest axons of the
57 peripheral nervous system: the dorsal root ganglion (DRG) nociceptor axons (12, 13).
58 Acute pain is normally important for preventing tissue damage (14, 15). However, in
59 conditions such as PDN, physiological pain transitions to pathological or neuropathic
60 pain that does not serve any important physiological function. The complex
61 pathophysiology underlying neuropathic pain in PDN(16) extends from primary afferent
62 terminals (16) to anatomical and functional changes in the brain and spinal cord, that
63 amplify nociceptive processing(16, 17). Diabetic patients(18) and experimental models
64 of PDN (19, 20) exhibit sensory neuron hyperexcitability, including spontaneous activity
65 of DRG nociceptor axons and the terminals of C-fiber nociceptors (21, 22). The
66 molecular pathways linking hyperexcitability to neuropathic pain and small-fiber

67 degeneration in PDN are unknown. This gap in knowledge represents a critical barrier
68 to progress in developing novel therapeutic approaches for PDN.

69 In our experiments, we identified DRG nociceptors via a molecular marker, the
70 sodium channel $Na_v1.8$(23). Approximately 75% of DRG sensory neurons express
71 $Na_v1.8$, including >90% of C-nociceptors, a population of C-low-threshold
72 mechanoreceptors and some Aδ-nociceptors and Aβ afferents(23). Thus, by focusing
73 on the properties of $Na_v1.8$-positive DRG neurons we are likely to discover key changes
74 in the behavior of DRG nociceptors in animal models of PDN.

75 One of the initial questions that must be addressed is what mechanisms trigger
76 $Na_v1.8$-positive DRG neuron hyperexcitability in diabetes? Promising hypotheses
77 include altered gene expression and posttranslational modification of key ion
78 channels(24, 25). For example, methylglyoxal, abundant during hyperglycemia(19, 20),
79 induces posttranslational modifications in $Na_v1.8$ sodium channels(26) that result in
80 nociceptor hyperexcitability and mechanical allodynia in rodents (20). In addition,
81 inflammatory mediators, including cytokines and chemokines, may increase $Na_v1.8$-
82 mediated currents by acutely activating $Na_v1.8$ ion channels through second-messenger
83 signaling or by enhancing channel expression(27-29). Consistent with this idea, we
84 have shown that chemokines and their receptors are expressed by DRG neurons (30,
85 31) and that chemokine signaling is important in generating neuropathic pain in
86 experimental models of PDN(30). However, the role of chemokines in generating
87 $Na_v1.8$-positive DRG neuron hyperexcitability, mechanical allodynia, and small-fiber
88 degeneration in PDN remains unclear.

89 Although the causes of PDN are likely to be multifactorial, they include
90 inflammatory processes(32). Inflammatory markers, such as interleukins IL-6, IL-2, and
91 tumor necrosis factor-α (TNF-α), are elevated in hyperglycemia, suggesting a chronic,
92 low-grade inflammatory state in diabetic patients(33, 34). Moreover, patients with higher
93 plasma TNF-α have a greater risk of PDN(33, 35, 36). Expression of the chemokine
94 receptor CXCR4, a G-protein-coupled, seven-span transmembrane receptor (GPCR),
95 was elevated in a peripheral nerve microarray analysis of patients with progressive
96 diabetic neuropathy(37). Consistent with this finding, we showed that, in the high-fat diet
97 (HFD) mouse model of PDN (38), CXCR4 and its ligand, the chemokine CXCL12 (also
98 called stromal-derived factor-1), are crucial in the generation of mechanical allodynia
99 (30), a pain hypersensitivity behavior associated with PDN in mice(30, 39), and
100 humans(40, 41).

101 In light of these findings, we have now examined the mechanistic relationships
102 between CXCL12/CXCR4 signaling, hyperexcitability in $Na_v1.8$-positive DRG neurons,
103 small-fiber degeneration and mechanical allodynia in the HFD mouse model of PDN.
104 We used electrophysiology, imaging, and chemogenetics to demonstrate that
105 CXCL12/CXCR4 signaling is key to development of $Na_v1.8$-positive DRG neuron
106 hyperexcitability, which is directly responsible for small-fiber degeneration and
107 mechanical allodynia. Hence, therapies that target this mechanism represent a novel
108 approach for PDN.
109
110
111

112 **RESULTS**

113 **Mechanical allodynia preceded small-fiber degeneration in diabetic mice.**

114 Neuropathic pain and small-fiber neuropathy are well-recognized complications
115 of type II diabetes, both in humans and animal models(10, 38). However, the temporal
116 correlation between the onset of neuropathic pain behavior and small-fiber neuropathy
117 has not been established. We set out to investigate this temporal relationship by
118 measuring mechanical allodynia, a particular pain hypersensitivity behavior normally
119 associated with PDN. We used the high-fat diet (HFD) mouse model of PDN. In this
120 model, mice fed with a diet high in fat content develop glucose intolerance, obesity,
121 mechanical allodynia, and small-fiber degeneration over a period of 10 weeks(30, 38,
122 39). Hence, the key hallmarks of human PDN are recapitulated in the HFD model.

123 DRG neuron subtypes are identified using molecular markers (42-44). Because
124 >90% of DRG nociceptors express $Na_v1.8$(23), we targeted our studies to this
125 population. To investigate the onset of small-fiber degeneration, we utilized a molecular
126 genetic strategy of crossing $Na_v1.8$-Cre mice (45) with Ai9 (td-Tomato) mice (46). In the
127 resulting $Na_v1.8$-Cre;Ai9 mice, $Na_v1.8$-positive DRG neurons were labeled red with td-
128 Tomato reporter protein following Cre-dependent recombination, making it possible to
129 visualize $Na_v1.8$-positive neuron cell bodies in the DRG and their afferents in the dorsal
130 horn of spinal cord and the skin (14, 23) (Supplemental Figure 1, A).

131 The $Na_v1.8$-Cre;Ai9 mice were fed an HFD for 10 weeks (30, 39). The mice
132 gained weight (Supplemental Figure 1, B) and became glucose intolerant 6 weeks after
133 HFD onset (Supplemental Figure 1, C). We next examined small-fiber degeneration in
134 skin samples of $Na_v1.8$-Cre;Ai9 mice using confocal microscopy. Starting at 8 weeks,

135 HFD mice displayed a dramatic reduction in intra-epidermal nerve fiber density (IENF
136 density), expressed as the number of nerves crossing the epidermal-dermal junction as
137 a function of length, relative to control (RD) mice. There was no difference in IENF
138 density between RD and HFD mice at 2, 4 or 6 weeks (Figure 1, A-C). These results
139 were verified by immunolabeling skin samples from Na_v1.8-Cre;Ai9 mice that had been
140 on either RD or HFD for 2 or 8 weeks with an antibody against the protein gene product
141 9.5 (PGP 9.5), a pan-neuronal marker used for calculating IENF density and for
142 diagnosing small-fiber neuropathies(13, 47). This independent verification excluded the
143 possibility that the results reflected abnormal td-Tomato expression or transport in HFD
144 mice (Supplemental Figure 1, D).

145 We next determined the onset of mechanical allodynia by quantifying the
146 withdrawal threshold of the hindpaw in response to stimulation with flexible von Frey
147 filaments applied in order of ascending force. The von Frey experiments were
148 conducted using random experimental group assignments by blinded investigators.
149 Beginning at 6 weeks, Na_v1.8-Cre;Ai9 mice fed the HFD exhibited a significantly
150 reduced withdrawal threshold compared to RD control mice, indicating the development
151 of mechanical allodynia (Figure 1, D). No statistically significant differences were noted
152 between RD and HFD mice 2 and 4 weeks after diet commencement. Hence, HFD mice
153 developed mechanical allodynia two weeks prior to small-fiber degeneration.

154

155 **Increased intracellular calcium influx into DRG neurons in diabetic mice**

156 The molecular cascade linking neuropathic pain behavior to small-fiber
157 degeneration in diabetes is incompletely understood. One phenomenon that could
158 potentially explain both is enhanced $Na_v1.8$-positive DRG neuron excitability. We
159 assessed this hyperexcitability by measuring changes in internal calcium concentration
160 ($[Ca^{2+}]_i$) in these neurons as PDN developed, using a functional imaging technique
161 employing acutely isolated whole DRG explants. We initially used a knock-in mouse line
162 that expressed the genetically encoded $[Ca^{2+}]_i$ indicator protein GCaMP3 under the
163 control of the PIRT promoter, which directs expression of GCaMP3 in >95% of DRG
164 neurons(48). Acutely excised DRG explants were isolated from Pirt-GCaMP3 mice 2, 4,
165 6, 8, 10 and 12 weeks after starting HFD or RD. We measured the number of DRG
166 neurons responding with $[Ca^{2+}]_i$ transients to low and high concentrations of stimuli (i.e.,
167 capsaicin and high potassium buffer). In DRG explants from mice that had been on HFD
168 for at least 6 weeks, the number of DRG neurons responding to a low concentration of
169 capsaicin or potassium was significantly higher than in DRG explants isolated from RD
170 mice (Supplemental Figure 2, A). In contrast, the number of DRG neurons responding
171 to low capsaicin or potassium after 2 or 4 weeks of HFD or RD did not differ
172 (Supplemental Figure 2, B).

173 Given the cellular diversity and functional heterogeneity of DRG neurons (42-44,
174 49), we wanted to monitor $[Ca^{2+}]_i$ in $Na_v1.8$-positive DRG neurons. Therefore, we
175 selectively expressed the $[Ca^{2+}]_i$ indicator protein GCaMP6 (50) in these neurons by
176 crossing $Na_v1.8$-Cre mice(45) with conditional reporter GCaMP6 mice (Ai96$^{flox/flox}$;RCL-
177 GCaMP6s)(50). We then performed imaging experiments on acutely isolated DRG
178 explants from these mice 2 and 8 weeks after starting HFD or RD (Supplemental video

179 1-4). We measured the number of $Na_v1.8$-positive DRG neurons responding with $[Ca^{2+}]_i$
180 transients to both low and high concentrations of capsaicin and potassium. When mice
181 had been on a HFD for 8 weeks, $Na_v1.8$-positive DRG neurons were more likely to
182 respond to lower concentrations of capsaicin and potassium compared to neurons from
183 RD mice (Figure 2, A-D). In contrast, the number of neurons responding to low
184 capsaicin or potassium after 2 weeks of HFD or RD did not differ (Figure 2, E-H).
185 Confirming the results in Pirt-GCamP3 mice, these results demonstrate the
186 development of $Na_v1.8$-positive DRG neuron hyperexcitability in the HFD model of PDN.
187 To determine whether this excitability was specific to $Na_v1.8$-positive DRG
188 neurons, we expressed GCaMP6 (50) in proprioceptive DRG neurons by crossing
189 parvalbumin-Cre mice, which have been used to study proprioceptor-lineage(51-53),
190 with GCaMP6 mice (Ai96$^{flox/flox}$;RCL-GCaMP6s)(50). We then imaged acutely isolated
191 DRG explants 2 and 8 weeks after starting HFD or RD and measured the number of
192 parvalbumin-positive DRG neurons responding with $[Ca^{2+}]_i$ transients to low and high
193 concentrations of capsaicin and high potassium buffer. Parvalbumin-positive DRG
194 neurons did not respond to either concentration of capsaicin and their responses to high
195 potassium buffer after 2 or 8 weeks of HFD or RD did not differ (Figure 2, I and J).

196

197 **Diabetic $Na_v1.8$-positive DRG neurons were hyperexcitable**

198 The increased sensitivity of $Na_v1.8$-positive DRG neurons from HFD mice to
199 capsaicin and potassium suggested hyperexcitability, which we tested directly in
200 primary DRG cultures. We made current-clamp recordings of td-Tomato-labeled $Na_v1.8$-
201 positive neurons from $Na_v1.8$-Cre;Ai9 mice fed HFD or RD for 10 weeks. These neurons

202 exhibited a significantly lower rheobase compared to neurons from RD mice (Figure 3,
203 A-C). No significant differences were observed in resting membrane potential or action
204 potential overshoot, but firing frequency was increased in $Na_v1.8$-positive neurons from
205 HFD compared to RD mice (Figure 3, G-O). These electrophysiological properties
206 support the conclusion that $Na_v1.8$-positive DRG neurons from HFD mice become
207 hyperexcitable.

208

209 **CXCR4 chemokine receptor deletion from $Na_v1.8$-positive DRG neurons prevented**
210 **mechanical allodynia and small-fiber degeneration in diabetic mice**

211 What factors drive $Na_v1.8$-positive DRG neuron hyperexcitability in PDN
212 pathology? We previously reported that excitatory effects of chemokines are important
213 in development and maintenance of pain behaviors in neuropathic pain models (31, 54)
214 and that CXCR4 signaling is important for the development of mechanical allodynia in
215 HFD mice(30).

216 To extend these findings, we deleted CXCR4 receptors from $Na_v1.8$-positive
217 DRG neurons by crossing $Na_v1.8$-Cre;Ai9 mice with CXCR4-floxed mice
218 ($CXCR4^{flox/flox}$)(55). This manipulation did not cause developmental defects(56), as the
219 number of $Na_v1.8$-positive DRG neurons labeled with td-Tomato was no different in
220 $Na_v1.8$-Cre;Ai9;$CXCR4^{flox/+}$ heterozygous and $Na_v1.8$-Cre;Ai9;$CXCR4^{flox/flox}$
221 homozygous mice (Supplemental Figure 3, A and B). Furthermore, we found no
222 significant differences in the numbers of td-Tomato-positive DRG neurons that were
223 also positive for IB4 (Supplemental Figure 3, A and B), which identifies non-peptidergic

224 nociceptive neurons(14, 57), demonstrating that these mice have normal segregation of
225 peptidergic versus non-peptidergic nociceptors after sensory neurogenesis(58, 59).
226 These mice also had normal metabolic profiles. Both Na_v1.8-Cre;Ai9;CXCR4$^{flox/+}$
227 heterozygous and Na_v1.8-Cre;Ai9;CXCR4$^{flox/flox}$ homozygous mice fed HFD developed
228 obesity (Supplemental Figure 3, C) and glucose intolerance (Supplemental Figure 3, D)
229 like wild-type mice.

230 We tested for mechanical allodynia using the von Frey withdrawal threshold
231 paradigm, as described above. In Na_v1.8-Cre;Ai9;CXCR4$^{flox/+}$ heterozygous HFD mice,
232 the withdrawal threshold was significantly reduced compared to RD mice, indicating the
233 development of mechanical allodynia (Figure 4, A). In contrast, Na_v1.8-
234 Cre;Ai9;CXCR4$^{flox/flox}$ homozygous HFD mice showed normal withdrawal thresholds
235 (Figure 4, A), indicating that CXCR4 receptors in Na_v1.8-positive DRG neurons are
236 necessary for the establishment of mechanical allodynia in this model of PDN. We did
237 not observe mechanical allodynia in RD mice with chemokine receptor CXCR4 deletion
238 from Na_v1.8-positive DRG neurons (Na_v1.8-Cre;Ai9;CXCR4$^{flox/flox}$ homozygous) (Figure
239 4, A), so CXCR4 deletion did not alter mechanical sensation.

240 We next tested whether excitatory CXCL12/CXCR4 signaling in Na_v1.8-positive
241 neurons was necessary for small-fiber degeneration. Using confocal microscopy, we
242 examined skin innervation in both Na_v1.8-Cre;Ai9;CXCR4$^{flox/+}$ heterozygous and Na_v1.8-
243 Cre;Ai9;CXCR4$^{flox/flox}$ homozygous mice fed RD or HFD for 10 weeks. CXCR4 deletion
244 from Na_v1.8-positive DRG neurons significantly improved skin innervation in diabetic
245 mice (Figure 4, B and C). In contrast, heterozygous HFD mice had substantially
246 depleted nerve terminals (Figure 4, B and C). These results were verified by

247 immunolabeling using a PGP 9.5 antibody on the same skin samples providing an
248 independent verification for the fiber density measurements (Supplemental Figure 4).
249 Skin innervation was normal in Na_v1.8-Cre;Ai9;CXCR4$^{flox/+}$ and Na_v1.8-
250 Cre;Ai9;CXCR4$^{flox/flox}$ RD mice (Figure 4, B and C; and Supplemental Figure 4),
251 demonstrating that CXCR4 deletion from Na_v1.8-positive DRG neurons did not interfere
252 with normal neurite outgrowth.

253

254 **Excitatory CXCL12/CXCR4 signaling was enhanced in diabetic Na_v1.8-positive**
255 **DRG neurons**

256 The above results demonstrate that CXCL12/CXCR4 signaling in Na_v1.8-positive
257 DRG neurons is necessary for mechanical allodynia and small-fiber degeneration in
258 PDN. What is the mechanism for this effect? Our central hypothesis is that
259 CXCL12/CXCR4 signaling triggers hyperexcitability and $[Ca^{2+}]_i$ increases in Na_v1.8-
260 positive DRG neurons, which result in mechanical allodynia and axonal degeneration.
261 To test this hypothesis, we performed current-clamp experiments on cultured DRG
262 neurons from HFD and RD Na_v1.8-Cre;Ai9 mice. Application of the chemokine CXCL12
263 (50 nM) increased the firing frequency of Na_v1.8-positive neurons (Figure 5, A-F). This
264 increase was significantly greater in neurons from HFD mice (Figure 5, G-I). These
265 results are consistent with a role for CXCL12/CXCR4 signaling in generating Na_v1.8-
266 positive DRG neuron hyperexcitability.

267 Excitatory CXCL12/CXCR4 signaling was enhanced at 6 weeks of HFD
268 treatment, around the time of onset of mechanical allodynia and preceding the onset of

269 small-fiber degeneration. Indeed, $[Ca^{2+}]_i$ transients in acutely excised DRG explants
270 from Pirt-GCaMP3 transgenic mice showed that CXCL12 produced responses in
271 significantly more neurons 6 weeks after starting HFD (Supplemental Figure 5, A). In
272 contrast, the number of DRG neurons responding to CXCL12 after 2 or 4 weeks of HFD
273 or RD did not differ (Supplemental Figure 5, B).

274 To demonstrate that this phenomenon was specific for $Na_v1.8$-positive neurons,
275 we performed similar $[Ca^{2+}]_i$ imaging experiments on acutely excised DRG explants
276 from $Na_v1.8$-Cre::GCaMP6 mice 2 and 8 weeks after starting HFD or RD (Supplemental
277 video 5-8). Significantly more $Na_v1.8$-positive DRG neurons responded with increased
278 $[Ca^{2+}]_i$ after application of CXCL12 (100 nM) when mice had been on a HFD for 8 weeks
279 versus RD (Figure 6, A, C and D), but no difference was found after 2 weeks (Figure 6,
280 B, E and F). Additionally, DRG explants from paralbumin-Cre::GCaMP6 mice on RD or
281 HFD for 2 and 8 weeks did not respond with $[Ca^{2+}]_i$ transients upon application of
282 CXCL12 (Supplemental Table 2). These results are consistent with the possibility that
283 CXCL12/CXCR4 signaling is important in the development of $Na_v1.8$-positive DRG
284 neuron hyperexcitability in PDN.

285

286 **Reducing $Na_v1.8$-positive DRG neuron excitability prevented and reversed**
287 **mechanical allodynia and small-fiber degeneration in diabetic mice**

288 If this hyperexcitability is responsible for mechanical allodynia and small-fiber
289 degeneration, then reducing hyperexcitability should have a significant impact on both
290 phenomena. To reduce the excitability of $Na_v1.8$-positive DRG neurons in vivo over the

291 long term in freely behaving animals, we elected to use a chemogenetic platform
292 genetically introducing DREADD receptors (designer receptors exclusively activated by
293 designer drugs) into Na_v1.8-positive DRG neurons. We used an inhibitory DREADD
294 receptor based on an engineered muscarinic acetylcholine receptor M_4 (PDi), which
295 works via activation of the inhibitory $G_{i/o}$ protein pathway (60). Activation of this receptor
296 with the small molecule agonist clozapine-N-oxide (CNO) or its metabolite clozapine
297 inhibits neuronal activity (for review (61-63)). We expressed inhibitory hM_4 DREADD
298 (PDi) receptors in Na_v1.8-positive DRG neurons by crossing Na_v1.8-Cre;Ai9 mice with a
299 mouse line that enables the conditional expression of DREADD receptors (62) (Figure
300 7, A). We stained DRG taken from resulting Na_v1.8-Cre;Ai9;RC::PDi mice. We were
301 able to visualize PDis with immunohistochemistry using an antibody against HA as in
302 this construct the inhibitory PDi DREADD contains an HA tag(62) (Figure 7A). To
303 visualize non-peptidergic neurons, we used the IB4 Isolectin. Indeed we demonstrate
304 that PDis were expressed in all Na_v1.8-positive DRG neurons, and the percentage of
305 IB4-positive non-peptidergic neurons(14, 57, 64) expressing PDis in mice on RD or HFD
306 did not differ (Figure 7, B and C).

307 In vitro electrophysiology confirmed that CNO application reduced activity in
308 Na_v1.8-positive DRG neurons expressing inhibitory PDi receptors (Figure 8, A-C) as
309 previously demonstrated in other types of neurons (62). Specifically, in current-clamp
310 studies, CNO significantly reduced evoked action-potential frequency in cultured
311 Na_v1.8-positive DRG neurons from RD (Figure 8, A-C and G) and HFD Na_v1.8-
312 Cre;Ai9;RC::PDi mice (Figure 8, H). When we incubated RD cultures overnight with
313 pertussis toxin, CNO failed to produce any effects, indicating that the inhibitory effects

314 observed were transduced through $G_{i/o}$, as expected (Figure 8, D-F and I). Additionally,
315 CNO reversibly reduced capsaicin-induced $[Ca^{2+}]_i$ signals in DRG explants from mice
316 encoding GCaMP6 together with PDis in Na_v1.8-positive neurons (Na_v1.8-
317 Cre;RC::PDi;GCaMP6 mice) (Figure 8, J and K).

318 DREADD-independent effects of CNO have been reported (65), so we verified
319 that CNO did not change the firing frequencies of DRG neurons from Na_v1.8-Cre;Ai9
320 mice not expressing PDis in RD (Supplemental Figure 6, A-C and G) or HFD mice
321 (Supplemental Figure 6, D-F and G). In summary, these results demonstrate that
322 activating PDis in Na_v1.8-positive DRG neurons had a reversible, CNO-dependent,
323 inhibitory effect on their excitability.

324 Additionally CNO reversed mechanical allodynia in HFD Na_v1.8-Cre;Ai9;RC::PDi
325 mice expressing inhibitory DREADDs but not in HFD Na_v1.8-Cre;Ai9 mice non
326 expressing inhibitory DREADDs in vivo. Indeed using the von Frey pain behavioral
327 assay, we observed that HFD Na_v1.8-Cre;RC::PDi mice had significantly lower
328 withdrawal threshold for mechanical stimulation compared to animals on RD
329 (Supplemental Figure 7, A). However, one hour after a single intraperitoneal injection of
330 CNO (10 mg/kg), the withdrawal threshold increased, returning to baseline four hours
331 after injection (Supplemental Figure 7, A). Injecting CNO did not reverse mechanical
332 allodynia in diabetic Na_v1.8-Cre;Ai9 mice not expressing PDis (Supplemental Figure 7,
333 B), indicating CNO had no DREADD-independent effects. Both Na_v1.8-Cre;Ai9:RC::PDi
334 (Supplemental Figure 8, A and B) and Na_v1.8-Cre;Ai9 mice (Supplemental Figure 8, C
335 and D) fed HFD displayed weight gain and glucose intolerance.

336 Our previous results suggested that small-fiber degeneration occurred 2 weeks
337 after the onset of neuronal hyperexcitability (Figure 1, A-C, Supplemental Figure 2).
338 Thus, to evaluate the consequences of reducing Na_v1.8-positive DRG neuronal
339 hyperexcitability on small-fiber degeneration in PDN, we needed to achieve long-term
340 activation of DREADD receptors in vivo. To do this, we delivered CNO to mice
341 continuously using osmotic minipumps implanted intraperitoneally in Na_v1.8-
342 Cre;Ai9;RC::PDi mice between the second and eighth week (Figure 9, A). Continuous
343 CNO infusion did not alter the metabolic profile in mice expressing PDis, as HFD
344 induced obesity and glucose intolerance in Na_v1.8-Cre;RC::PDi infused with either CNO
345 or saline (Supplemental Figure 9, A-C). Additionally, we performed von Frey pain
346 behavioral studies and demonstrate that when CNO was continuously infused from
347 weeks 2-8, HFD mice no longer developed mechanical allodynia (Figure 9, B).
348 However, mice continuously infused with saline over the same period, developed
349 mechanical allodynia after 6 weeks on HFD (Figure 9, B). These results are consistent
350 with the possibility that CXCL12/CXCR4-mediated hyperexcitability of Na_v1.8-positive
351 DRG neurons is responsible for mechanical allodynia.

352 We next evaluated the consequences of reducing hyperexcitability on small-fiber
353 degeneration. Long-term chemogenetic reduction of Na_v1.8-positive DRG neuron
354 hyperexcitability significantly improved skin innervation in HFD mice (Figure 9, C and
355 D). Micrographs of skin from Na_v1.8-Cre;Ai9;RC::PDi RD control mice infused with
356 saline or CNO pumps showed normal skin innervation (Figure 9, C and D). In contrast,
357 HFD Na_v1.8-Cre;Ai9;RC::PDi mice with saline pumps exhibited greatly reduced
358 innervation (Figure 9, C and D). However, HFD mice with CNO pumps showed

359 significantly improved innervation, which was not statistically different from that of RD
360 mice (Figure 9, C and D). These results were verified by immunolabeling using a PGP
361 9.5 antibody on the same skin sample providing an independent verification for the fiber
362 density measurements (Supplemental Figure 10, A-C). These data demonstrate that
363 reducing the hyperexcitability of Na_v1.8-positive DRG neurons prevented small-fiber
364 degeneration.

365 We next tested whether similar treatment could reverse these phenomena once
366 they were established. We fitted Na_v1.8-Cre;Ai9;RC::PDi mice with osmotic mini-pumps
367 containing CNO or saline 10 weeks after starting HFD (Figure 10, A). By then, the mice
368 had developed obesity, glucose intolerance, mechanical allodynia, and small-fiber
369 degeneration. The obesity and glucose intolerance continued in HFD mice
370 (Supplemental Figure 9, D-F), but CNO infusion reversed mechanical allodynia, while it
371 persisted in saline-infused mice (Figure 10, B). After four weeks of CNO infusion, small-
372 fiber degeneration was completely reversed (Figure 10, C and D). These observations
373 were confirmed with PGP 9.5 antibody immunolabelling on skin samples from the same
374 mice (Supplemental Figure 11, A-C), as an independent verification for our fiber density
375 measurements. We further established that CNO infusion did not affect mechanical
376 allodynia or small-fiber degeneration in Na_v1.8-Cre;Ai9 mice that were not expressing
377 DREADDs, regardless of diet, at 2-8 weeks (Supplemental Figure 12, A-D) or 10-14
378 weeks (Supplemental Figure 13, A-D). Hence, these effects of CNO are DREADD
379 dependent.

380

381 **Increasing Na_v1.8-positive DRG neuron excitability accelerated small-fiber**

382 **degeneration in diabetic mice**

383 Next, we hypothesized that increasing neuronal excitability would accelerate
384 mechanical allodynia and small-fiber degeneration. To test this hypothesis, we again
385 utilized a chemogenetic approach in which we expressed excitatory hM_3Dq
386 DREADDs(66) in $Na_v1.8$-positive DRG neurons. We used a mouse line with a Cre-
387 responsive (Rosa-CAG=loxh M_3Dq [RC::L-hM_3Dq]) (66) allele that also encodes EGFP
388 and an hM_3Dq-mCherry fusion protein. Cre activity inverts hM_3Dq-mCherry, producing
389 the proper orientation for transcription. RC::L-hM_3Dq therefore expresses EGFP without
390 recombinase activity and hM_3Dq-mCherry after Cre-mediated recombination (Figure 11,
391 A). Using confocal microscopy, we confirmed expression of hM_3Dq DREADDs in
392 $Na_v1.8$-positive DRG neurons and the dorsal horn of spinal cord (14, 23) (Figure 11, B).
393 Fura-2 based $[Ca^{2+}]i$ imaging of $Na_v1.8$-positive DRG neurons cultured from $Na_v1.8$-
394 Cre;RC::L-hM_3Dq mice demonstrated that CNO elicited robust $[Ca^{2+}]_i$ signals in cells
395 expressing the receptor (red), but not in cells without it (green) (Figure 11, C-E).
396 Furthermore, in vitro current clamp experiments showed that addition of CNO to $Na_v1.8$-
397 positive DRG neurons depolarized the membrane potential and increased the frequency
398 of evoked action potentials in cultures from $Na_v1.8$-Cre;RC::L-hM_3Dq mice but not from
399 $Na_v1.8$-Cre;Ai9 control mice (Figure 11, F-J and Supplemental Table 1).

400 Next we investigated the effects of long-term activation of hM_3Dqs in vivo. We
401 delivered CNO using osmotic mini-pumps placed intraperitoneally in $Na_v1.8$-Cre;RC::L-
402 M_3Dq mice from 2 to 4 weeks after commencement of HFD or RD (Figure 12, A). After
403 four weeks on HFD, mice had not yet developed glucose intolerance (Supplemental
404 Figure 14, A-C). We found that mice fed either diet developed mechanical allodynia if

405 CNO was continuously delivered from 2 to 4 weeks (Figure 12, B). Long-term
406 chemogenetic activation of $Na_v1.8$-positive DRG neurons also significantly accelerated
407 small-fiber degeneration in HFD mice (Figure 12, C and D). Confocal micrographs from
408 $Na_v1.8$-Cre;RC::L-hM_3Dq mice after 4 weeks on RD or HFD with saline pumps showed
409 normal skin innervation. In contrast, $Na_v1.8$-Cre;RC::L-hM_3Dq mice on HFD for 4 weeks
410 with a CNO pump showed substantial depletion of nerve terminals (Figure 12, C and D)
411 demonstrating accelerated pathology. In contrast, $Na_v1.8$-Cre;RC::L-hM_3Dq mice with
412 CNO infusion on RD did not develop small-fiber degeneration, at least after 4 weeks,
413 the latest time we examined (Figure 12, C and D), indicating that increased excitability
414 without diabetes was not sufficient to cause small-fiber degeneration.
415
416
417
418
419
420
421
422
423
424
425
426
427

428 **DISCUSSION**

429 The results of our experiments demonstrated that excitatory CXCL12/CXCR4
430 signaling is a key factor in generating mechanical allodynia and small-fiber
431 degeneration, two important features of PDN. We could prevent and reverse these
432 phenomena by selective deletion of CXCR4 receptors or by chemogenetically limiting
433 the excitability of $Na_v1.8$-positive DRG neurons in the HFD mouse model of PDN. As
434 activating CXCR4 receptors increased excitability and $[Ca^{2+}]i$ of these neurons, we
435 hypothesize that these effects may be responsible for the CXCR4-mediated mechanical
436 allodynia and small-fiber degeneration. Hence, these studies indicate that CXCR4-
437 induced hyperexcitability of $Na_v1.8$-positive DRG neurons represents a novel molecular
438 pathway linking mechanical allodynia and axonal degeneration in diabetes, suggesting
439 a new target for disease modifying therapy, which is currently unavailable for PDN
440 patients(6).

441 Painful symptoms vary among PDN patients(40), leading to different sensory
442 phenotypes(40, 41) with different molecular mechanisms(25). In PDN patients,
443 mechanical allodynia is commonly observed together with thermal hypoesthesia,
444 particularly at later stages of the disease(40, 41). Similarly, in the HFD model, mice
445 ultimately develop thermal hypoalgesia and mechanical allodynia, but not until 16 weeks
446 after starting HFD(38). After 10 weeks on HFD, mice display mechanical allodynia
447 without thermal hypoalgesia(30, 39). Given that sensory phenotypes are heterogeneous
448 and vary with disease stage (40), we decided to focus our investigation on mechanical
449 allodynia rather then on thermal pain behaviors. Mechanical allodynia is common in
450 PDN patients(30, 39), though the relative contribution of its static and dynamic

451 components, which are important in the clinic, may not be precisely duplicated in mouse
452 models(25, 41). Regardless, our studies introduce the novel suggestion that CXCR4
453 chemokine signaling is an important upstream mediator driving $Na_v1.8$-positive DRG
454 neuronal hyperexcitability, mechanical allodynia, and small-fiber degeneration in the
455 HFD model. Hence, modulation of proalgesic chemokine signaling may provide an
456 opportunity for disease modification. Thus, these results have the potential for
457 transforming the way small-fiber degeneration is treated, replacing the largely ineffective
458 approaches that are currently available for patients afflicted with PDN(6).

459 We demonstrated that the development of mechanical allodynia was inhibited
460 following selective deletion of CXCR4 receptors and associated reduction of
461 hyperexcitability in $Na_v1.8$-positive DRG neurons. The subtypes of DRG neurons
462 traditionally linked to mechanical allodynia are C-fibers (67-70), low-threshold C-
463 mechanoreceptors, and Aδ-mechanoreceptors (71-74). However, mechanical allodynia
464 is also mediated by low-threshold Aβ-mechanoreceptors (71, 72). Given that all of these
465 neuronal populations express $Na_v1.8$ to some degree(23), our studies do not completely
466 deconvolute the nature of the subtypes of neurons within the $Na_v1.8$ population that are
467 specifically associated with the occurrence of mechanical allodynia, something that
468 could be achieved in future studies.

469 An additional limitation concerns the role of CXCR4-induced DRG hyperexcitability
470 in the pathogenesis of axonal degeneration. One possibility is that blocking CXCR4
471 signaling protects against chronic increased $[Ca^{2+}]_i$ which produces axonal
472 degeneration, as previously suggested(75) in the central(76) and peripheral
473 neurons(77-79). In particular, increased $[Ca^{2+}]_i$ is responsible for DRG neurite

474 degeneration and contributes to nerve degeneration in a genetic model of small-fiber
475 neuropathy(80). On the other hand, some reports have identified potentially beneficial
476 effects of $[Ca^{2+}]_i$ on axonal stability in a model of axon injury(81, 82). Hence, the precise
477 characteristics of $[Ca^{2+}]_i$ in DRG neurons, including magnitude and acute or chronic
478 signaling, may lead to different endpoints of axon structure and function.

479 Increased $[Ca^{2+}]_i$ might contribute to axonal damage by altering mitochondrial
480 function(83), including calcium homeostasis(84). Mitochondrial abnormalities occur in
481 animal models of diabetes(32, 85). Specifically, DRG neurons show downregulation of
482 mitochondrial respiratory chain complex proteins(86) and reduced respiratory chain
483 activity(87). Thus, sustained CXCR4 signaling in $Na_v1.8$-positive DRG neurons might
484 initiate a cascade resulting in hyperexcitability and $[Ca^{2+}]_i$ increases that could
485 overwhelm the mitochondrial homeostatic mechanisms compromised by diabetes(32,
486 85), leading to small-fiber degeneration. Our observation that chemogenetic activation
487 of $Na_v1.8$-positive DRG neurons accelerated small-fiber degeneration only in HFD mice
488 (Figure 12, D), supports this hypothesis.

489 Our chemogenetic approach revealed novel mechanisms underlying the
490 development of mechanical allodynia and small-fiber degeneration in PDN. DREADDs
491 are widely employed to manipulate neural excitability (for review (61, 88) but they have
492 some limitations. Inhibitory PDi expression in C-fibers using the TRPV1-Cre allele
493 resulted in altered channel activity and second messenger signaling even without CNO,
494 presumably due to constitutive activity of overexpressed DREADD receptors in these
495 experiments(89). Accordingly, we included saline controls to ensure that our findings
496 were related to activation by CNO. We did not observe CNO-independent changes,

497 perhaps because we used a different promoter to drive Cre expression ($Na_v1.8$-Cre
498 instead of TRPV1-Cre).

499 Recent reports have also suggested that there may be DREADD-independent
500 effects of CNO(65) and have raised the possibility that CNO can rapidly convert to
501 clozapine in vivo(63). To control for this possibility, we established that CNO infusion did
502 not affect mechanical allodynia or small-fiber degeneration in $Na_v1.8$-Cre;Ai9 mice that
503 were not expressing DREADDs, regardless of diet, at 2-8 weeks (Supplemental Figure
504 12, A-D) or 10-14 weeks (Supplemental Figure 13, A-D). Hence, all effects of CNO we
505 observed were DREADD dependent. All the controls for the chemogenetic platform
506 listed above are essential for validating our experiments as the data presented here
507 represent the first time that any intervention has been shown to prevent and even
508 reverse, not only mechanical allodynia but also small-fiber degeneration, in a diabetic
509 model.

510 In summary, our results identify CXCL12/CXCR4 signaling as the initiator of a novel
511 pathway linking hyperexcitability and increased $[Ca^{2+}]_i$ in $Na_v1.8$-positive DRG neurons
512 to mechanical allodynia and small-fiber degeneration in PDN. From a translational
513 perspective, we propose that blocking CXCR4 signaling or $Na_v1.8$-positive DRG neuron
514 hyperexcitability may represent a novel approach for the treatment of this intractable
515 and widespread affliction. Indeed, reduction of proalgesic CXCL12/CXCR4 signaling
516 could abolish persistent excitability and increased $[Ca^{2+}]_i$, preventing not only
517 neuropathic pain behavior but also the development of small-fiber degeneration. We
518 also predict that drugs that reduce $Na_v1.8$-expressing DRG neuronal hyperexcitability,
519 such as specific sodium channel blockers (90, 91), might effectively treat PDN.

520 Moreover, the relationship between hyperexcitability, calcium overload, and axonal
521 degeneration is likely to inform studies of other neurodegenerative diseases, such as
522 ALS(92) or PD(93), that involve similar underlying events.
523
524
525
526
527
528
529
530
531
532
533
534
535
536
537
538
539
540
541
542

543 **MATERIAL & METHODS**

544 **Animals:** Animals were housed with food and water *ad libitum* on a 12-hour light cycle.
545 We utilized the following mouse lines: Na_v1.8-Cre;Ai9, Pirt-GCaMP3, Na_v1.8-
546 Cre::GCaMP6, parvalbumin-cre::GCaMP6, Na_v1.8-Cre;;RC::PDi mice, Na_v1.8-
547 Cre;Ai9;RC::PDi, Na_v1.8-Cre;RC::PDi;GCamP6, Na_v1.8-Cre;RC::L-hM_3Dq, Na_v1.8-
548 Cre;Ai9;CXCR4$^{flox/+}$ heterozygotes and Na_v1.8-Cre;Ai9;CXCR4$^{flox/flox}$ homozygotes.

549

550 **High-fat diet:** HFD is a common rodent model of type-II diabetes (38). Mice were fed
551 42% fat (Envigo TD88137) for 10 weeks. Control mice were fed regular diet (11% fat).
552 After 10 weeks on RD or HFD, a glucose tolerance test was performed as described
553 (38). To compare "diabetic" versus "non-diabetic" HFD mice, we set the cutoff for
554 diabetes ($\geq$140 mg/dL) at 2 SDs above the mean for glucose at 2 hours after glucose
555 challenge in 129 wild-type littermate RD mice (39, 94).

556

557 **Detection of cutaneous innervation:** Skin samples were processed as previously
558 described(39). **Confocal analysis:** samples were imaged by confocal microscopy
559 (Olympus fv10i, fluoView software). Composite Z-stack images were obtained and
560 processed using Fiji (NIH). The epidermal-dermal junction was outlined by a blinded
561 observer who also noted its length. At least 3 other blinded reviewers counted the
562 nerves crossing this line using the Cell Counter plugin.

563

564 **Behavioral testing:** von Frey behavioral studies were performed as previously
565 described (30, 31). von Frey experiments were conducted using random experimental
566 group assignments (diet (RD or HFD) and treatment assignments). Investigators that
567 performed von Frey tests and endpoint analysis were blinded to the experimental
568 conditions. We have experience with randomized allocation and blinded analysis using
569 this mouse model with sequenced numbering of mice at weaning(30, 39).

570

571 **Calcium imaging in DRG explants:** L4 and L5 PirtGCaMP3 and Na_v1.8-
572 Cre;RC::PDi;GCaMP6 mice DRGs were dissected, incubated in ACSF at room
573 temperature, and mounted on the stage of a Yokogawa CSU-X1 & CSU-W1 upright
574 spinning-disk confocal microscope (3i, Intelligent Imaging Innovations, Inc, CO)
575 equipped with an electron multiplication CCD camera(48). Activity of selected neurons
576 of the explants expressing GCaMP3 or GCaMP6 (green fluorescence) was examined
577 based on peak amplitude of fluorescence change ($\Delta F/F0$) for spontaneous activity
578 compared with that of the stimulus. Fiji (NIH) software was used to analyze $[Ca^{2+}]_i$
579 imaging data using standard functions and a custom macro. Different concentrations of
580 potassium (K^+) (10 and 50 mM) or capsaicin (cap) (1, 2 and 10 μM), CNO (8 μM) and
581 CXCL12 (100 nM) were applied.

582

583 **Preparation of primary cultures of DRG neurons:** DRG sensory neurons from
584 diabetic Na_v1.8-Cre;Ai9 mice, Na_v1.8-Cre;Ai9;RC::PDi mice and Na_v1.8-Cre;RC::L-
585 hM_3Dq mice were dissociated as described (31) after 10 weeks on either RD or HFD.

586 **Electrophysiological recordings from DRG neurons**. For current-clamp recordings,
587 patch electrodes with a resistance of 5–7 MΩ were filled with (in mM) 140 KCl, 0.5
588 EGTA, 5 HEPES and 3-Mg-ATP, pH 7.3 (300 mOsmol). The resting membrane
589 potential was measured from each cell. Whole-cell, current-clamp recordings were
590 obtained as previously described (95) using a MultiClamp patch-clamp amplifier
591 (Molecular Devices). The data was captured with pClamp 10.0 software (Molecular
592 Devices) and calculated with Clampfit, Sigma Plot, Graph Pad Prism, and Igor. CNO
593 (2.5, 7.5 or 10 μM) and CXCL12 (50 nM) were applied to culture.

594

595 **Antibodies:** We used the following antibodies on DRG sections: HA-Tag (C29F4) rabbit
596 monoclonal antibody (Cell Signaling, Cat # 3724, 1:250), and I-isolectin B4 (IB4
597 Isolectin GS-IB4 Alexa fluor conjugate 647 (Invitrogen, Cat # I32450 (1:100).
598 Secondary: Alexa fluor 488 goat anti-rabbit antibody (Invitrogen, 1:250). We used anti-
599 PGP9.5 Rabbit monoclonal antibody (Millipore #AB1761-I, 1:250) on skin sections.

600

601 **Immunohistochemical labeling:** Adult mice were deeply anesthetized with isoflurane
602 and transcardially perfused with saline followed by 4% paraformaldehyde. DRG (lumbar
603 level 2-4) and spinal cord were processed as previously described(30). Tissue sections
604 were analyzed by confocal microscopy.

605

606 **Intraperitoneal injection with clozapine-n-oxide**: CNO (10 mg/kg) (Sigma Aldrich) in
607 200 microliters of saline or saline were injected with a 25 gauge. Mice were tested for
608 pain 1 hour and 4 hours after injection.
609
610 **Chronic activation of DREADDs with CNO:** ALZET® Osmotic Pumps (Cupertino, CA,
611 USA) were surgically implanted intraperitoneally according to the manufacturer's
612 instructions in animals anesthetized with isoflurane. Pump model 2006 and 1004 were
613 used for constant delivery (0.15 µl/hr) of CNO (10 mg/kg/day) (VDM Biochemicals) or
614 saline for 6 weeks and 4 weeks, respectively.
615
616 **In vitro calcium imaging of DRG neurons.** Neurons from Na_v1.8-Cre;RC::L-hM_3Dq
617 mice were cultured as described (31). Their responses to CNO (7.5µM) were recorded
618 using Fura-2 based $[Ca^{2+}]$i imaging as previously described (30, 31). For all
619 experiments, capsaicin (100nM), high K+ (25 mM) and ATP (100µM) were added to the
620 cells.
621
622 **Statistical Analysis**: All statistical analysis was performed using Prism7.03 (GraphPad
623 Software, San Diego, CA, USA). For measurement of blood glucose and behavioral
624 testing the significance of differences between the control and the various treatment
625 groups, or between genotypes, was analyzed using one-way or two-way ANOVA,
626 mutiple comparison tests (Bonferroni). For calcium imaging experiments in vitro and in
627 vivo, the data were tested for statistical significance by Mann-Whitney test. The two-way

628 analysis of variance (ANOVA) with Dunnett's or Bonferroni multiple-comparison was
629 used to determine the IENF density. For the electrophysiological experiments, the data
630 were tested for statistical significance by Mann-Whitney test and one-way ANOVA,
631 post-hoc Tukey test. Student *t* tests were all 2-tailed. All values are expressed as mean
632 ± S.E.M, and $p < 0.05$ is considered significant.

633

634 **Study Approval:** All methods involving animals were approved by the Institutional
635 Animal Care and Use Committee at Northwestern University.

636

637

638

639

640

641

642

643

644

645

646

647 **AUTHOR CONTRIBUTIONS:**

648 NDJ performed von Frey behavioral studies, $[Ca^{2+}]_i$ imaging studies
649 immunohistochemical labeling, and confocal analysis. Mouse breeding, diet
650 administration, GTT, and IENF density counts were done by NDJ, CAR, BEH and HG.
651 BJB and SH performed electrophysiological studies. DR and AAB performed $[Ca^{2+}]_i$
652 imaging studies. DMM and NDJ performed statistical analysis. DMM and RJM
653 supervised the project. DMM drafted the manuscript, which was edited by RJM. All
654 authors read and approved the manuscript.

655

656

657

658

659

660

661

662

663

664

665

666 **ACKNOWLEDGEMENTS:** This work was supported by NIH K08 NS079482-01 (DMM),
667 NIH 5R01DA013141-14 (RJM), and NIH/Rush University Medical Center
668 1R01AR064251-01 (RJM). All statistical analysis was reviewed by the Statistical Core at
669 Northwestern University. We thank Dr. Rajeshwar Awatramani for helpful discussions.
670 We thank Alexandra Fredrickson for helping with the evaluation of IENF density. We
671 thank Dr. Susan Dymecki, Dr. Xinzhong, Dong, Dr. John Wood, Dr. Savio Chan and Dr.
672 Patricia Jensen for generous gifts of mice (RC::PDi, Pirt-GCaMP3, Na_v1.8-Cre, Parvalb-
673 Cre and RC::L-hM_3Dq, respectively).

674

675

676

677

678

679

680

681

682

683

684

685 **REFERENCE:**

686 1. American Diabetes A. Diagnosis and classification of diabetes mellitus. *Diabetes care.*
687 2011;34 Suppl 1(S62-9.
688 2. Spallone V, Lacerenza M, Rossi A, Sicuteri R, and Marchettini P. Painful diabetic
689 polyneuropathy: approach to diagnosis and management. *The Clinical journal of pain.*
690 2012;28(8):726-43.
691 3. Zimmet PZ, Magliano DJ, Herman WH, and Shaw JE. Diabetes: a 21st century
692 challenge. *The lancet Diabetes & endocrinology.* 2014;2(1):56-64.
693 4. Menke A, Casagrande S, Geiss L, and Cowie CC. Prevalence of and Trends in Diabetes
694 Among Adults in the United States, 1988-2012. *Jama.* 2015;314(10):1021-9.
695 5. daCosta DiBonaventura M, Cappelleri JC, and Joshi AV. A longitudinal assessment of
696 painful diabetic peripheral neuropathy on health status, productivity, and health care
697 utilization and cost. *Pain medicine.* 2011;12(1):118-26.
698 6. Bril V, England J, Franklin GM, Backonja M, Cohen J, Del Toro D, Feldman E, Iverson
699 DJ, Perkins B, Russell JW, et al. Evidence-based guideline: Treatment of painful diabetic
700 neuropathy: report of the American Academy of Neurology, the American Association of
701 Neuromuscular and Electrodiagnostic Medicine, and the American Academy of Physical
702 Medicine and Rehabilitation. *Neurology.* 2011;76(20):1758-65.
703 7. Quilici S, Chancellor J, Lothgren M, Simon D, Said G, Le TK, Garcia-Cebrian A, and
704 Monz B. Meta-analysis of duloxetine vs. pregabalin and gabapentin in the treatment of
705 diabetic peripheral neuropathic pain. *BMC neurology.* 2009;9(6.
706 8. Callaghan BC, Cheng HT, Stables CL, Smith AL, and Feldman EL. Diabetic neuropathy:
707 clinical manifestations and current treatments. *The Lancet Neurology.* 2012;11(6):521-34.
708 9. Finnerup NB, Attal N, Haroutounian S, McNicol E, Baron R, Dworkin RH, Gilron I,
709 Haanpaa M, Hansson P, Jensen TS, et al. Pharmacotherapy for neuropathic pain in adults:
710 a systematic review and meta-analysis. *The Lancet Neurology.* 2015;14(2):162-73.
711 10. Divisova S, Vlckova E, Srotova I, Kincova S, Skorna M, Dusek L, Dubovy P, and
712 Bednarik J. Intraepidermal nerve-fibre density as a biomarker of the course of neuropathy
713 in patients with Type 2 diabetes mellitus. *Diabetic medicine : a journal of the British*
714 *Diabetic Association.* 2015.
715 11. Latremoliere A, and Woolf CJ. Central sensitization: a generator of pain hypersensitivity
716 by central neural plasticity. *The journal of pain : official journal of the American Pain*
717 *Society.* 2009;10(9):895-926.
718 12. Lauria G, and Devigili G. Skin biopsy as a diagnostic tool in peripheral neuropathy.
719 *Nature clinical practice Neurology.* 2007;3(10):546-57.
720 13. Sommer C, and Lauria G. Skin biopsy in the management of peripheral neuropathy. *The*
721 *Lancet Neurology.* 2007;6(7):632-42.
722 14. Basbaum AI, Bautista DM, Scherrer G, and Julius D. Cellular and molecular mechanisms
723 of pain. *Cell.* 2009;139(2):267-84.
724 15. Woolf CJ. Central sensitization: uncovering the relation between pain and plasticity.
725 *Anesthesiology.* 2007;106(4):864-7.
726 16. Feldman EL, Nave KA, Jensen TS, and Bennett DL. New Horizons in Diabetic
727 Neuropathy: Mechanisms, Bioenergetics, and Pain. *Neuron.* 2017;93(6):1296-313.
728 17. Tesfaye S, Boulton AJ, and Dickenson AH. Mechanisms and management of diabetic
729 painful distal symmetrical polyneuropathy. *Diabetes care.* 2013;36(9):2456-65.

730 18. Orstavik K, Namer B, Schmidt R, Schmelz M, Hilliges M, Weidner C, Carr RW,
731 Handwerker H, Jorum E, and Torebjork HE. Abnormal function of C-fibers in patients
732 with diabetic neuropathy. *The Journal of neuroscience : the official journal of the Society*
733 *for Neuroscience.* 2006;26(44):11287-94.
734 19. Andersson DA, Gentry C, Light E, Vastani N, Vallortigara J, Bierhaus A, Fleming T, and
735 Bevan S. Methylglyoxal evokes pain by stimulating TRPA1. *PloS one.*
736 2013;8(10):e77986.
737 20. Bierhaus A, Fleming T, Stoyanov S, Leffler A, Babes A, Neacsu C, Sauer SK, Eberhardt
738 M, Schnolzer M, Lasitschka F, et al. Methylglyoxal modification of Nav1.8 facilitates
739 nociceptive neuron firing and causes hyperalgesia in diabetic neuropathy. *Nature*
740 *medicine.* 2012;18(6):926-33.
741 21. Orstavik K, and Jorum E. Microneurographic findings of relevance to pain in patients
742 with erythromelalgia and patients with diabetic neuropathy. *Neuroscience letters.*
743 2010;470(3):180-4.
744 22. Serra J, Duan WR, Locke C, Sola R, Liu W, and Nothaft W. Effects of a T-type calcium
745 channel blocker, ABT-639, on spontaneous activity in C-nociceptors in patients with
746 painful diabetic neuropathy: a randomized controlled trial. *Pain.* 2015;156(11):2175-83.
747 23. Shields SD, Ahn HS, Yang Y, Han C, Seal RP, Wood JN, Waxman SG, and Dib-Hajj
748 SD. Nav1.8 expression is not restricted to nociceptors in mouse peripheral nervous
749 system. *Pain.* 2012;153(10):2017-30.
750 24. Lauria G, Ziegler D, Malik R, Merkies IS, Waxman SG, Faber CG, and group PS. The
751 role of sodium channels in painful diabetic and idiopathic neuropathy. *Current diabetes*
752 *reports.* 2014;14(10):538.
753 25. von Hehn CA, Baron R, and Woolf CJ. Deconstructing the neuropathic pain phenotype to
754 reveal neural mechanisms. *Neuron.* 2012;73(4):638-52.
755 26. de Lera Ruiz M, and Kraus RL. Voltage-Gated Sodium Channels: Structure, Function,
756 Pharmacology, and Clinical Indications. *Journal of medicinal chemistry.*
757 2015;58(18):7093-118.
758 27. Yang F, Sun W, Yang Y, Wang Y, Li CL, Fu H, Wang XL, Yang F, He T, and Chen J.
759 SDF1-CXCR4 signaling contributes to persistent pain and hypersensitivity via regulating
760 excitability of primary nociceptive neurons: involvement of ERK-dependent Nav1.8 up-
761 regulation. *Journal of neuroinflammation.* 2015;12(219.
762 28. Kao DJ, Li AH, Chen JC, Luo RS, Chen YL, Lu JC, and Wang HL. CC chemokine
763 ligand 2 upregulates the current density and expression of TRPV1 channels and Nav1.8
764 sodium channels in dorsal root ganglion neurons. *Journal of neuroinflammation.*
765 2012;9(189.
766 29. Wang JG, Strong JA, Xie W, Yang RH, Coyle DE, Wick DM, Dorsey ED, and Zhang
767 JM. The chemokine CXCL1/growth related oncogene increases sodium currents and
768 neuronal excitability in small diameter sensory neurons. *Molecular pain.* 2008;4(38.
769 30. Menichella DM, Abdelhak B, Ren D, Shum A, Frietag C, and Miller RJ. CXCR4
770 chemokine receptor signaling mediates pain in diabetic neuropathy. *Molecular pain.*
771 2014;10(42.
772 31. Bhangoo SK, Ren D, Miller RJ, Chan DM, Ripsch MS, Weiss C, McGinnis C, and White
773 FA. CXCR4 chemokine receptor signaling mediates pain hypersensitivity in association
774 with antiretroviral toxic neuropathy. *Brain, behavior, and immunity.* 2007;21(5):581-91.

775 32. Vincent AM, Callaghan BC, Smith AL, and Feldman EL. Diabetic neuropathy: cellular
776 mechanisms as therapeutic targets. *Nature reviews Neurology.* 2011;7(10):573-83.
777 33. Kampoli AM, Tousoulis D, Briasoulis A, Latsios G, Papageorgiou N, and Stefanadis C.
778 Potential pathogenic inflammatory mechanisms of endothelial dysfunction induced by
779 type 2 diabetes mellitus. *Current pharmaceutical design.* 2011;17(37):4147-58.
780 34. Sjoholm A, and Nystrom T. Endothelial inflammation in insulin resistance. *Lancet.*
781 2005;365(9459):610-2.
782 35. Purwata TE. High TNF-alpha plasma levels and macrophages iNOS and TNF-alpha
783 expression as risk factors for painful diabetic neuropathy. *Journal of pain research.*
784 2011;4(169-75.
785 36. Uceyler N, Rogausch JP, Toyka KV, and Sommer C. Differential expression of cytokines
786 in painful and painless neuropathies. *Neurology.* 2007;69(1):42-9.
787 37. Hur J, Sullivan KA, Pande M, Hong Y, Sima AA, Jagadish HV, Kretzler M, and Feldman
788 EL. The identification of gene expression profiles associated with progression of human
789 diabetic neuropathy. *Brain : a journal of neurology.* 2011;134(Pt 11):3222-35.
790 38. Obrosova IG, Ilnytska O, Lyzogubov VV, Pavlov IA, Mashtalir N, Nadler JL, and Drel
791 VR. High-fat diet induced neuropathy of pre-diabetes and obesity: effects of "healthy"
792 diet and aldose reductase inhibition. *Diabetes.* 2007;56(10):2598-608.
793 39. Menichella DM, Jayaraj ND, Wilson HM, Ren D, Flood K, Wang XQ, Shum A, Miller
794 RJ, and Paller AS. Ganglioside GM3 synthase depletion reverses neuropathic pain and
795 small fiber neuropathy in diet-induced diabetic mice. *Molecular pain.* 2016;12(
796 40. Baron R, Tolle TR, Gockel U, Brosz M, and Freynhagen R. A cross-sectional cohort
797 survey in 2100 patients with painful diabetic neuropathy and postherpetic neuralgia:
798 Differences in demographic data and sensory symptoms. *Pain.* 2009;146(1-2):34-40.
799 41. Themistocleous AC, Ramirez JD, Shillo PR, Lees JG, Selvarajah D, Orengo C, Tesfaye
800 S, Rice AS, and Bennett DL. The Pain in Neuropathy Study (PiNS): a cross-sectional
801 observational study determining the somatosensory phenotype of painful and painless
802 diabetic neuropathy. *Pain.* 2016;157(5):1132-45.
803 42. Chiu IM, Barrett LB, Williams EK, Strochlic DE, Lee S, Weyer AD, Lou S, Bryman GS,
804 Roberson DP, Ghasemlou N, et al. Transcriptional profiling at whole population and
805 single cell levels reveals somatosensory neuron molecular diversity. *eLife.* 2014;3(
806 43. Usoskin D, Furlan A, Islam S, Abdo H, Lonnerberg P, Lou D, Hjerling-Leffler J,
807 Haeggstrom J, Kharchenko O, Kharchenko PV, et al. Unbiased classification of sensory
808 neuron types by large-scale single-cell RNA sequencing. *Nature neuroscience.*
809 2015;18(1):145-53.
810 44. Li CL, Li KC, Wu D, Chen Y, Luo H, Zhao JR, Wang SS, Sun MM, Lu YJ, Zhong YQ,
811 et al. Somatosensory neuron types identified by high-coverage single-cell RNA-
812 sequencing and functional heterogeneity. *Cell research.* 2016;26(8):967.
813 45. Stirling LC, Forlani G, Baker MD, Wood JN, Matthews EA, Dickenson AH, and Nassar
814 MA. Nociceptor-specific gene deletion using heterozygous NaV1.8-Cre recombinase
815 mice. *Pain.* 2005;113(1-2):27-36.
816 46. Madisen L, Zwingman TA, Sunkin SM, Oh SW, Zariwala HA, Gu H, Ng LL, Palmiter
817 RD, Hawrylycz MJ, Jones AR, et al. A robust and high-throughput Cre reporting and
818 characterization system for the whole mouse brain. *Nature neuroscience.*
819 2010;13(1):133-40.

820 47. Lauria G, Lombardi R, Camozzi F, and Devigili G. Skin biopsy for the diagnosis of
821 peripheral neuropathy. *Histopathology.* 2009;54(3):273-85.
822 48. Han L, Ma C, Liu Q, Weng HJ, Cui Y, Tang Z, Kim Y, Nie H, Qu L, Patel KN, et al. A
823 subpopulation of nociceptors specifically linked to itch. *Nature neuroscience.*
824 2012;16(2):174-82.
825 49. Goswami SC, Mishra SK, Maric D, Kaszas K, Gonnella GL, Clokie SJ, Kominsky HD,
826 Gross JR, Keller JM, Mannes AJ, et al. Molecular signatures of mouse TRPV1-lineage
827 neurons revealed by RNA-Seq transcriptome analysis. *The journal of pain : official*
828 *journal of the American Pain Society.* 2014;15(12):1338-59.
829 50. Chen TW, Wardill TJ, Sun Y, Pulver SR, Renninger SL, Baohan A, Schreiter ER, Kerr
830 RA, Orger MB, Jayaraman V, et al. Ultrasensitive fluorescent proteins for imaging
831 neuronal activity. *Nature.* 2013;499(7458):295-300.
832 51. Hippenmeyer S, Vrieseling E, Sigrist M, Portmann T, Laengle C, Ladle DR, and Arber S.
833 A developmental switch in the response of DRG neurons to ETS transcription factor
834 signaling. *PLoS biology.* 2005;3(5):e159.
835 52. Niu J, Ding L, Li JJ, Kim H, Liu J, Li H, Moberly A, Badea TC, Duncan ID, Son YJ, et
836 al. Modality-based organization of ascending somatosensory axons in the direct dorsal
837 column pathway. *The Journal of neuroscience : the official journal of the Society for*
838 *Neuroscience.* 2013;33(45):17691-709.
839 53. de Nooij JC, Doobar S, and Jessell TM. Etv1 inactivation reveals proprioceptor
840 subclasses that reflect the level of NT3 expression in muscle targets. *Neuron.*
841 2013;77(6):1055-68.
842 54. White FA, Sun J, Waters SM, Ma C, Ren D, Ripsch M, Steflik J, Cortright DN, Lamotte
843 RH, and Miller RJ. Excitatory monocyte chemoattractant protein-1 signaling is up-
844 regulated in sensory neurons after chronic compression of the dorsal root ganglion.
845 *Proceedings of the National Academy of Sciences of the United States of America.*
846 2005;102(39):14092-7.
847 55. Mithal DS, Ren D, and Miller RJ. CXCR4 signaling regulates radial glial morphology
848 and cell fate during embryonic spinal cord development. *Glia.* 2013;61(8):1288-305.
849 56. Belmadani A, Jung H, Ren D, and Miller RJ. The chemokine SDF-1/CXCL12 regulates
850 the migration of melanocyte progenitors in mouse hair follicles. *Differentiation; research*
851 *in biological diversity.* 2009;77(4):395-411.
852 57. Stucky CL, Rossi J, Airaksinen MS, and Lewin GR. GFR alpha2/neurturin signalling
853 regulates noxious heat transduction in isolectin B4-binding mouse sensory neurons. *The*
854 *Journal of physiology.* 2002;545(Pt 1):43-50.
855 58. Snider WD, and McMahon SB. Tackling pain at the source: new ideas about nociceptors.
856 *Neuron.* 1998;20(4):629-32.
857 59. Bennett DL, Averill S, Clary DO, Priestley JV, and McMahon SB. Postnatal changes in
858 the expression of the trkA high-affinity NGF receptor in primary sensory neurons. *The*
859 *European journal of neuroscience.* 1996;8(10):2204-8.
860 60. Armbruster BN, Li X, Pausch MH, Herlitze S, and Roth BL. Evolving the lock to fit the
861 key to create a family of G protein-coupled receptors potently activated by an inert
862 ligand. *Proceedings of the National Academy of Sciences of the United States of America.*
863 2007;104(12):5163-8.

61. Urban DJ, and Roth BL. DREADDs (designer receptors exclusively activated by designer drugs): chemogenetic tools with therapeutic utility. *Annual review of pharmacology and toxicology.* 2015;55(399-417.
62. Ray RS, Corcoran AE, Brust RD, Kim JC, Richerson GB, Nattie E, and Dymecki SM. Impaired respiratory and body temperature control upon acute serotonergic neuron inhibition. *Science.* 2011;333(6042):637-42.
63. Gomez JL, Bonaventura J, Lesniak W, Mathews WB, Sysa-Shah P, Rodriguez LA, Ellis RJ, Richie CT, Harvey BK, Dannals RF, et al. Chemogenetics revealed: DREADD occupancy and activation via converted clozapine. *Science.* 2017;357(6350):503-7.
64. Vulchanova L, Riedl MS, Shuster SJ, Stone LS, Hargreaves KM, Buell G, Surprenant A, North RA, and Elde R. P2X3 is expressed by DRG neurons that terminate in inner lamina II. *The European journal of neuroscience.* 1998;10(11):3470-8.
65. MacLaren DA, Browne RW, Shaw JK, Krishnan Radhakrishnan S, Khare P, Espana RA, and Clark SD. Clozapine N-Oxide Administration Produces Behavioral Effects in Long-Evans Rats: Implications for Designing DREADD Experiments. *eNeuro.* 2016;3(5).
66. Sciolino NR, Plummer NW, Chen YW, Alexander GM, Robertson SD, Dudek SM, McElligott ZA, and Jensen P. Recombinase-Dependent Mouse Lines for Chemogenetic Activation of Genetically Defined Cell Types. *Cell reports.* 2016;15(11):2563-73.
67. Ossipov MH, Bian D, Malan TP, Jr., Lai J, and Porreca F. Lack of involvement of capsaicin-sensitive primary afferents in nerve-ligation injury induced tactile allodynia in rats. *Pain.* 1999;79(2-3):127-33.
68. Minett MS, Falk S, Santana-Varela S, Bogdanov YD, Nassar MA, Heegaard AM, and Wood JN. Pain without nociceptors? Nav1.7-independent pain mechanisms. *Cell reports.* 2014;6(2):301-12.
69. Liu CN, Wall PD, Ben-Dor E, Michaelis M, Amir R, and Devor M. Tactile allodynia in the absence of C-fiber activation: altered firing properties of DRG neurons following spinal nerve injury. *Pain.* 2000;85(3):503-21.
70. King T, Qu C, Okun A, Mercado R, Ren J, Brion T, Lai J, and Porreca F. Contribution of afferent pathways to nerve injury-induced spontaneous pain and evoked hypersensitivity. *Pain.* 2011;152(9):1997-2005.
71. Abraira VE, and Ginty DD. The sensory neurons of touch. *Neuron.* 2013;79(4):618-39.
72. Li L, Rutlin M, Abraira VE, Cassidy C, Kus L, Gong S, Jankowski MP, Luo W, Heintz N, Koerber HR, et al. The functional organization of cutaneous low-threshold mechanosensory neurons. *Cell.* 2011;147(7):1615-27.
73. Seal RP, Wang X, Guan Y, Raja SN, Woodbury CJ, Basbaum AI, and Edwards RH. Injury-induced mechanical hypersensitivity requires C-low threshold mechanoreceptors. *Nature.* 2009;462(7273):651-5.
74. Boada MD, Martin TJ, Peters CM, Hayashida K, Harris MH, Houle TT, Boyden ES, Eisenach JC, and Ririe DG. Fast-conducting mechanoreceptors contribute to withdrawal behavior in normal and nerve injured rats. *Pain.* 2014;155(12):2646-55.
75. Wang JT, Medress ZA, and Barres BA. Axon degeneration: molecular mechanisms of a self-destruction pathway. *The Journal of cell biology.* 2012;196(1):7-18.
76. Coleman MP, and Perry VH. Axon pathology in neurological disease: a neglected therapeutic target. *Trends in neurosciences.* 2002;25(10):532-7.

908 77. Lehning EJ, Doshi R, Isaksson N, Stys PK, and LoPachin RM, Jr. Mechanisms of injury-
909 induced calcium entry into peripheral nerve myelinated axons: role of reverse sodium-
910 calcium exchange. *Journal of neurochemistry.* 1996;66(2):493-500.
911 78. Persson AK, Hoeijmakers JG, Estacion M, Black JA, and Waxman SG. Sodium
912 Channels, Mitochondria, and Axonal Degeneration in Peripheral Neuropathy. *Trends in*
913 *molecular medicine.* 2016;22(5):377-90.
914 79. Vargas ME, Yamagishi Y, Tessier-Lavigne M, and Sagasti A. Live Imaging of Calcium
915 Dynamics during Axon Degeneration Reveals Two Functionally Distinct Phases of
916 Calcium Influx. *The Journal of neuroscience : the official journal of the Society for*
917 *Neuroscience.* 2015;35(45):15026-38.
918 80. Estacion M, Vohra BP, Liu S, Hoeijmakers J, Faber CG, Merkies IS, Lauria G, Black JA,
919 and Waxman SG. Ca2+ toxicity due to reverse Na+/Ca2+ exchange contributes to
920 degeneration of neurites of DRG neurons induced by a neuropathy-associated Nav1.7
921 mutation. *Journal of neurophysiology.* 2015;114(3):1554-64.
922 81. Cho Y, Sloutsky R, Naegle KM, and Cavalli V. Injury-induced HDAC5 nuclear export is
923 essential for axon regeneration. *Cell.* 2013;155(4):894-908.
924 82. Cho Y, and Cavalli V. HDAC5 is a novel injury-regulated tubulin deacetylase controlling
925 axon regeneration. *The EMBO journal.* 2012;31(14):3063-78.
926 83. Bernardi P, and Rasola A. Calcium and cell death: the mitochondrial connection. *Sub-*
927 *cellular biochemistry.* 2007;45(481-506.
928 84. Rasola A, and Bernardi P. The mitochondrial permeability transition pore and its
929 involvement in cell death and in disease pathogenesis. *Apoptosis : an international*
930 *journal on programmed cell death.* 2007;12(5):815-33.
931 85. Vincent AM, Edwards JL, McLean LL, Hong Y, Cerri F, Lopez I, Quattrini A, and
932 Feldman EL. Mitochondrial biogenesis and fission in axons in cell culture and animal
933 models of diabetic neuropathy. *Acta neuropathologica.* 2010;120(4):477-89.
934 86. Roy Chowdhury SK, Smith DR, Saleh A, Schapansky J, Marquez A, Gomes S, Akude E,
935 Morrow D, Calcutt NA, and Fernyhough P. Impaired adenosine monophosphate-
936 activated protein kinase signalling in dorsal root ganglia neurons is linked to
937 mitochondrial dysfunction and peripheral neuropathy in diabetes. *Brain : a journal of*
938 *neurology.* 2012;135(Pt 6):1751-66.
939 87. Chowdhury SK, Zherebitskaya E, Smith DR, Akude E, Chattopadhyay S, Jolivalt CG,
940 Calcutt NA, and Fernyhough P. Mitochondrial respiratory chain dysfunction in dorsal
941 root ganglia of streptozotocin-induced diabetic rats and its correction by insulin
942 treatment. *Diabetes.* 2010;59(4):1082-91.
943 88. Zhu H, and Roth BL. DREADD: a chemogenetic GPCR signaling platform. *The*
944 *international journal of neuropsychopharmacology / official scientific journal of the*
945 *Collegium Internationale Neuropsychopharmacologicum.* 2014;18(1).
946 89. Saloman JL, Scheff NN, Snyder LM, Ross SE, Davis BM, and Gold MS. Gi-DREADD
947 Expression in Peripheral Nerves Produces Ligand-Dependent Analgesia, as well as
948 Ligand-Independent Functional Changes in Sensory Neurons. *The Journal of*
949 *neuroscience : the official journal of the Society for Neuroscience.* 2016;36(42):10769-
950 81.
951 90. Dib-Hajj SD, Yang Y, Black JA, and Waxman SG. The Na(V)1.7 sodium channel: from
952 molecule to man. *Nature reviews Neuroscience.* 2013;14(1):49-62.

953 91. Eijkelkamp N, Linley JE, Baker MD, Minett MS, Cregg R, Werdehausen R, Rugiero F,
954 and Wood JN. Neurological perspectives on voltage-gated sodium channels. *Brain : a*
955 *journal of neurology.* 2012;135(Pt 9):2585-612.
956 92. Wainger BJ, Kiskinis E, Mellin C, Wiskow O, Han SS, Sandoe J, Perez NP, Williams
957 LA, Lee S, Boulting G, et al. Intrinsic membrane hyperexcitability of amyotrophic lateral
958 sclerosis patient-derived motor neurons. *Cell reports.* 2014;7(1):1-11.
959 93. Lieberman OJ, Choi SJ, Kanter E, Saverchenko A, Frier MD, Fiore GM, Wu M,
960 Kondapalli J, Zampese E, Surmeier DJ, et al. alpha-Synuclein-Dependent Calcium Entry
961 Underlies Differential Sensitivity of Cultured SN and VTA Dopaminergic Neurons to a
962 Parkinsonian Neurotoxin. *eNeuro.* 2017;4(6).
963 94. Fenner D, Odili S, Hong HK, Kobayashi Y, Kohsaka A, Siepka SM, Vitaterna MH, Chen
964 P, Zelent B, Grimsby J, et al. Generation of N-ethyl-N-nitrosourea (ENU) diabetes
965 models in mice demonstrates genotype-specific action of glucokinase activators. *The*
966 *Journal of biological chemistry.* 2011;286(45):39560-72.
967 95. Cummins TR, Dib-Hajj SD, Black JA, Akopian AN, Wood JN, and Waxman SG. A
968 novel persistent tetrodotoxin-resistant sodium current in SNS-null and wild-type small
969 primary sensory neurons. *The Journal of neuroscience : the official journal of the Society*
970 *for Neuroscience.* 1999;19(24):RC43.

971

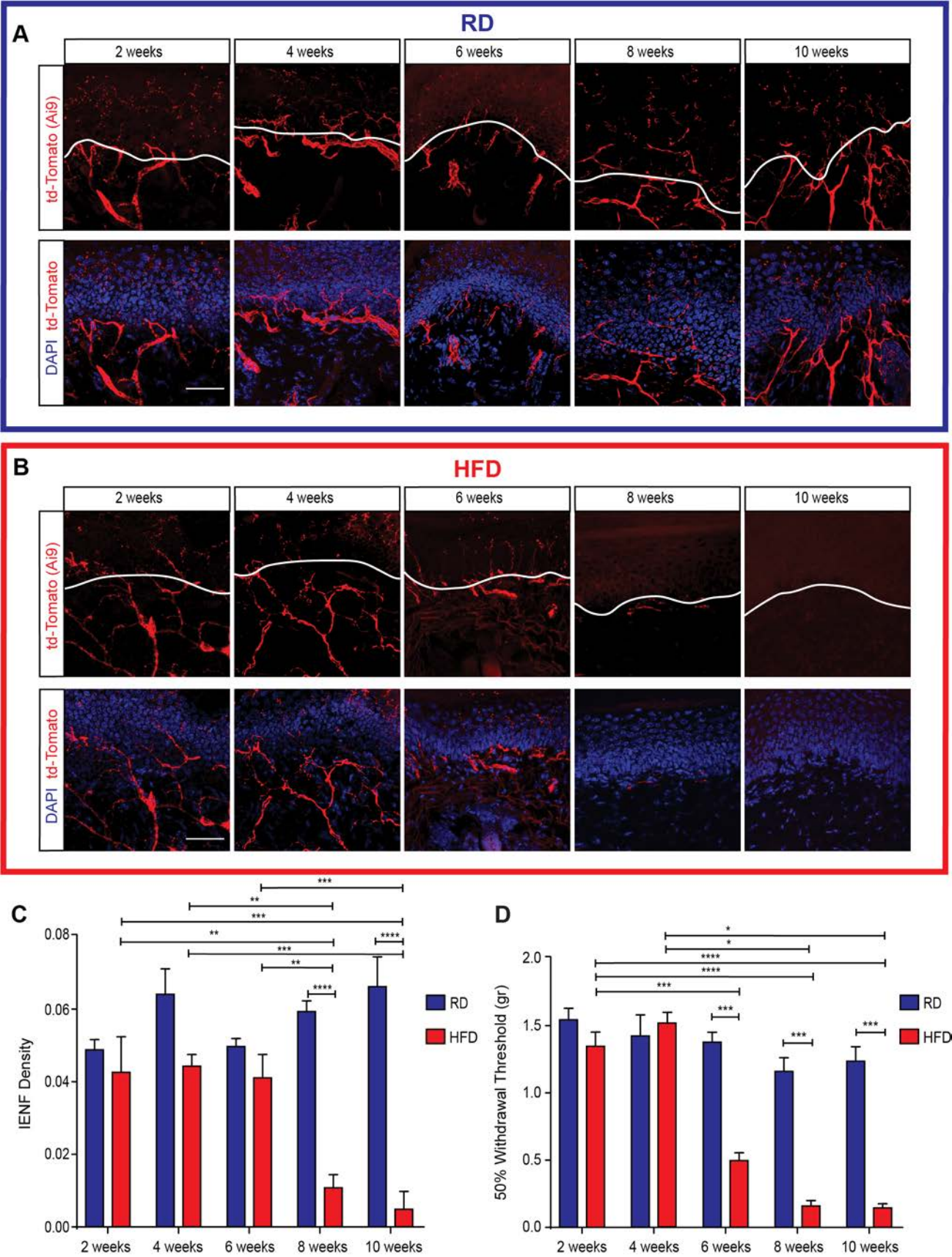
A
RD
2 weeks
4 weeks
6 weeks
8 weeks
10 weeks
td-Tomato (Ai9)
DAPI td-Tomato
B
HFD
2 weeks
4 weeks
6 weeks
8 weeks
10 weeks
td-Tomato (Ai9)
DAPI td-Tomato
C
IENF Density
0.08
0.06
0.04
0.02
0.00
2 weeks
4 weeks
6 weeks
8 weeks
10 weeks
RD
HFD
D
50% Withdrawal Threshold (gr)
2.0
1.5
1.0
0.5
0.0
2 weeks
4 weeks
6 weeks
8 weeks
10 weeks
RD
HFD

Figure 1. Onset of small-fiber degeneration and mechanical allodynia in mice fed a high-fat diet. (**A**). Confocal analysis of skin sections from $Na_v1.8$-Cre;Ai9 mice fed a regular diet (RD, **blue**) showed normal innervation. $Na_v1.8$-positive fibers genetically labeled with td-Tomato are visualized in red. Sections were stained with a nuclear marker (DAPI, blue staining). (**B**) Skin sections from diabetic $Na_v1.8$-Cre;Ai9 mice (HFD, **red**) showing decreased innervation commencing 8 weeks after the start of the diet. (Scale bar=50μm). (**C**) This effect was quantified using intra-epidermal nerve density (IENF density) and the epidermal-dermal junction is outlined in white. (**, $p<0.01$, ***, $p<0.001$, ****, $p<0.0001$) (n=6 for all groups with 3 non-contiguous sections analyzed per sample). (**D**) von Frey testing demonstrated onset of mechanical allodynia in diabetic $Na_v1.8$-Cre;Ai9 mice after 6 weeks on HFD but not in RD mice (*, $p<0.05$, ***, $p<0.001$, ****, $p<0.0001$) (n=7/group). Values are expressed as mean ± S.E.M. p-values were calculated using two-way ANOVA, Bonferroni multiple comparison test.

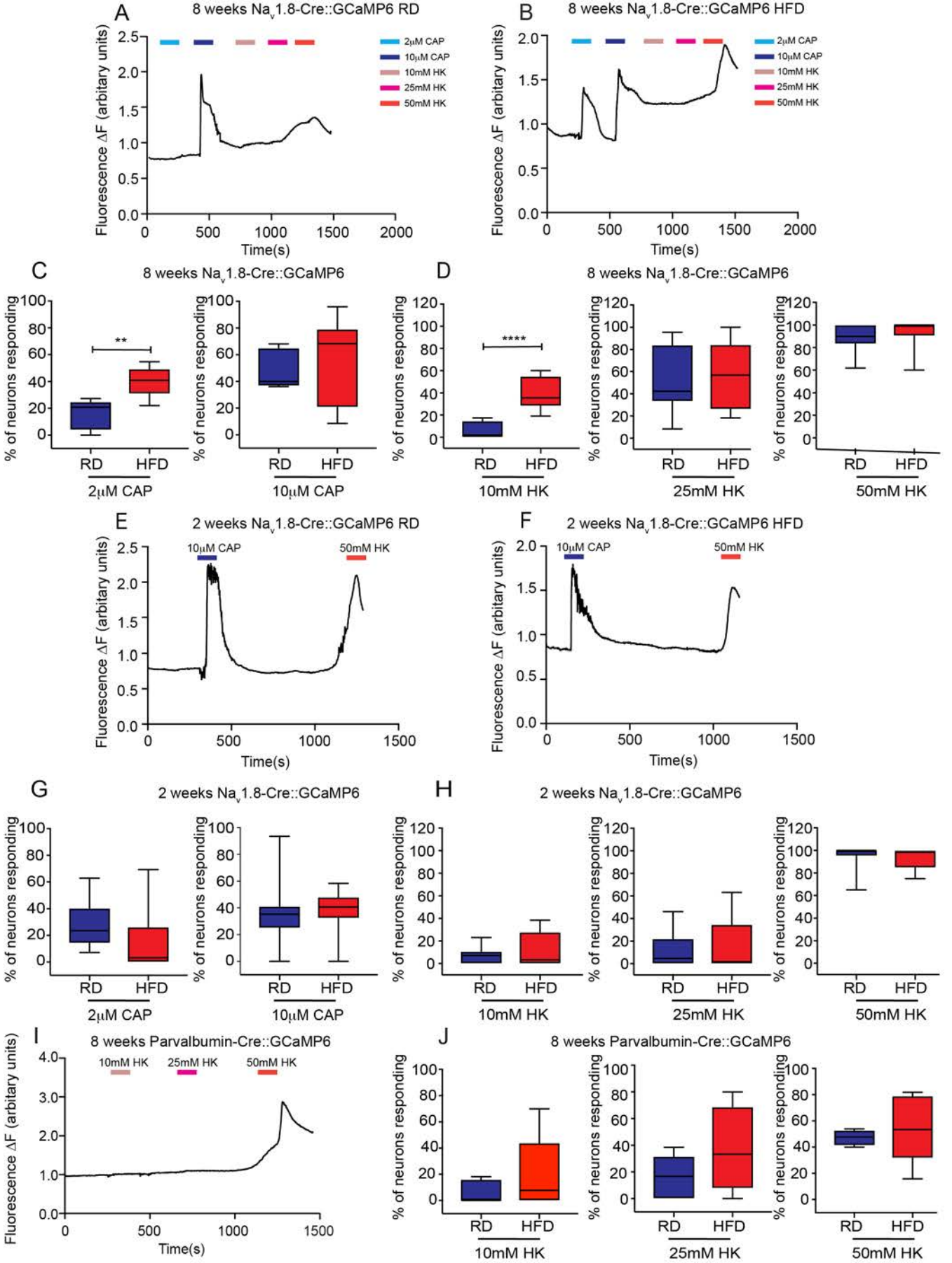
A
8 weeks Nav1.8-Cre::GCaMP6 RD
2μM CAP
10μM CAP
10mM HK
25mM HK
50mM HK
Fluorescence ΔF (arbitary units)
Time(s)
B
8 weeks Nav1.8-Cre::GCaMP6 HFD
C
8 weeks Nav1.8-Cre::GCaMP6
% of neurons responding
RD
HFD
2μM CAP
10μM CAP
D
10mM HK
25mM HK
50mM HK
E
2 weeks Nav1.8-Cre::GCaMP6 RD
F
2 weeks Nav1.8-Cre::GCaMP6 HFD
G
2 weeks Nav1.8-Cre::GCaMP6
H
I
8 weeks Parvalbumin-Cre::GCaMP6
J

Figure 2. $Na_v1.8$-positive DRG neurons displayed increased $[Ca^{2+}]i$ in mice fed a high-fat diet. (A, B) Representative traces of $[Ca^{2+}]i$ in acutely excised explants from $Na_v1.8$-Cre;GCaMP6 mice after 8 weeks on (**A**) RD or (**B**) HFD. The number of $Na_v1.8$-positive neurons was quantified to assess the response to either (**C**) 2μM or 10μM capsaicin (**, $p<0.01$) (RD n=381 neurons, 11 explant; HFD n=519 neurons, 17 explants) or (**D**) 10mM, 25mM or 50mM high potassium buffer (HK) (****, $p<0.0001$) (RD n=381 neurons, 11 explants; HFD n=519 neurons, 17 explants). Capsaicin- or HK-responsive DRG neurons are reported as a percentage of total neurons that responded to 50mM HK. (**E, F**) These same experiments were performed at 2 weeks on (**E**) RD or (**F**) HFD. (**G, H**) No difference was found in the number of neurons responding to (**G**) capsaicin or (**H**) high potassium buffer (RD n=381 neurons, 11 explants; HFD n=231 neurons, 10 explants). (**I, J**) In DRG explants from parvalbumin-Cre;GCaMP6 mice, there were no significant differences between RD and HFD after eight weeks (RD n=88 neurons, 6 explants; HFD n=118 neurons, 9 explants). Values are expressed as mean ± S.E.M. p-values were calculated using by Mann-Whitney test.

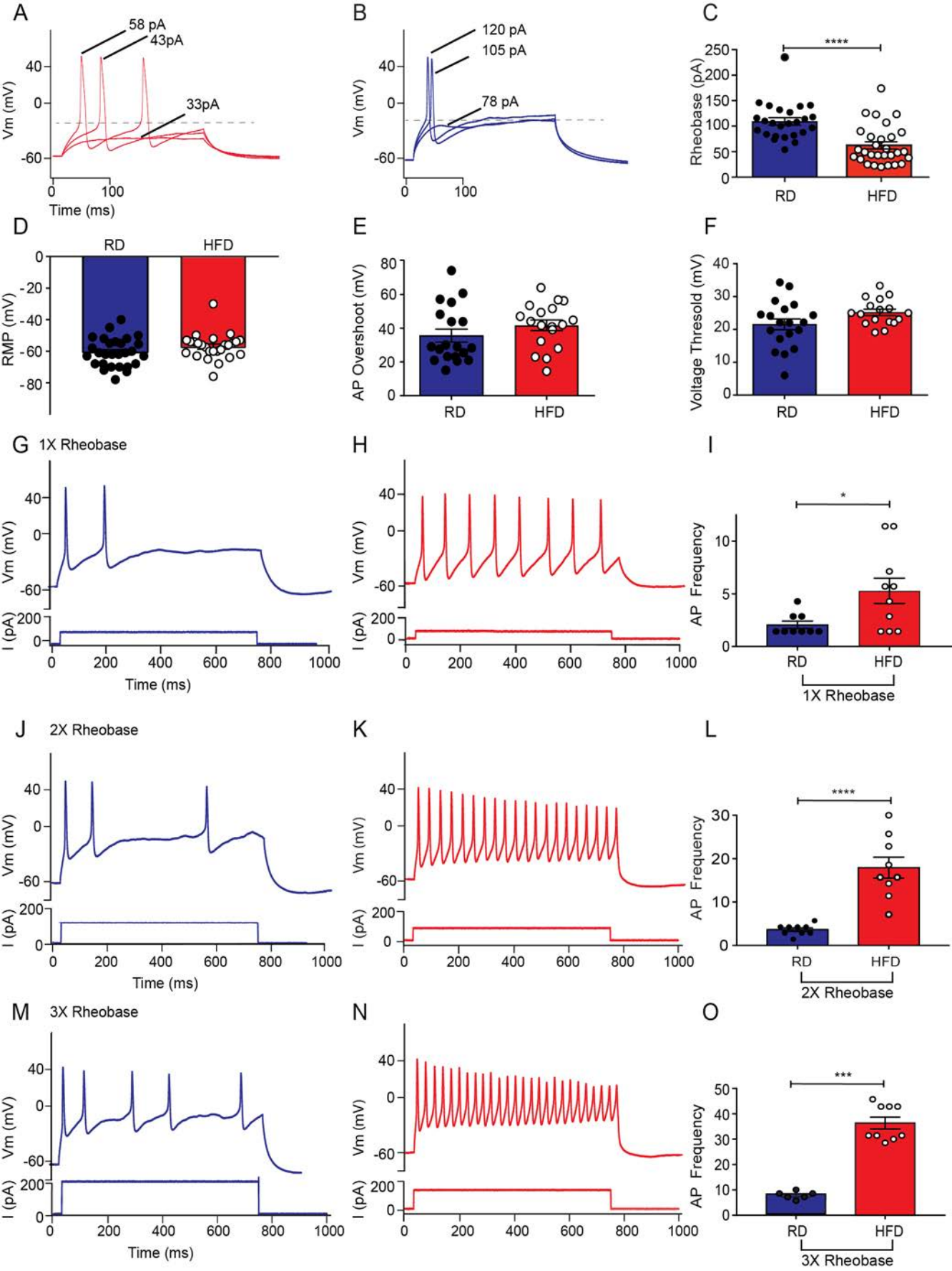
A
58 pA
43pA
33pA
Vm (mV)
Time (ms)
B
120 pA
105 pA
78 pA
Vm (mV)
C
Rheobase (pA)
****
RD
HFD
D
RD
HFD
RMP (mV)
E
AP Overshoot (mV)
RD
HFD
F
Voltage Thresold (mV)
RD
HFD
G 1X Rheobase
Vm (mV)
I (pA)
Time (ms)
H
Vm (mV)
I (pA)
I
AP Frequency
*
RD
HFD
1X Rheobase
J 2X Rheobase
Vm (mV)
I (pA)
Time (ms)
K
Vm (mV)
I (pA)
L
AP Frequency
****
RD
HFD
2X Rheobase
M 3X Rheobase
Vm (mV)
I (pA)
Time (ms)
N
Vm (mV)
I (pA)
O
AP Frequency
***
RD
HFD
3X Rheobase

Figure 3. Na_v1.8-positive DRG neurons displayed hyperexcitability in mice fed a high-fat diet. (**A, B**) Current-clamp recordings of DRG primary cultures from Na_v1.8-Cre;Ai9 mice. Na_v1.8-positive DRG neurons from HFD mice (**A**, **red**) (n=29) exhibited a lower rheobase compared to neurons from RD mice (**B**, **blue)** (n=25). (**C**) A significant decrease in rheobase was observed in HFD neurons (****, $p<0.0001$). (**D**) Resting membrane potentials (RPM), (**E**) action potential (AP) overshoot, and (**F**) voltage threshold for action-potential generation remained unchanged. (**G-O**) Representative current steps and associated voltage recordings are displayed for RD (blue) or HFD (red) DRG neurons where (**G, H**) 1X rheobase current (n=9; n=10), (**J, K**) 2X (n=9; n=9) or (**M, N**) 3X (n=6; n=9) was injected for 700 milliseconds. (**H, K and N**) There was an increase of frequency of firing in HFD neurons compared to (**G, J and M**) neurons from RD mice. There was a significant increase in the firing frequency in HFD DRGs compared to RD DRGs after (**I**) 1X (*, $p<0.05$), (**L**) 2X (****, $p<0.0001$), and (**O**) 3X (***, $p<0.001$) rheobase current injections respectively. Values are expressed as mean ± S.E.M. p-values were calculated using Mann-Whitney test.

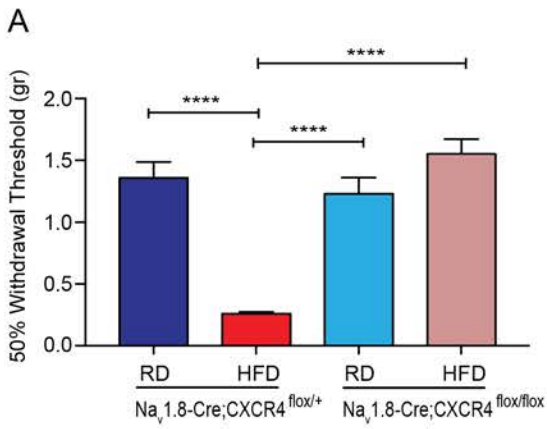
A
50% Withdrawal Threshold (gr)
2.0
1.5
1.0
0.5
0.0
****
****
****
RD
HFD
RD
HFD
Nav1.8-Cre;CXCR4 flox/+
Nav1.8-Cre;CXCR4 flox/flox

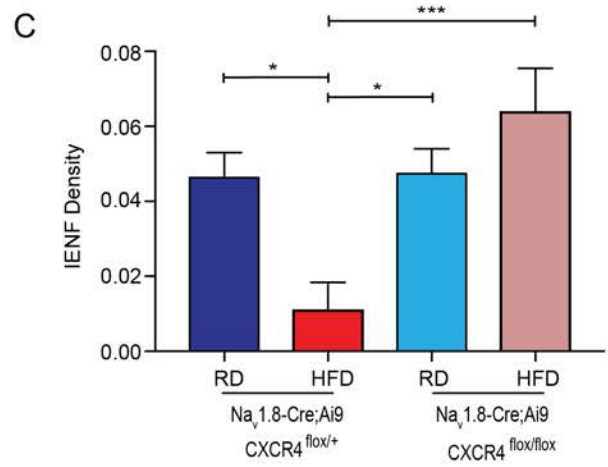
C
IENF Density
0.08
0.06
0.04
0.02
0.00
*
*
***
RD
HFD
RD
HFD
Nav1.8-Cre;Ai9
CXCR4 flox/+
Nav1.8-Cre;Ai9
CXCR4 flox/flox

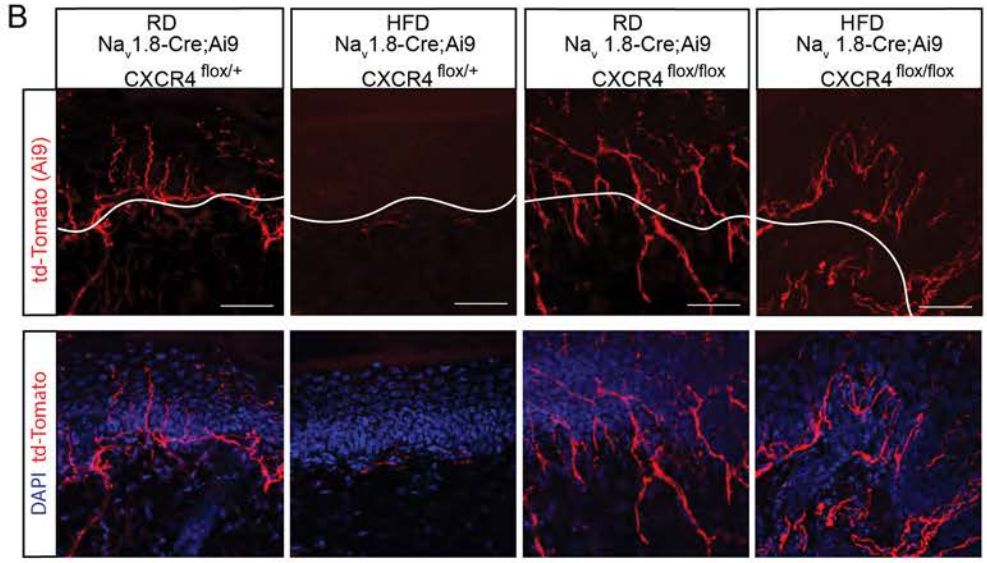
B
RD
Nav1.8-Cre;Ai9
CXCR4 flox/+
HFD
Nav1.8-Cre;Ai9
CXCR4 flox/+
RD
Nav 1.8-Cre;Ai9
CXCR4 flox/flox
HFD
Nav 1.8-Cre;Ai9
CXCR4 flox/flox
td-Tomato (Ai9)
DAPI td-Tomato

Figure 4. Selective chemokine receptor CXCR4 deletion from Na_v1.8-postive DRG neurons prevented the development of mechanical allodynia and small-fiber degeneration in HFD-induced PDN. (**A**) von Frey testing demonstrated that in HFD (red) Na_v1.8-Cre;Ai9;CXCR4$^{flox/+}$, which had a heterozygous deletion of CXCR4 from Na_v1.8-postive DRG neurons, the withdrawal threshold was significantly reduced compared to Na_v1.8-Cre;Ai9;CXCR4$^{flox/+}$ mice on RD (**dark blue**) and to mice with a homozygous deletion of CXCR4 (Na_v1.8-Cre;Ai9;CXCR4$^{flox/flox}$) on RD **(light blue).** In contrast, Na_v1.8-Cre;Ai9;CXCR4$^{flox/flox}$ **(pink)** mice on HFD showed normalization of the withdrawal thresholds (****, $p<0.0001$) (n=6/group). (**B**) Confocal analysis of skin from mice with both heterozygous and homozygous deletions of CXCR4 from Na_v1.8-postive DRG neurons on either RD or HFD showing td-Tomato (**red**), and merged images with the nuclear marker DAPI (**blue**). Na_v1.8-Cre;Ai9;CXCR4$^{flox/+}$ RD mice had normal skin innervation whereas the same mice on HFD had reduced innervation. However, selective homozygous deletion of CXCR4 for mice on HFD prevented small-fiber degeneration. Scale bar=50μm. (**C**) This effect was quantified using intra-epidermal nerve density (IENF density) and the epidermal-dermal junction is outlined in white (*, $p<0.05$, ***, $p<0.001$) (n=7 for all groups with 3 non-contiguous sections analyzed per sample). Values are expressed as mean $\pm$ S.E.M. p-values were calculated using one-way ANOVA, Bonferroni mutliple comparison test.

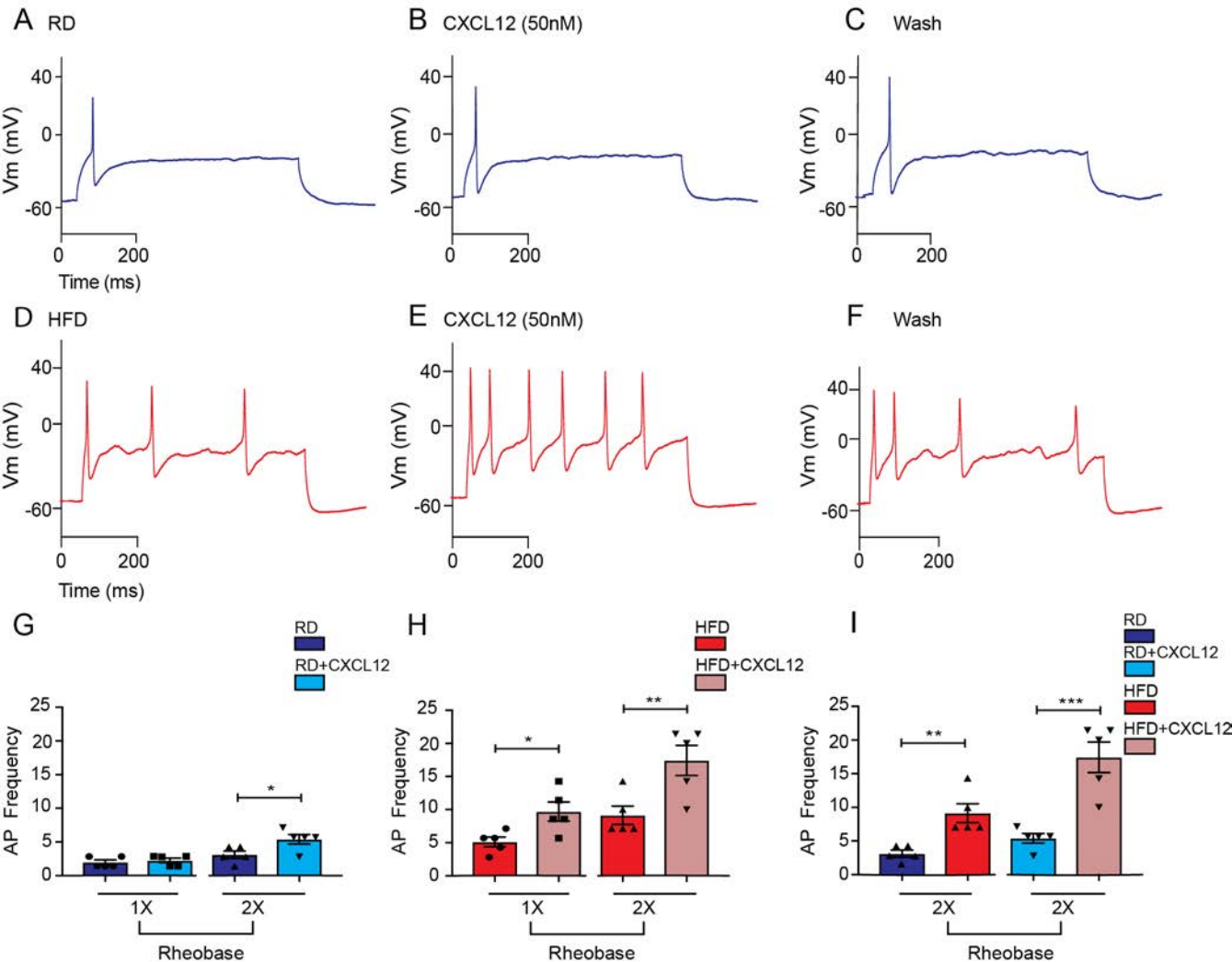
A RD
B CXCL12 (50nM)
C Wash
D HFD
E CXCL12 (50nM)
F Wash
Vm (mV)
40
0
-60
0
200
Time (ms)
G
H
I
RD
RD+CXCL12
HFD
HFD+CXCL12
AP Frequency
25
20
15
10
5
0
*
**
***
1X
2X
Rheobase

Figure 5. CXCL12/CXCR4 signaling produced increased firing frequencies in HFD-induced diabetic Na_v1.8-positive DRG neurons. (**A**) Current clamp recordings of DRG primary cultures from Na_v1.8-Cre;Ai9 mice. A typical illustration of action potentials generated using depolarizing current injection from a RD Na_v1.8-positive DRG neuron (**blue**) in response to a 700 milliseconds (ms) input of 1X rheobase current injection from the resting membrane potential (V_m) (-57 mV). (**B**) Application of CXCL12 (50 nM) produced no change in firing of this neuron after current injection. (**C**) Results after a 5 minute wash. (**D**) Representative traces from a diabetic HFD fed Na_v1.8-positive DRG neuron (**red**) firing multiple action potentials in response to a 700 ms input of 1X rheobase depolarizing current injections. (**E, F**) An increase in firing frequency of HFD Na_v1.8-positive neurons was observed after (**E**) CXCL12 (50nM) application and (**F**) after wash. (**G, I**) The frequency of firing for each of these treatments was quantified. (**G**) A significant increase in action potential (AP) frequency occurred after CXCL12 treatment in 2X rheobase current pulses in RD Na_v1.8-positive DRG neurons (*, $p<0.05$) (n=5). (**H**) Significant increases in frequency observed after CXCL12 in HFD Na_v1.8-positive DRG neurons (**red**) after 1X and 2X rheobase depolarizing current injections from the resting membrane potentials are presented (*, $p<0.05$, **, $p<0.01$) (n=5/group). (**I**) A comparison between RD and HFD after CXCL12 application showed significant increases in AP frequency in HFD (**, $p<0.01$, ***, $p<0.001$) (n=5/group). Values are expressed as mean ± S.E.M. p-values were calculated using Mann-Whitney test.

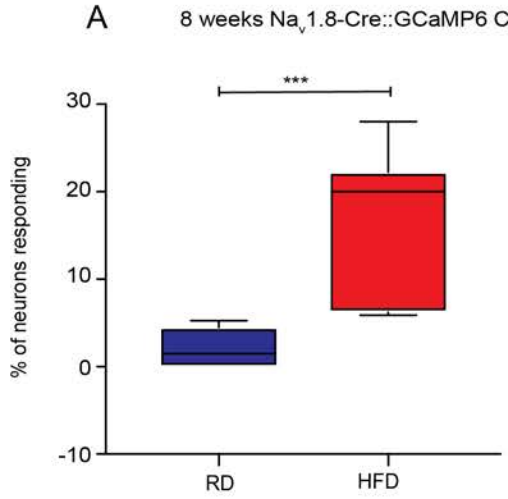
A
8 weeks Nav1.8-Cre::GCaMP6 CXCL12
***
% of neurons responding
30
20
10
0
-10
RD
HFD

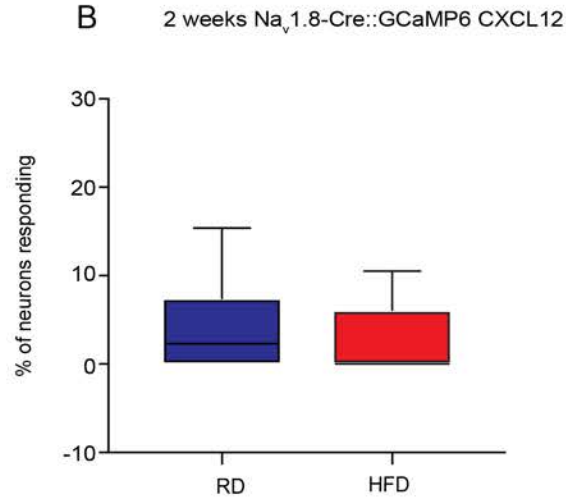
B
2 weeks Nav1.8-Cre::GCaMP6 CXCL12
% of neurons responding
30
20
10
0
-10
RD
HFD

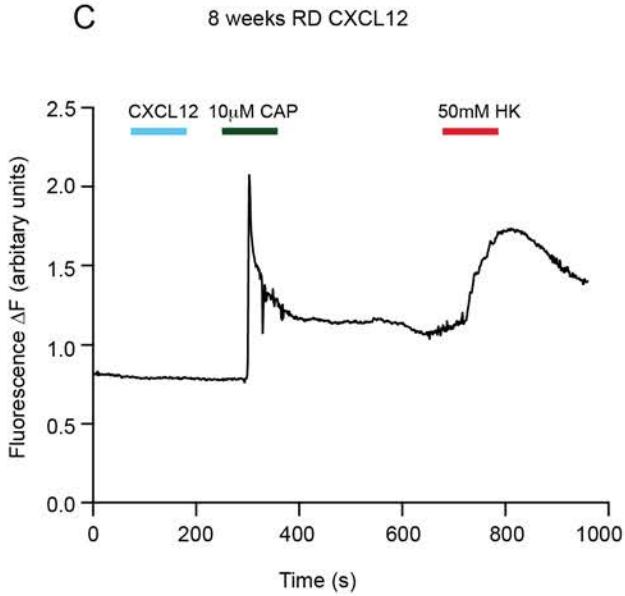
C
8 weeks RD CXCL12
CXCL12
10μM CAP
50mM HK
Fluorescence ΔF (arbitary units)
2.5
2.0
1.5
1.0
0.5
0.0
0
200
400
600
800
1000
Time (s)

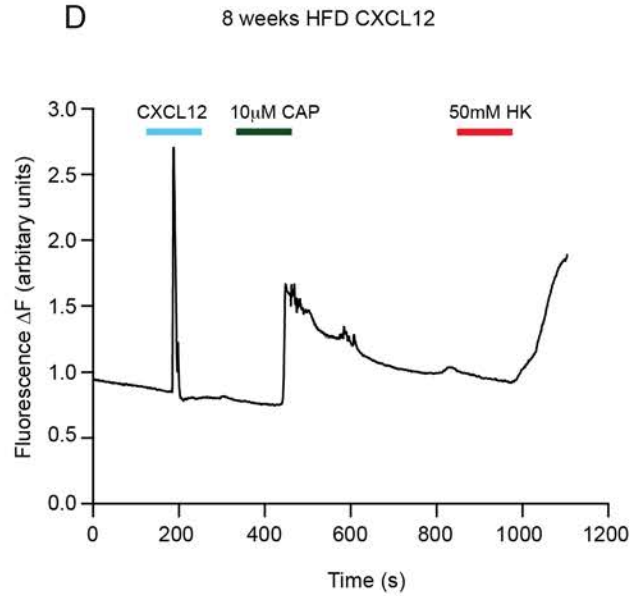
D
8 weeks HFD CXCL12
CXCL12
10μM CAP
50mM HK
Fluorescence ΔF (arbitary units)
3.0
2.5
2.0
1.5
1.0
0.5
0.0
0
200
400
600
800
1000
1200
Time (s)

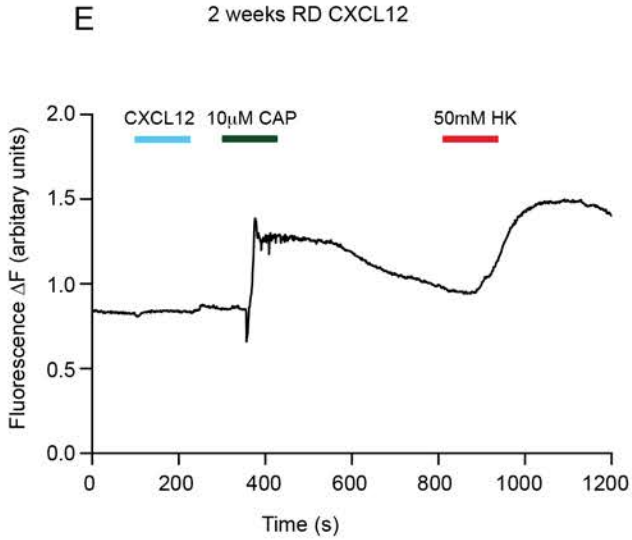
E
2 weeks RD CXCL12
CXCL12
10μM CAP
50mM HK
Fluorescence ΔF (arbitary units)
2.0
1.5
1.0
0.5
0.0
0
200
400
600
800
1000
1200
Time (s)

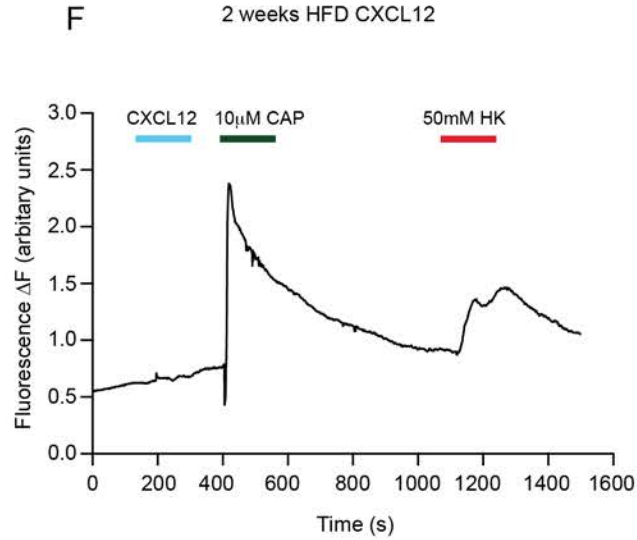
F
2 weeks HFD CXCL12
CXCL12
10μM CAP
50mM HK
Fluorescence ΔF (arbitary units)
3.0
2.5
2.0
1.5
1.0
0.5
0.0
0
200
400
600
800
1000
1200
1400
1600
Time (s)

Figure 6. CXCR4 activation produced more frequent calcium responses in Na_v1.8-positive DRG neurons from mice on HFD. (**A, B**) $[Ca^{2+}]$i responses of acutely excised DRG explants from RD (**blue**) and HFD (**red**) Na_v1.8-Cre;GCaMP6 mice at 8 **(A)** and 2 (**B)** weeks after starting the diet. A significantly higher number of Na_v1.8-positive DRG neurons responded with increased $[Ca^{2+}]_i$ after application of CXCL12 (100nM) when mice had been on a HFD for 8 weeks compared with mice fed with RD **(A).** Data is shown as capsaicin or HK responsive DRG neurons as a percentage of total neurons that responded to 50mM HK. (***, $p<0.001$) (RD n=333 neurons; 13 explants; HFD =519 neurons, 17 explants). (**C-F**) Representative traces of $[Ca^{2+}]$i transients in DRG explants from Na_v1.8-Cre;GCaMP6 mice. Explants were treated with capsaicin (CAP 10μM) and high potassium buffer (HK 50mM). (**C, D)** After 8 weeks on HFD more neurons responded to CXCL12 than on RD (**E, F**) Experiments were performed after 2 weeks on RD or HFD and showed no difference in response to CXCL12 (RD n=381 neurons, 11 explants; HFD n=231 neurons, 10 explants). Values are expressed as mean $\pm$ S.E.M. p-values were calculated using Mann-Whitney test.

A

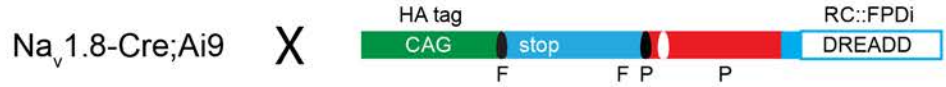
Na$_v$1.8-Cre;Ai9
X
HA tag
CAG
stop
F
F P
P
RC::FPDi
DREADD

B

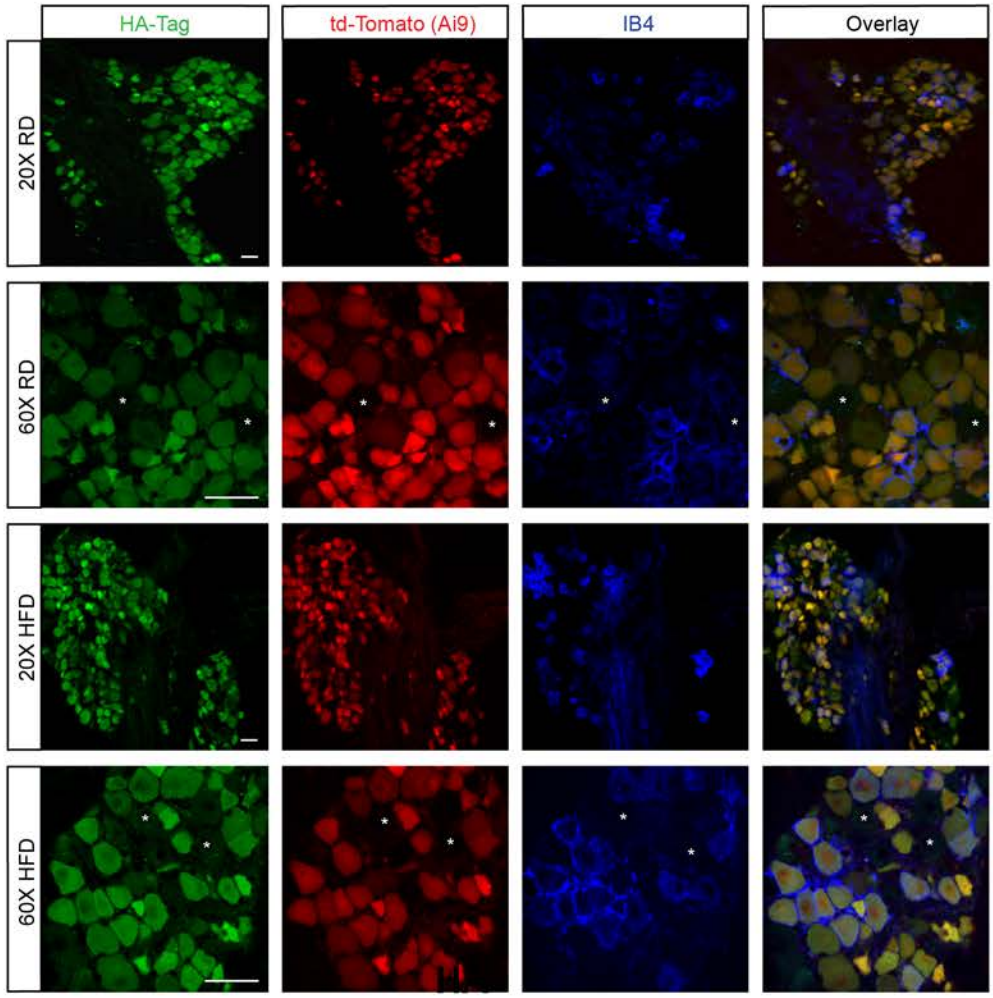
HA-Tag
td-Tomato (Ai9)
IB4
Overlay
20X RD
60X RD
20X HFD
60X HFD

C

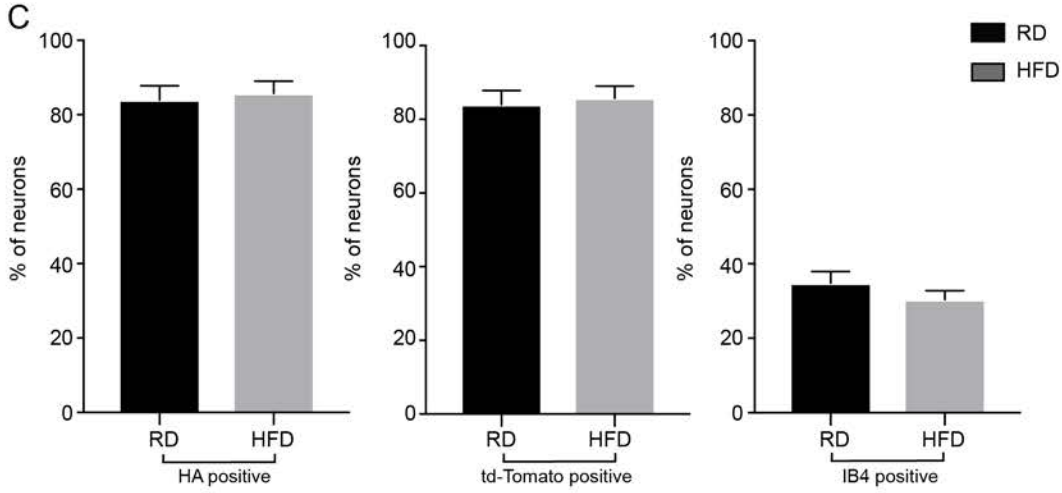
RD
HFD
% of neurons
100
80
60
40
20
0
RD
HFD
HA positive
td-Tomato positive
IB4 positive

Figure 7. Expression of inhibitory DREADD receptor PDi in Na_v1.8-positive DRG neurons. (A) Breeding scheme and genetic constructs used to generate the Na_v1.8-Cre;Ai9;RC::PDi inhibitory DREADD mice; the inhibitory PDi DREADD receptor (PDi DREADDs) has an HA-tag and Na_v1.8-positive DRG neurons are genetically labeled in red with td-Tomato. (**B**) Confocal micrographs of DRGs from RD **(top**) and HFD (**bottom**) PDi DREADD mice (Na_v1.8-Cre;Ai9;RC::PDi). These images show PDi DREADDs tagged with an HA epitope (**green**), Na_v1.8 td-Tomato expressing neurons (**red**) and IB4 positive neurons (**blue**). PDi DREADDs were found in small and medium diameter DRG neurons some of which were IB4 positive and some were IB4 negative. Large diameter neurons (*) did not express PDi DREADDs. Scale bar=50μm. (**C**) The percentage of PDi DREADDs expressing neurons as determined by the HA tag, td-Tomato Na_v1.8 neurons, non-peptidergic IB4 positive neurons were quantified. RD DRGs had 83.9±3.4% HA or td-Tomato positive neurons whereas HFD DRGs had 85.7±3.8% HA or td-Tomato. RD DRGs had 34.8±3.2% IB4 positive neurons whereas HFD DRGs had 35.4±2.4%. There were no significant differences in the sizes of these populations between DRGs from RD and HFD PDi DREADDs expressing mice (n=278 neurons (RD); n=227 (HFD)). Values are expressed as mean ± S.E.M. p-values were calculated using Mann-Whitney test.

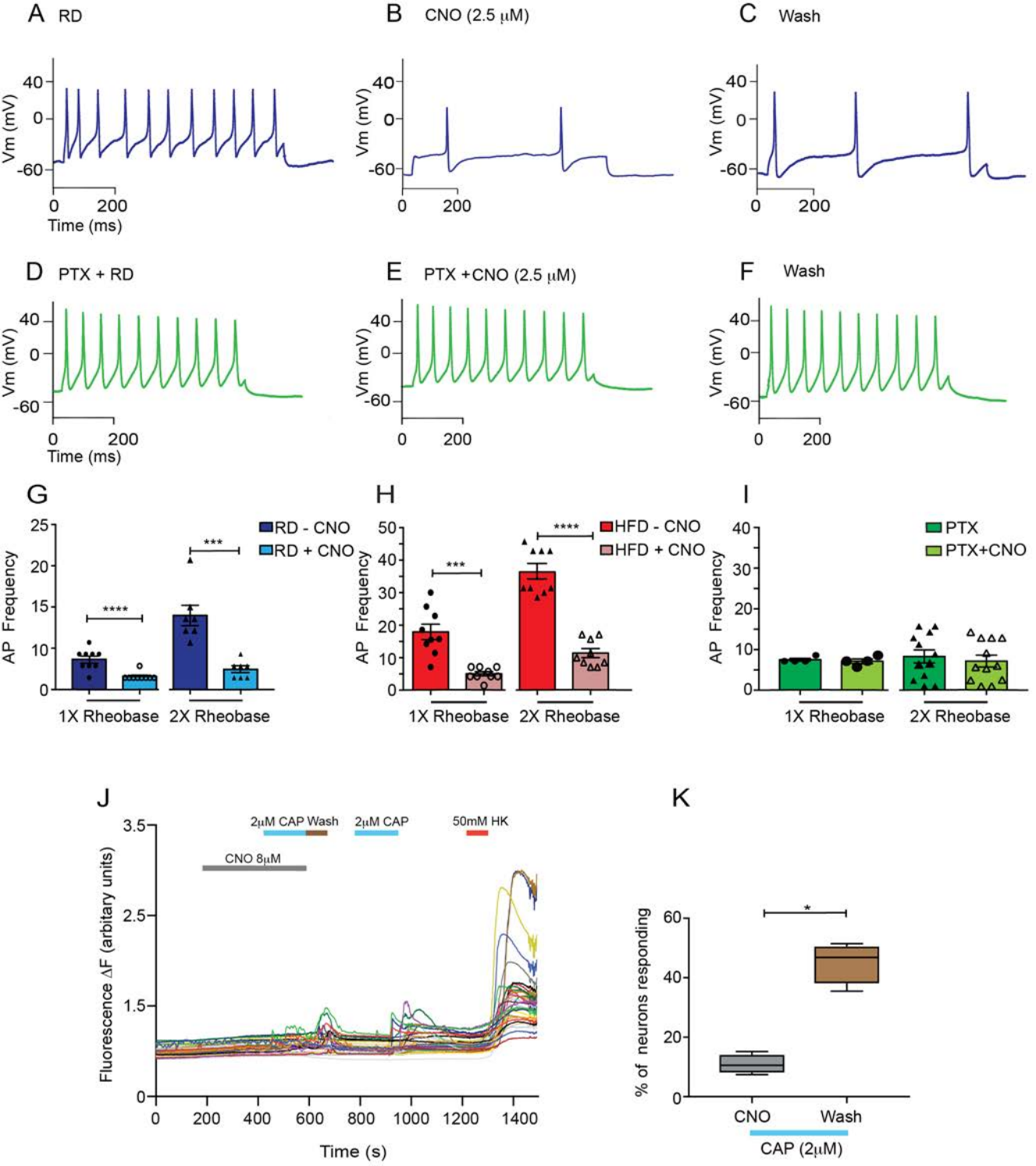
A RD
B CNO (2.5 μM)
C Wash
D PTX + RD
E PTX +CNO (2.5 μM)
F Wash
Vm (mV)
Time (ms)
G
H
I
AP Frequency
RD - CNO
RD + CNO
HFD - CNO
HFD + CNO
PTX
PTX+CNO
1X Rheobase
2X Rheobase
J
2μM CAP Wash
2μM CAP
50mM HK
CNO 8μM
Fluorescence ΔF (arbitary units)
Time (s)
K
% of neurons responding
CNO
Wash
CAP (2μM)

Figure 8. Chemogenetic inhibition of Na_v1.8-positive DRG neurons expressing the inhibitory DREADD receptor PDi is G-protein mediated. (**A**) Current clamp recordings from inhibitory PDi expressing Na_v1.8-positive neurons in primary cultures isolated from Na_v1.8-Cre;Ai9;RC::PDi fed a RD **(blue).** (**B**) Application of CNO (2.5μM) reduced the action potential (AP) frequency and (**C**) washing out the CNO partially restored the firing rate. (**D-F**) Overnight incubation of RD DRG cultures with pertussis toxin (PTX, **green**) abolished the inhibitory effect of CNO. (**G**) In RD Na_v1.8-positive DRG neurons expressing DREADD receptors there was a significant decrease in action potential frequency after application of CNO at both 1X and 2X rheobase (***, $p<0.001$, ****, $p<0.0001$) (n=7, 9 respectively). (**H**) The same mice fed HFD also showed a decrease in AP frequency after application of CNO (***, $p<0.001$, ****, $p<0.0001$) (n=9 for both groups). (**I**) Overnight incubation of DRG cultures with pertussis toxin abolished the inhibitory effects of CNO. There was no difference in AP frequency after preincubation with PTX and application of CNO at either 1X or 2X rheobase (n=4, 12 respectively). (**J**) $[Ca^{2+}]i$ responses in DRG explants from Na_v1.8 Cre;RC::PDi;GCaMP6 mice, showed that $[Ca^{2+}]i$ responses after addition of capsaicin (CAP 2μM) were inhibited during incubation with CNO (8μM for 5 minutes). After washing, Na_v1.8-positive DRG neurons showed restored $[Ca^{2+}]i$ transients to capsaicin (CAP 2μM) and high potassium buffer (HK 10mM) (n=120 neurons; 10 explants). (**K**) The responses to lower concentrations of capsaicin were quantified as the responses to capsaicin as a percentage of total HK responsive neurons. (*, $p<0.05$). Values are expressed as mean ± S.E.M. p-values were calculated by Mann-Whitney test.

A

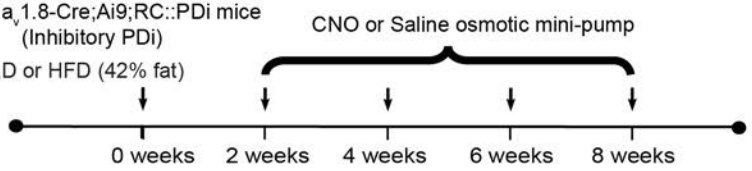
Na$_v$1.8-Cre;Ai9;RC::PDi mice
(Inhibitory PDi)
RD or HFD (42% fat)
CNO or Saline osmotic mini-pump
0 weeks
2 weeks
4 weeks
6 weeks
8 weeks

B

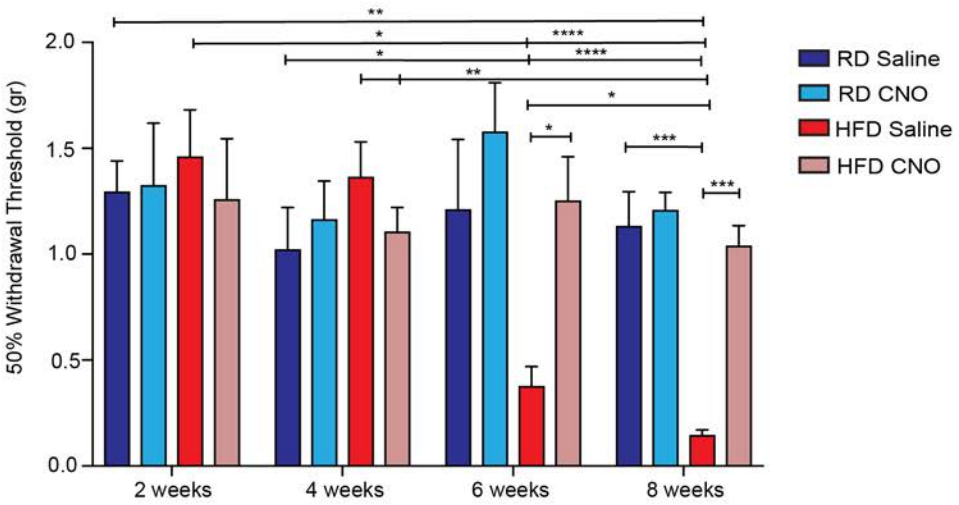
50% Withdrawal Threshold (gr)
2.0
1.5
1.0
0.5
0.0
2 weeks
4 weeks
6 weeks
8 weeks
RD Saline
RD CNO
HFD Saline
HFD CNO
**
*
****
*
****
**
*
*
***
***

C

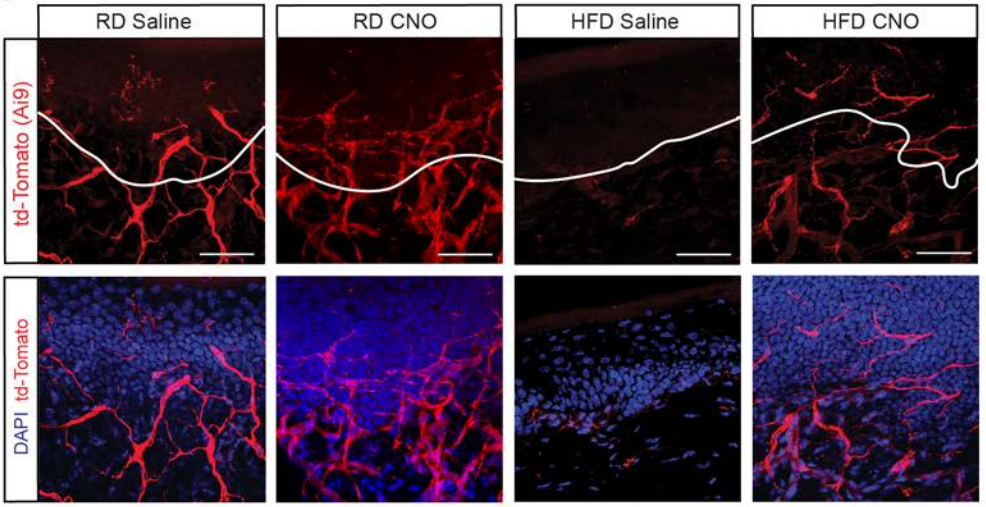
RD Saline
RD CNO
HFD Saline
HFD CNO
td-Tomato (Ai9)
DAPI td-Tomato

D

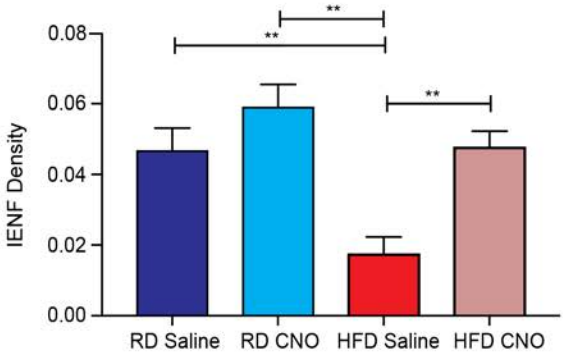
IENF Density
0.08
0.06
0.04
0.02
0.00
**
**
**
RD Saline
RD CNO
HFD Saline
HFD CNO

Figure 9. Long-term chemogenetic inhibition of Na_v1.8-positive DRG neurons prevented mechanical allodynia and small-fiber degeneration in HFD fed mice. (**A**) Na_v1.8-Cre;Ai9;RC::PDi mice were fitted with osmotic mini-pumps i.p. infusing either CNO (10mg/kg/day) or saline between 2-8 weeks of either RD or HFD. Each arrow represents a time point where pain behavior was assessed. (**B**) von Frey testing was performed on Na_v1.8-Cre;Ai9;RC::PDi mice at 2, 4, 6, and 8 weeks after implantation of an osmotic mini-pump intraperitoneally (i.p.) that delivered CNO (10mg/kg/day) or saline to RD or HFD fed mice. Mice on HFD showed a reduced withdrawal threshold starting at 6 weeks, which was reversed following CNO treatment (*, $p<0.05$, **, $p<0.01$, ***, $p<0.001$, ****, $p<0.0001$) (n=9/group). (**C**) Confocal micrographs of skin from these mice show td-Tomato in the Na_v1.8 fibers (**red**) and merged images with the nuclear marker DAPI (**blue**). Mice on RD given either saline or CNO showed normal skin innervation. In diabetic HFD mice given saline there was a reduction in skin innervation, but it was reversed for mice on HFD given CNO. Scale bar=50μm. (**D**) This effect was quantified using intra-epidermal nerve density (IENF density) and the epidermal-dermal junction is outlined in white-showing that CNO infusion prevented small-fiber degeneration of mice on HFD (**, $p<0.01$) (n=6/group with 3 non-continuous sections analyzed per sample). Values are expressed as mean $\pm$ SEM. p-values were calculated using two-way ANOVA, Bonferroni multiple comparison test.

A

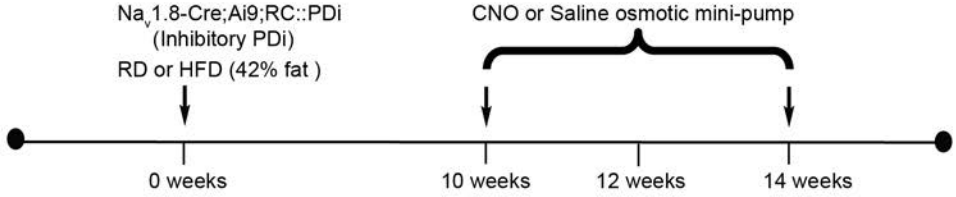
Na$_v$1.8-Cre;Ai9;RC::PDi
(Inhibitory PDi)
RD or HFD (42% fat)
CNO or Saline osmotic mini-pump
0 weeks
10 weeks
12 weeks
14 weeks

B

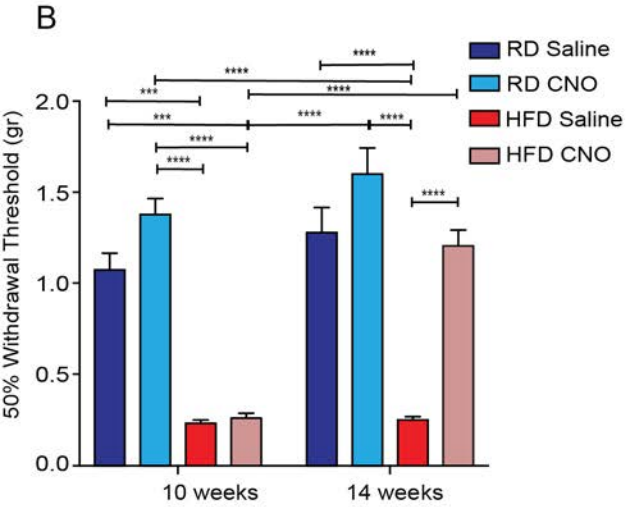
RD Saline
RD CNO
HFD Saline
HFD CNO
50% Withdrawal Threshold (gr)
2.0
1.5
1.0
0.5
0.0
10 weeks
14 weeks
***
****

D

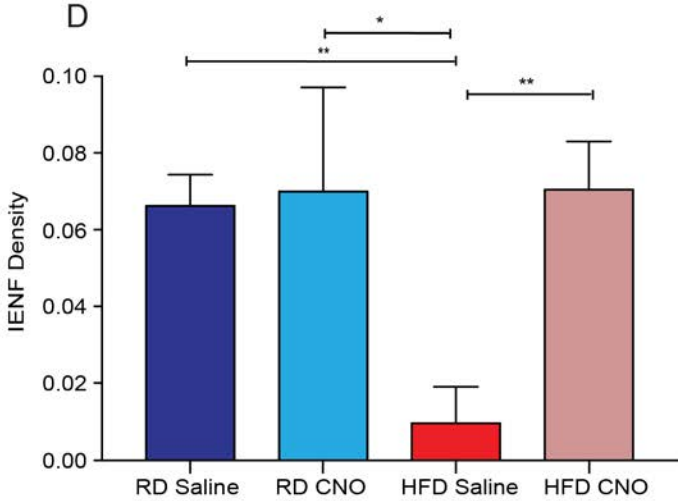
IENF Density
0.10
0.08
0.06
0.04
0.02
0.00
RD Saline
RD CNO
HFD Saline
HFD CNO
*
**

C

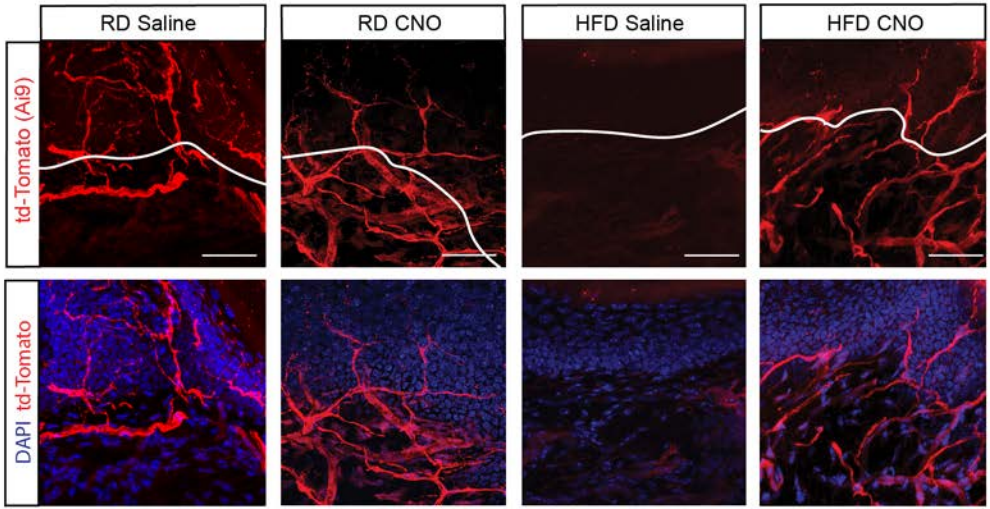
RD Saline
RD CNO
HFD Saline
HFD CNO
td-Tomato (Ai9)
DAPI td-Tomato

Figure 10. Chemogenetic inhibition of Na_v1.8-positive DRG neurons can reverse small-fiber degeneration and mechanical allodynia in HFD fed mice. (**A**) Experimental protocol for osmotic mini-pump implantation in Na_v1.8-Cre;Ai9;RC::PDi mice. Na_v1.8-Cre;Ai9;RC::PDi mice were put on RD or HFD for 10 weeks and then implanted intraperitoneally with an osmotic mini-pump delivering saline or CNO (10mg/kg/day) for 4 weeks to determine if CNO could reverse the effects of the HFD. Each arrow represents a time point where pain behavior was assessed. (**B**) von Frey pain behavior testing demonstrated the presence of mechanical allodynia (reduction in withdrawal threshold) in HFD fed mice after 10 weeks on diet. This mechanical allodynia was reduced after continuous treatment with CNO tested at the 14 weeks time point (***, $p<0.001$, ****, $p<0.0001$) (n=6/group). (**C, D**) Confocal micrographs from skin of Na_v1.8-Cre;Ai9;RC::PDi. td-Tomato expressing Na_v1.8 fibers (**red**) and merged images with the nuclear marker DAPI (**blue**) are shown**.** (**C**) Control mice on a RD with saline or CNO pumps showed normal skin innervation. HFD mice implanted with a saline pump showed reduced skin innervation. HFD mice fitted with CNO pumps showed a significant improvement in skin innervation. Scale bar=50μm. (**D**) This effect was quantified using intra-epidermal nerve density (IENF density and the intra-epidermal dermal junction is outlined in white (*, $p<0.05$, **, $p<0.01$) (n=6/group with 3 non-contiguous sections analyzed per sample). Values are expressed as mean $\pm$ SEM. p-values were calculated using two-way ANOVA, Bonferroni multiple comparison test.

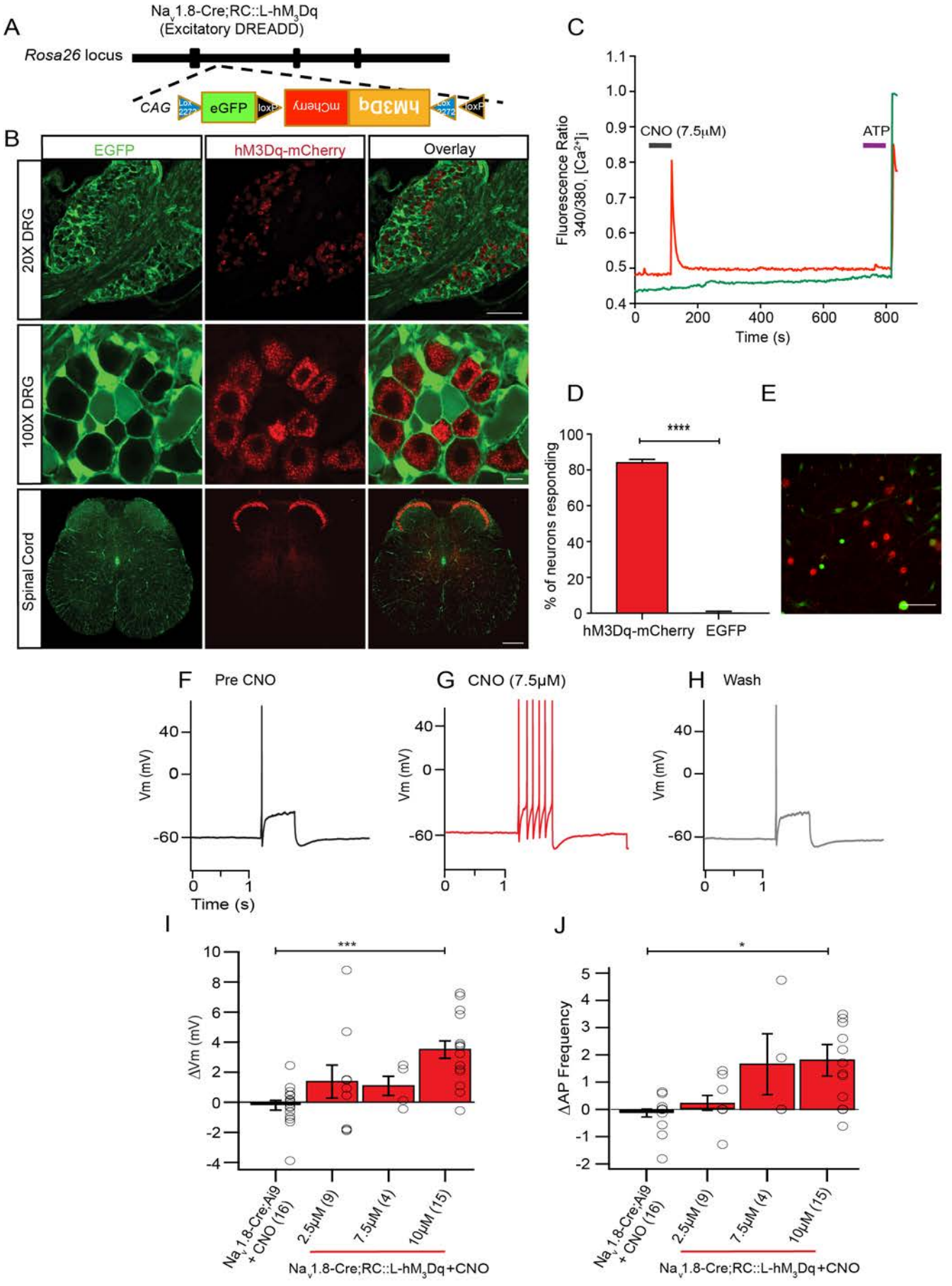
A
Nav1.8-Cre;RC::L-hM3Dq
(Excitatory DREADD)
Rosa26 locus
CAG
eGFP
mCherry
hM3Dq
B
EGFP
hM3Dq-mCherry
Overlay
20X DRG
100X DRG
Spinal Cord
C
CNO (7.5μM)
ATP
Fluorescence Ratio 340/380, [Ca2+]i
Time (s)
D
E
% of neurons responding
hM3Dq-mCherry
EGFP
F Pre CNO
G CNO (7.5μM)
H Wash
Vm (mV)
Time (s)
I
ΔVm (mV)
J
ΔAP Frequency
Nav1.8-Cre;Ai9 + CNO (16)
2.5μM (9)
7.5μM (4)
10μM (15)
Nav1.8-Cre;RC::L-hM3Dq+CNO

Figure 11. Chemogenetic activation of hM_3Dq excitatory DREADD receptors in $Na_v1.8$-positive DRG neurons led to increased neuronal excitability. (**A**) The $Na_v1.8$-Cre;RC::L-hM_3Dq construct used in these experiments was designed so that $Na_v1.8$-positive DRG neurons expressed m-Cherry fused hM_3Dq excitatory DREADD receptors, whereas all other cells expressed EGFP. (**B**) Representative images from DRGs (**top and middle)** and spinal cords (**bottom**) showing $Na_v1.8$-positive DRG neurons expressing m-Cherry fused hM_3Dq excitatory DREADD receptors whereas all other cells expressed EGFP. Magnification of 20x (**top**) and 100x (**middle**), 10x (**bottom**) (scale bar=150μm, 10μm, 150μm respectively). (**C-E**) DRG neurons were cultured from hM_3Dq excitatory DREADD mice and subjected to Fura-2 based $[Ca^{2+}]i$ imaging; only cells expressing the hM_3Dq DREADD receptors had $[Ca^{2+}]i$ responses to CNO (7.5μM) (**red**) whereas all other EGFP expressing cells did not respond (**green**). (**D**) Quantification of the percentage of neurons responding to CNO (84.042±1.9%) (****, $p<0.0001$, using a Mann-Whitney test) (n=94). (**E**) A representative image of the neurons used for $[Ca^{2+}]i$ imaging. Scale bar=50μm. (**F-J**) DRG primary cultures were prepared from these hM_3Dq excitatory DREADD mice and mCherry expressing cells were recorded. (**G**) Treatment with CNO (7.5μM) along with a depolarizing current step lead to increased action potential (AP) frequency compared with (**F**) the current step alone or (**H**) after wash. (**I**) Changes in membrane voltage and (**J**) the AP frequency were quantified for various concentrations of CNO. These same experiments were performed in $Na_v1.8$ td-Tomato DRG neurons that did not express DREADD receptors ($Na_v1.8$-Cre;Ai9 mice). (**I, J**) Compared to the control cells not expressing the hM_3Dq excitatory DREADD (**green)**, DREADD expressing cells (**red**) had significantly higher voltage membrane (V_m) and action potential

frequencies (*, $p<0.05$, ***, $p<0.001$ using one-way ANOVA, post-hoc Tukey test) (n=16). Values are expressed as mean ± S.E.M.

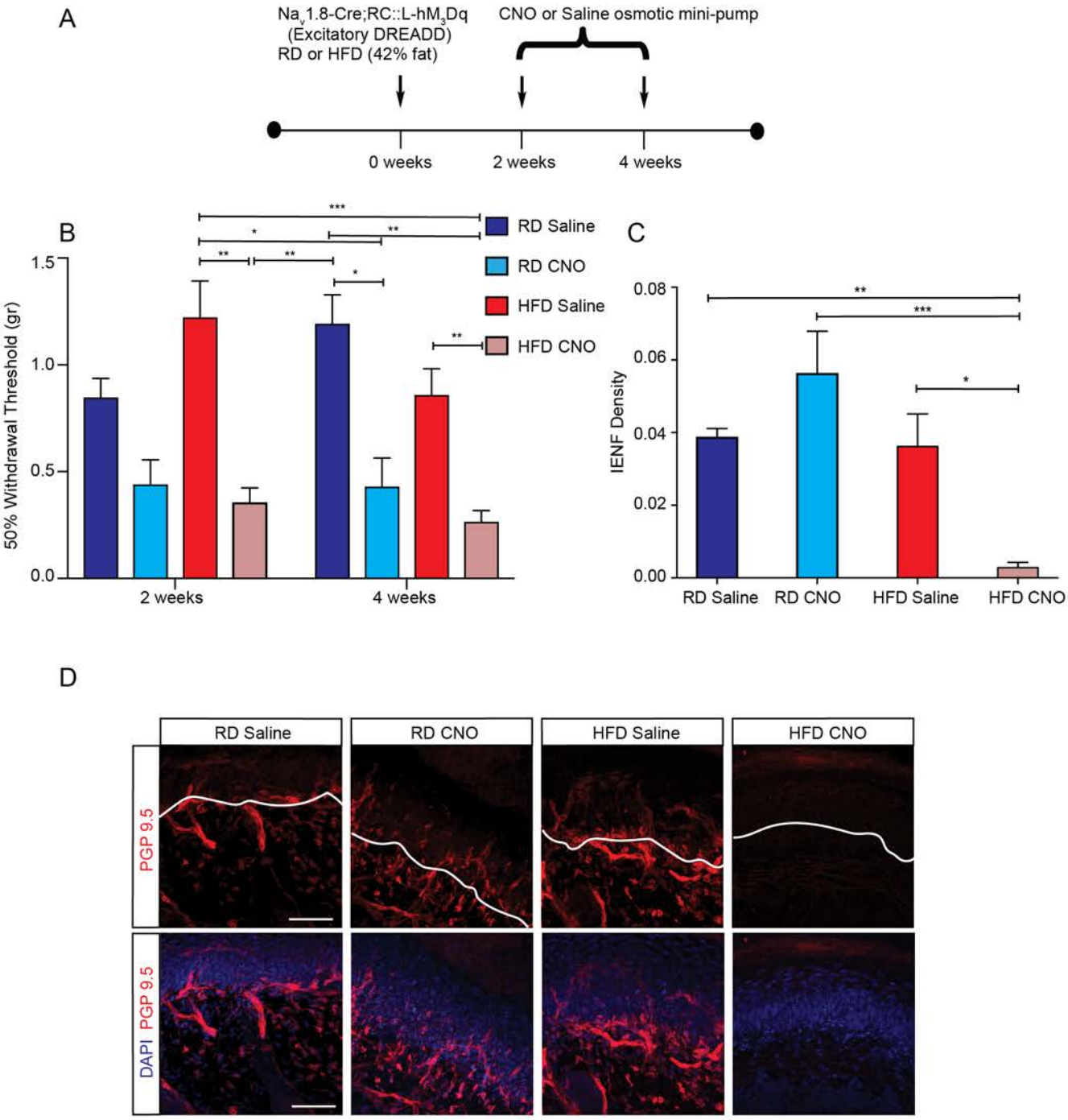
A
Na$_v$1.8-Cre;RC::L-hM$_3$Dq
(Excitatory DREADD)
RD or HFD (42% fat)
CNO or Saline osmotic mini-pump
0 weeks
2 weeks
4 weeks
B
50% Withdrawal Threshold (gr)
1.5
1.0
0.5
0.0
2 weeks
4 weeks
RD Saline
RD CNO
HFD Saline
HFD CNO
C
IENF Density
0.08
0.06
0.04
0.02
0.00
RD Saline
RD CNO
HFD Saline
HFD CNO
D
RD Saline
RD CNO
HFD Saline
HFD CNO
PGP 9.5
DAPI PGP 9.5

Figure 12. Long-term chemogenetic activation of Na_v1.8-positive DRG neurons resulted in a significant acceleration in the development of mechanical allodynia and small-fiber degeneration and in HFD fed mice. (**A**) Experimental setup of osmotic mini-pump implantation in Na_v1.8-Cre;RC::L-hM_3Dq mice. Na_v1.8-Cre;RC::L-hM_3Dq mice that expressed excitatory hM_3Dq DREADD receptors were fed either RD or HFD and had a osmotic mini-pump implanted intraperitoneally, which administered either saline or CNO (10mg/kg/day) for the period from 2 to 4 weeks following the commencement of HFD or RD. (**B**) von Frey pain behavior testing demonstrated the onset of mechanical allodynia (reduction in withdrawal threshold) in HFD fed mice (**red**) after 2 or 4 weeks following CNO administration. The RD mice (**blue**) also showed a reduction of withdrawal threshold after 4 weeks of CNO administration (*, $p<0.05$, **, $p<0.01$, ***, $p<0.001$) (n=6/group). (**C, D**) Confocal micrographs of skin from Na_v1.8-Cre;RC::L-hM_3Dq mice on RD for 4 weeks with saline pumps showed normal skin innervation using PGP 9.5 (pseudo-colored **red**). Sections were co-labeled with a nuclear marker DAPI (blue staining). In contrast, HFD mice with CNO pumps showed significant depletion of nerve terminals. Interestingly, in RD mice increased excitability, produced by hM_3Dq DREADD receptors, alone was not able to induce small-fiber degeneration in the absence of diabetes. Scale bar=50μm. (**C**) This effect was quantified using intra-epidermal nerve density (IENF density) and the epidermal-dermal junction is outlined in white (*, $p<0.05$, **, $p<0.01$, ***, $p<0.001$) (n=6 from each group with 3 non-contiguous sections analyzed per sample). p-values were calculated using one-way ANOVA, Bonferroni multiple comparison test.

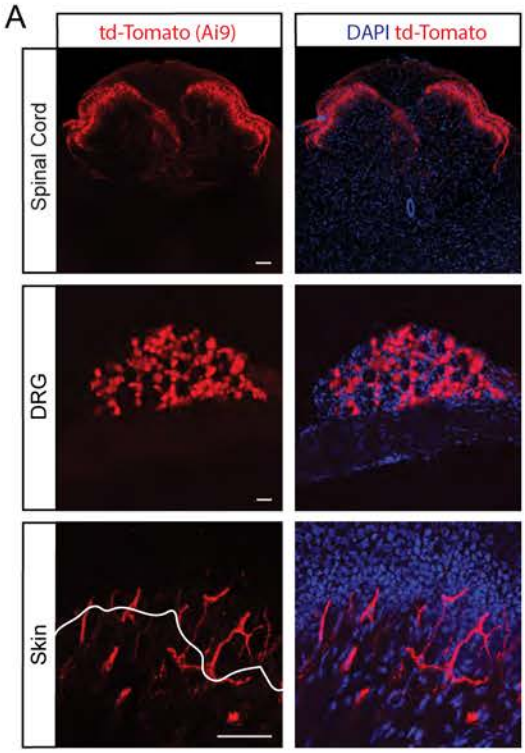
A
td-Tomato (Ai9)
DAPI td-Tomato
Spinal Cord
DRG
Skin

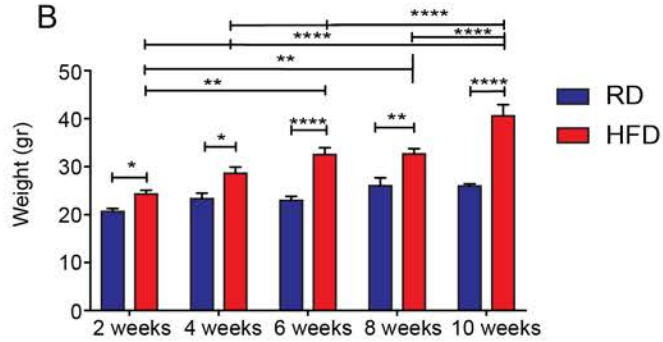
B
Weight (gr)
0
10
20
30
40
50
2 weeks
4 weeks
6 weeks
8 weeks
10 weeks
RD
HFD
*
**
****

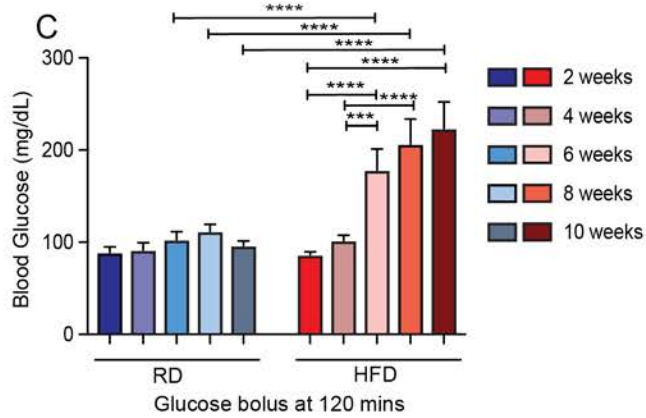
C
Blood Glucose (mg/dL)
0
100
200
300
RD
HFD
Glucose bolus at 120 mins
2 weeks
4 weeks
6 weeks
8 weeks
10 weeks
***
****

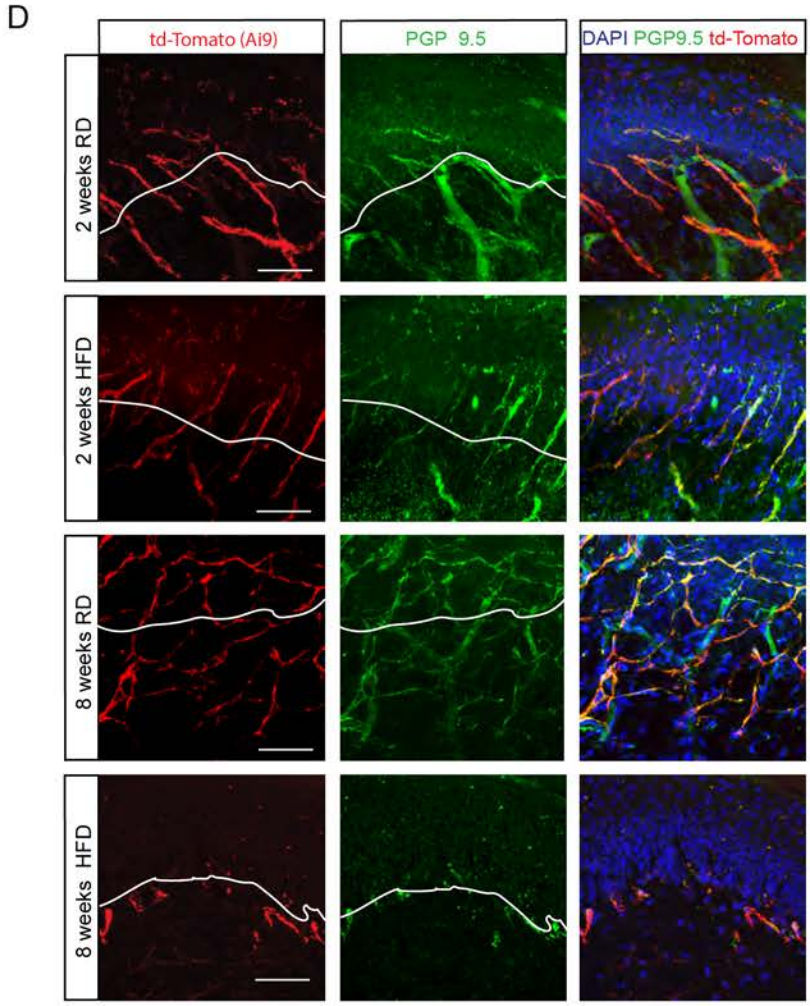
D
td-Tomato (Ai9)
PGP 9.5
DAPI PGP9.5 td-Tomato
2 weeks RD
2 weeks HFD
8 weeks RD
8 weeks HFD

Supplemental Figure 1. Validation of the Na_v1.8-Cre system. (**A**) Confocal micrographs of spinal cord, DRG and skin taken from Na_v1.8-Cre;Ai9 mice showing Na_v1.8-positive neurons in the DRG and Na_v1.8-afferents in spinal cord and skin labeled with td-Tomato (**red**). Sections were co-labeled with a nuclear marker DAPI (**blue**). Magnification 10x (**top**), 20x (**middle**), 60x (**bottom**) (scale bar=50μm). (**B**) Weights of Na_v1.8-Cre;Ai9 mice in grams (gr) fed either RD (**blue**) or HFD (**red**) over a 10 week period (*, $p<0.05$, **, $p<0.01$, ****, $p<0.0001$.) (n= 8/group). (**C**) Blood glucose levels for both RD and HFD at various lengths of time on each diet, blood glucose levels were taken 120 minutes after injection of glucose (45% D-glucose solution (2mg glucose/1g animal body weight)) (***, $p<0.001$, ****, $P<0.0001$) (n=8/group). p-values were calculated using two-way ANOVA , Bonferroni multiple comparison test. (**D**) Confocal micrographs of skin taken from Na_v1.8-Cre;Ai9 mice that had been on either RD or HFD for 2 or 8 weeks showing td-Tomato (**red**), PGP 9.5 (**green**), and DAPI a nuclear marker (**blue**). At 8 weeks HFD mice showed a reduced number of nerve fibers crossing the epidermal-dermal junction (outlined in white). Magnification 60x (scale bar=50μm). Values are expressed as mean ± S.E.M.

A

Pirt-GCaMP3 mice 6-12 weeks

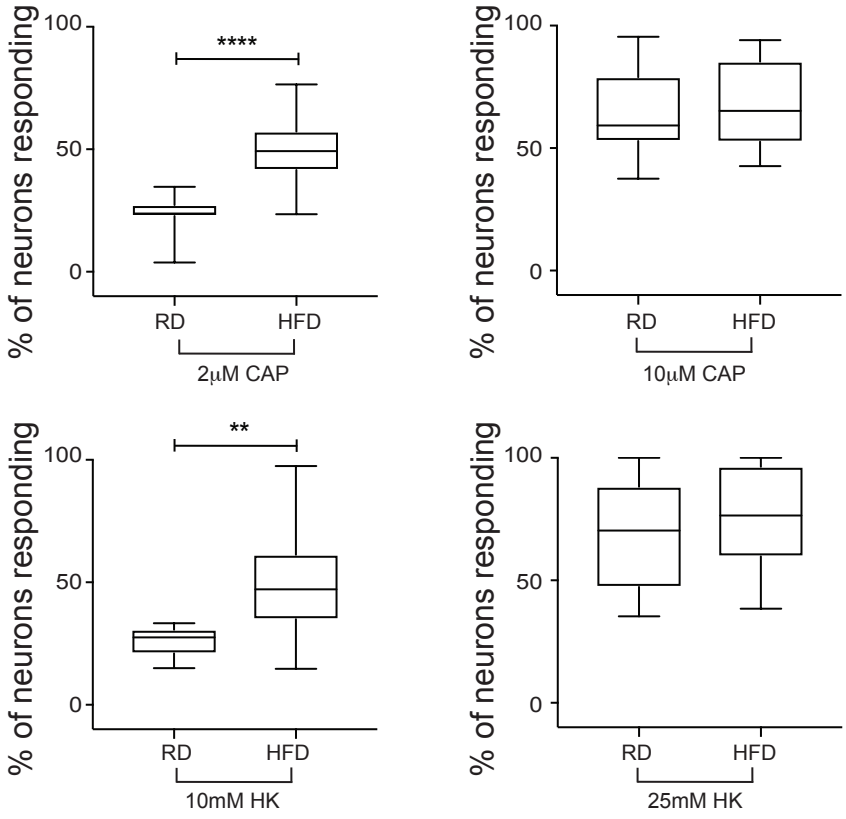

B

Pirt-GCaMP3 mice 2-4 weeks

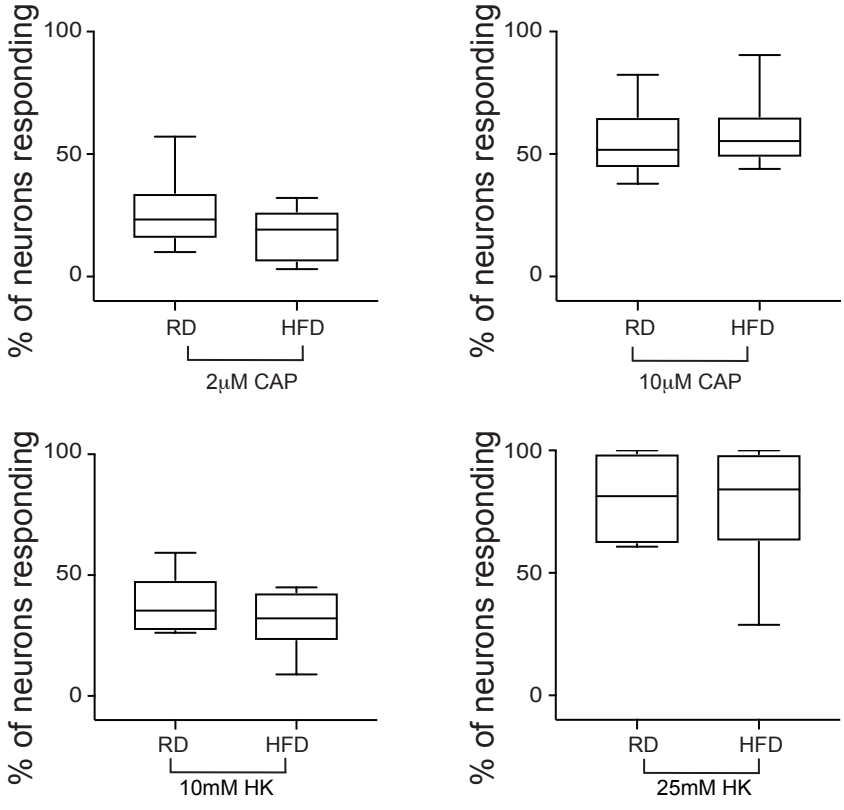

Supplemental Figure 2. Onset of increased [Ca^{2+}]i responses in diabetic DRG explants after 6 weeks on HFD. (**A, B**) [Ca^{2+}]i responses of acutely excised DRGs from Pirt-GCaMP3 mice to 2μM or 10μM capsaicin and 10mM, or 25mM high potassium buffer (HK). Data is shown as capsaicin or HK responsive DRG neurons as a percentage of total neurons that responded to 50mM HK. (**A**) Explants from HFD mice that had been on diet for 6-12 weeks showed increased responses to 2μM capsaicin compared to RD mice. There were also increased responses of HFD explants to 10mM HK compared to RD (**, $p<0.01$, ****, $p<0.0001$). At higher concentrations of capsaicin and HK there was no significant difference between RD and HFD mice (RD n=594 neurons n=18 explants; HFD n=844 neurons n=30 explants). (**B**) When these same experiments were done on explants from mice that had only been on RD or HFD for 2-4 weeks there was no significant difference in [Ca^{2+}]$_i$ responses to capsaicin or HK (RD n=347 neurons n=16 explants; HFD n=504 neurons n=20 explants). This showed that the increased [Ca^{2+}]i responses of Pirt-GCaMP3 explants are evident after 6 weeks on HFD. Values are expressed as mean ± S.E.M. p-values were calculated by Mann-Whitney test.

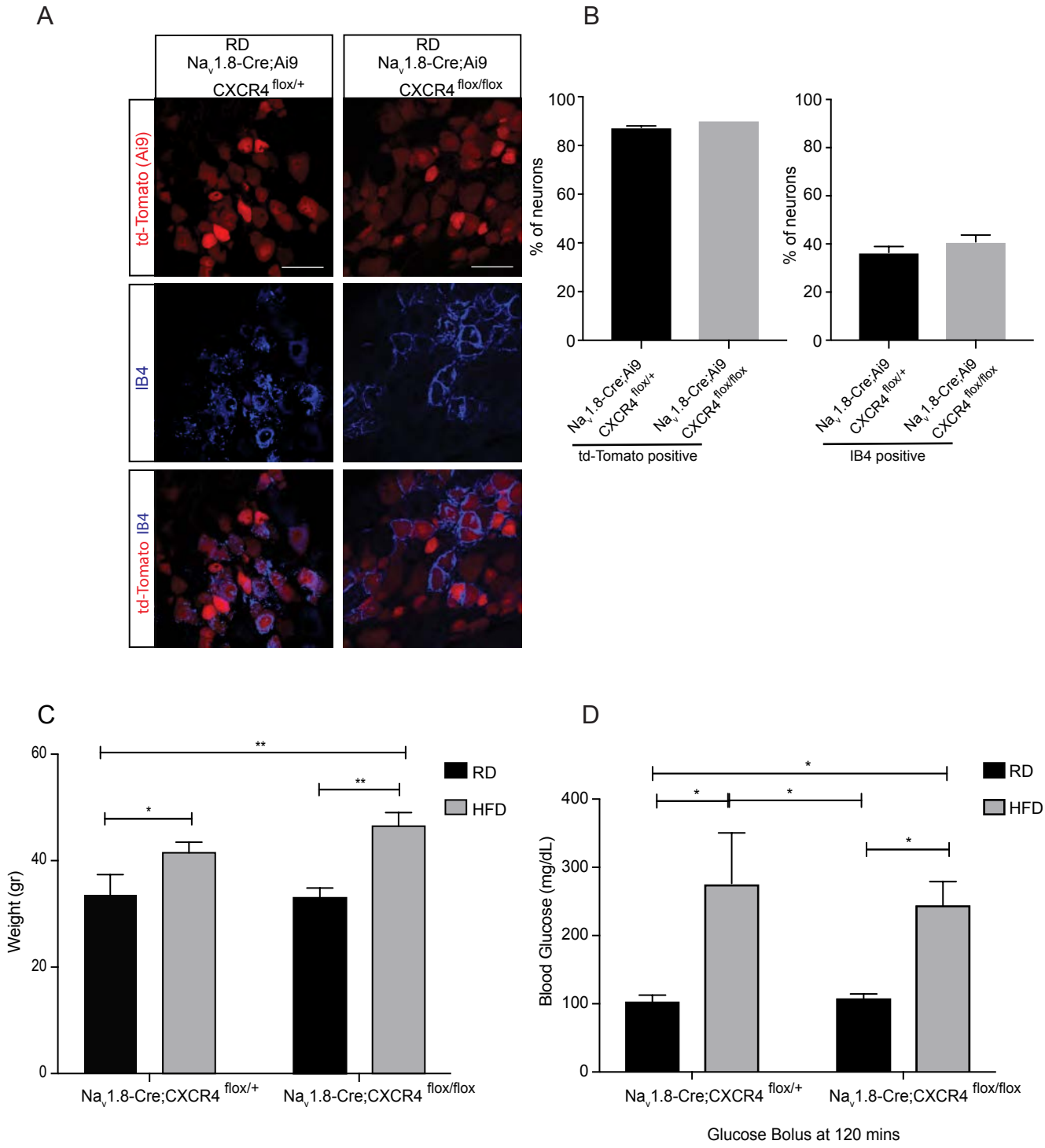
A
RD
Nav1.8-Cre;Ai9
CXCR4 flox/+
RD
Nav1.8-Cre;Ai9
CXCR4 flox/flox
td-Tomato (Ai9)
IB4
td-Tomato IB4
B
% of neurons
100
80
60
40
20
0
Nav1.8-Cre;Ai9 CXCR4 flox/+
Nav1.8-Cre;Ai9 CXCR4 flox/flox
td-Tomato positive
IB4 positive
C
Weight (gr)
60
40
20
0
**
*
**
RD
HFD
Nav1.8-Cre;CXCR4 flox/+
Nav1.8-Cre;CXCR4 flox/flox
D
Blood Glucose (mg/dL)
400
300
200
100
0
*
*
*
*
RD
HFD
Nav1.8-Cre;CXCR4 flox/+
Nav1.8-Cre;CXCR4 flox/flox
Glucose Bolus at 120 mins

Supplemental Figure 3. Selective deletion of CXCR4 receptors from Na_v1.8-positve DRG neurons did not alter the DRG neuronal phenotype or metabolic profile of mice fed HFD. (**A**) Confocal micrographs from DRGs from mice with either heterozygous deletion of CXCR4 (Na_v1.8-Cre;Ai9;CXCR4$^{flox/+}$) or homozygous deletion (Na_v1.8-Cre;Ai9;CXCR4$^{flox/flox}$), showing td-Tomato (**red**) labeling Na_v1.8-positive DRG neurons some of which are also labeled with a marker for non-peptidergic DRG neurons, IB4 (**blue**). Magnification 60x (scale bar=50μm). (**B**) The numbers of td-Tomato positive and IB4 positive neurons were quantified and there were no significant differences between mice with heterozygous (td-Tomato 85.5±0.5, IB4 36.4±2.5) and homozygous (td-Tomato 87.3±2.8, IB4 35.8±2.9) selective CXCR4 deletions (n=177, 154 neurons respectively). p-values were calculated by Mann-Whitney test. (**C**) Weights of mice in grams (gr) with either heterozygous deletion of CXCR4 (Na_v1.8-Cre;Ai9;CXCR4$^{flox/+}$) or homozygous deletion (Na_v1.8-Cre;Ai9;CXCR4$^{flox/flox}$) of CXCR4 from Na_v1.8-positive neurons(*, $p<0.05$, **, $p<0.01$) (n=6/group). (**D**) Blood glucose levels of the same mice 120 minutes after injection of glucose (45% D-glucose solution (2mg glucose/1gr animal body weight)) (*, $p<0.05$) (n=6/group). Values are expressed as mean ± S.E.M. p-values were calculated using one-way ANOVA, Bonferroni multiple comparison test.

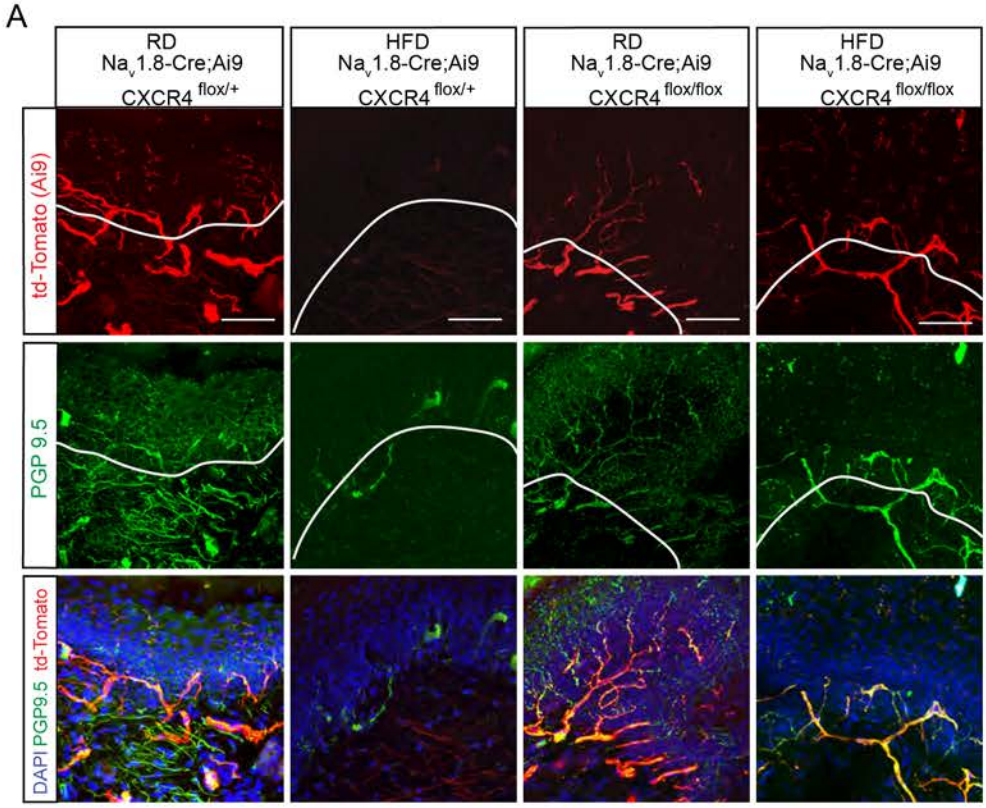
A
RD
Nav1.8-Cre;Ai9
CXCR4 flox/+
HFD
Nav1.8-Cre;Ai9
CXCR4 flox/+
RD
Nav1.8-Cre;Ai9
CXCR4 flox/flox
HFD
Nav1.8-Cre;Ai9
CXCR4 flox/flox
td-Tomato (Ai9)
PGP 9.5
DAPI PGP9.5 td-Tomato

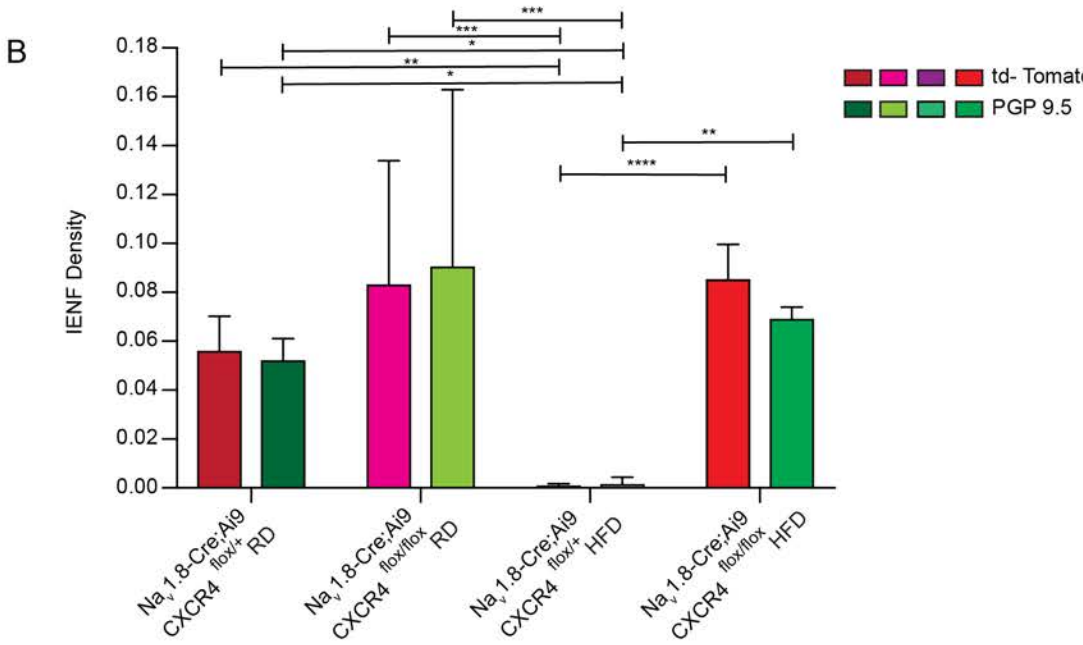
B
IENF Density
0.18
0.16
0.14
0.12
0.10
0.08
0.06
0.04
0.02
0.00
td- Tomato
PGP 9.5
***
***
*
**
*
**
****
Nav1.8-Cre;Ai9 CXCR4 flox/+ RD
Nav1.8-Cre;Ai9 CXCR4 flox/flox RD
Nav1.8-Cre;Ai9 CXCR4 flox/+ HFD
Nav1.8-Cre;Ai9 CXCR4 flox/flox HFD

Supplemental Figure 4. Selective chemokine receptor CXCR4 deletion from Na_v1.8-positive DRG neurons prevented the development of small-fiber degeneration in HFD-induced PDN. (**A**) Confocal analysis of skin from mice with either heterozygous (Na_v1.8-Cre;Ai9;CXCR4$^{flox/+}$) or homozygous deletion (Na_v1.8-Cre;Ai9;CXCR4$^{flox/flox}$) of CXCR4 on either RD or HFD showing td-Tomato (**red**), immunolabeling with antibody against the protein gene product 9.5 (PGP 9.5) (**green**), and merged images with the nuclear marker DAPI (**blue**). Na_v1.8-Cre;Ai9;CXCR4$^{flox/+}$ RD mice had normal skin innervation whereas the same mice on HFD had reduced innervation. However, selective homozygous deletion of CXCR4 for mice on HFD prevented small-fiber degeneration. Magnification 60x (scale bar=50μm). (**B**) This effect was quantified using intra-epidermal nerve density (IENF density) which is expressed as the number of nerves crossing the epidermal-dermal junction (outlined in white) as a function of epidermal-dermal junction length. IENF densities calculated using both td-Tomato labeled fibers (red or pink) and PGP 9.5 fibers (shades of green) (*, $p<0.05$, **, $p<0.01$, ***, $p<0.001$) (n=7 for all groups with 3 non-contiguous sections analyzed per sample). Values are expressed as mean $\pm$ S.E.M. p-values were calculated using a two-way ANOVA with Dunnett's Multiple Comparison test.

A Pirt-GCaMP3 mice 6-12 weeks CXCL12

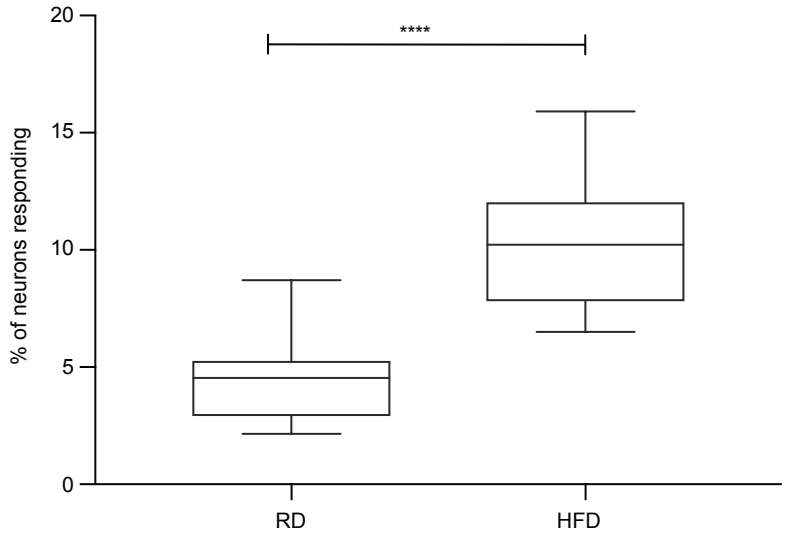

B Pirt-GCaMP3 mice 2-4 weeks CXCL12

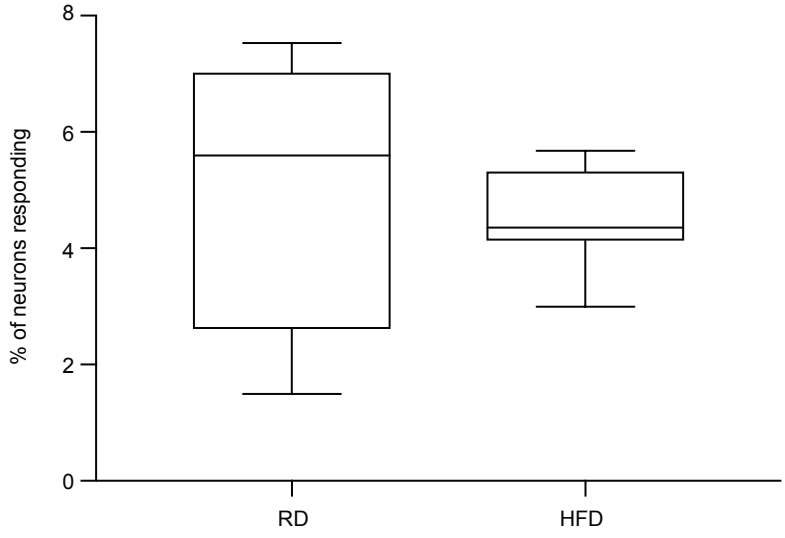

Supplemental Figure 5. Onset of increased [Ca^{2+}]i responses following CXCL12 application after 6 weeks on HFD. (**A, B**) [Ca^{2+}]i responses of acutely excised DRGs from Pirt-GCaMP3 mice to CXCL12. Data is shown as CXCL12 responsive DRG neurons as a percentage of total neurons that responded to a high potassium buffer (HK). (**A**) There were significantly more [Ca^{2+}]i responses to CXCL12 (100 nM) in explants from HFD mice compared to RD fed non-diabetic controls after 6-12 weeks on diet (****, $p<0.0001$) (HFD n=844 neurons n=30 explants; RD n=594 neurons n=18 explants). (**B**) In contrast, [Ca^{2+}]i responses to CXCL12 were not different after 2-4 weeks on HFD or on RD (HFD n=504 neurons n=20 explants; RD n=347 neurons n=16 explants). Values are expressed as mean ± S.E.M. p-values were calculated using Mann-Whitney test.

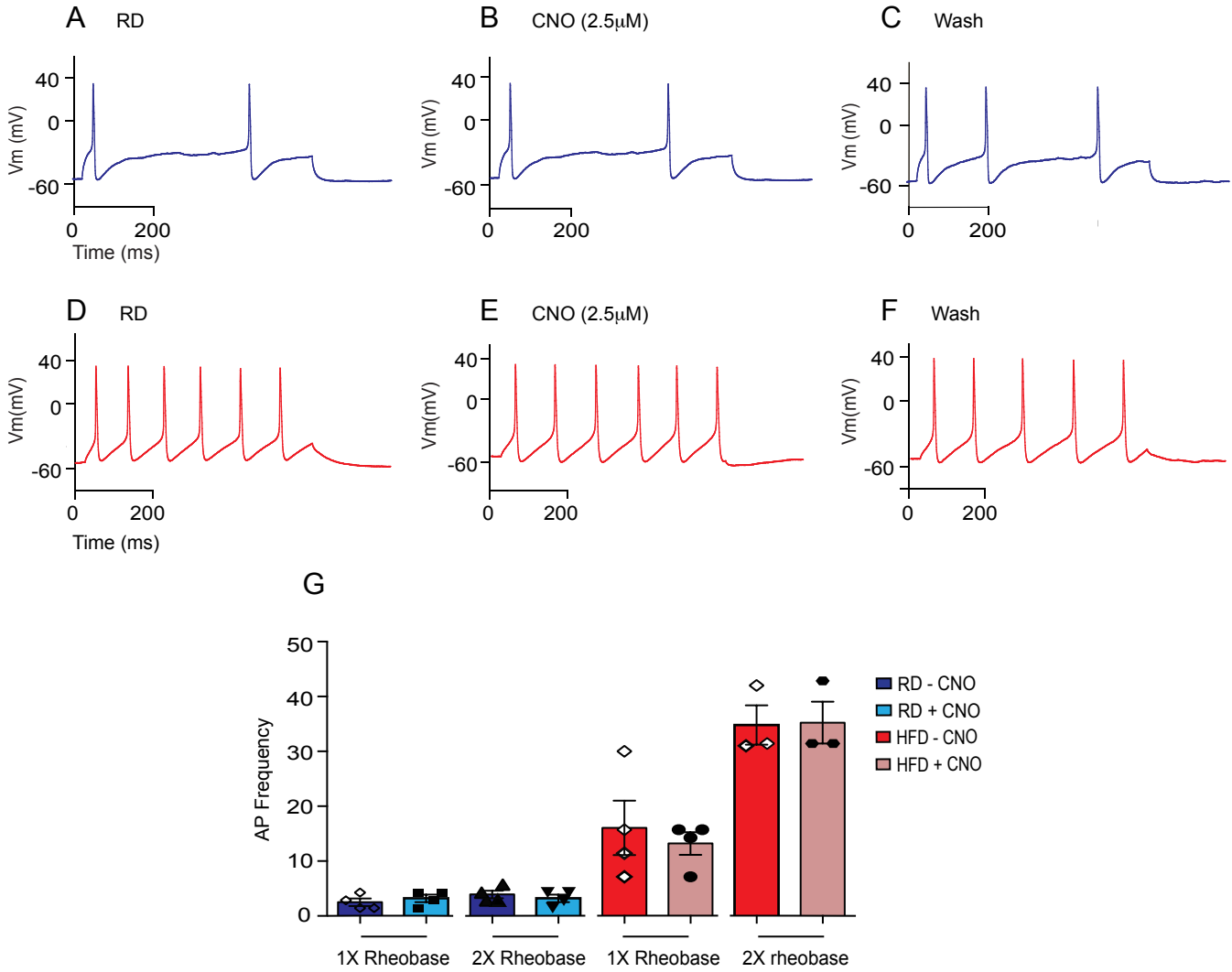
A
RD
B
CNO (2.5μM)
C
Wash
Vm (mV)
40
0
-60
0
200
Time (ms)
D
RD
E
CNO (2.5μM)
F
Wash
Vm(mV)
G
AP Frequency
50
40
30
20
10
0
1X Rheobase
2X Rheobase
1X Rheobase
2X rheobase
RD - CNO
RD + CNO
HFD - CNO
HFD + CNO

Supplemental Figure 6. Na_v1.8-positive DRG neurons that did not express DREADD receptors had no change in action potential frequency after CNO application. (**A-F**) Representative traces from a Na_v1.8-Cre;Ai9 primary cultured DRGs, which do not express DREADD receptors, from mice fed either RD (**A-C, blue**) or HFD (**D-F, red**). (**G**) In both RD and HFD application of 2.5μM CNO did not change the action potential frequency (AP frequency) at either 1X or 2X rheobase current injection (RD n=4 for 1X and 2X; HFD n=4 for 1X and n=3 for 2X). Values are expressed as mean ± S.E.M. p-values were calculated using Mann-Whitney test.

A

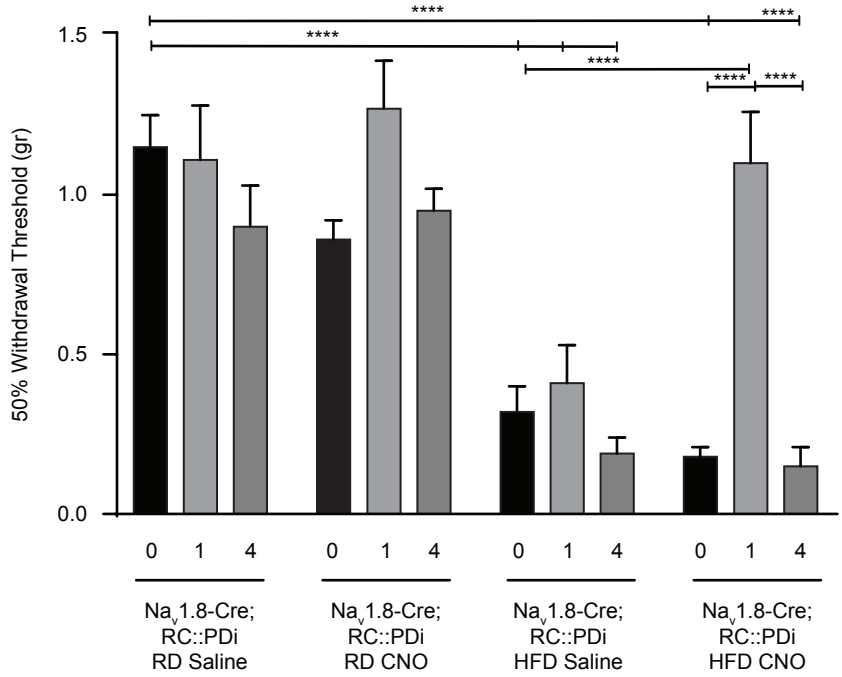
****
****
****
****
****
****
1.5
1.0
0.5
0.0
50% Withdrawal Threshold (gr)
0 1 4
0 1 4
0 1 4
0 1 4
Nav1.8-Cre;
RC::PDi
RD Saline
Nav1.8-Cre;
RC::PDi
RD CNO
Nav1.8-Cre;
RC::PDi
HFD Saline
Nav1.8-Cre;
RC::PDi
HFD CNO

B

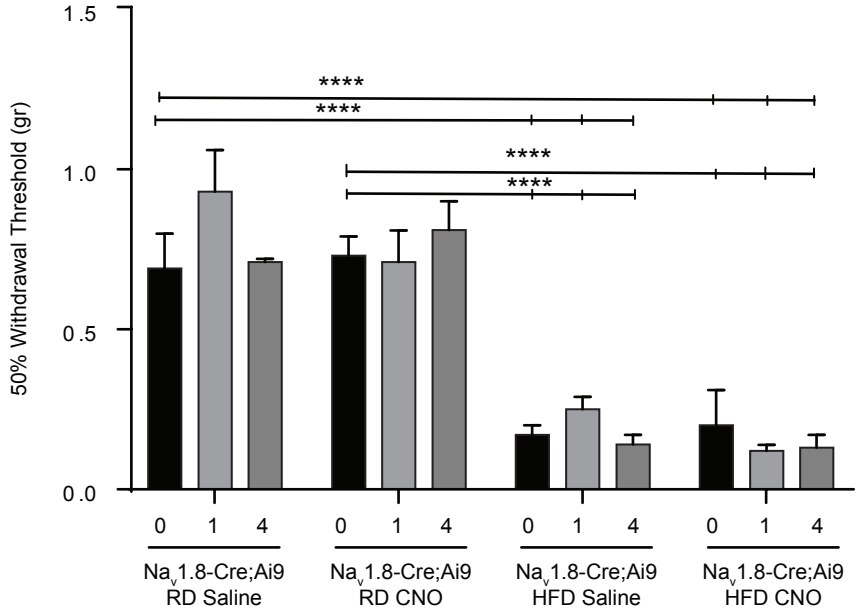
****
****
****
****
1.5
1.0
0.5
0.0
50% Withdrawal Threshold (gr)
0 1 4
0 1 4
0 1 4
0 1 4
Nav1.8-Cre;Ai9
RD Saline
Nav1.8-Cre;Ai9
RD CNO
Nav1.8-Cre;Ai9
HFD Saline
Nav1.8-Cre;Ai9
HFD CNO

Supplemental Figure 7. Injection of CNO decreases mechanical allodynia in inhibitory PDi DREADD expressing mice on HFD and had no effect on mice not expressing DREADD receptors. (**A**) von Frey behavioral testing for Na_v1.8-Cre:RC::PDi mice on either RD or HFD injected with a CNO (10 mg/kg) or saline intraperitoneally (i.p.). These mice expressed inhibitory DREADD receptors, PDi, in their Na_v1.8-positive DRG neurons and fed a HFD showed an increase in pain withdrawal threshold one hour after CNO injection, this effect was absent four hours after injection (****, $p<0.0001$) (n=16/group). (**B**) von Frey behavioral testing was also performed on Na_v1.8-Cre;Ai9 mice that do not express inhibitory DREADD receptors. Mice were fed either RD or HFD and given an i.p. injection of either CNO (10 mg/kg) or saline. Mice on HFD had decreased withdrawal thresholds as expected and injection of CNO had no effect (****, $p<0.0001$) (n=8/group). For both genotypes behavioral testing was done before the injection (time=0), one hour after the injection (time=1hr) and four hours after (time=4hr). Values are expressed as mean ± S.E.M. p-values were calculated using a two-way ANOVA, Bonferroni multiple comparison test.

Na$_v$1.8-Cre;RC::PDi mice
(Inhibitory PDi)

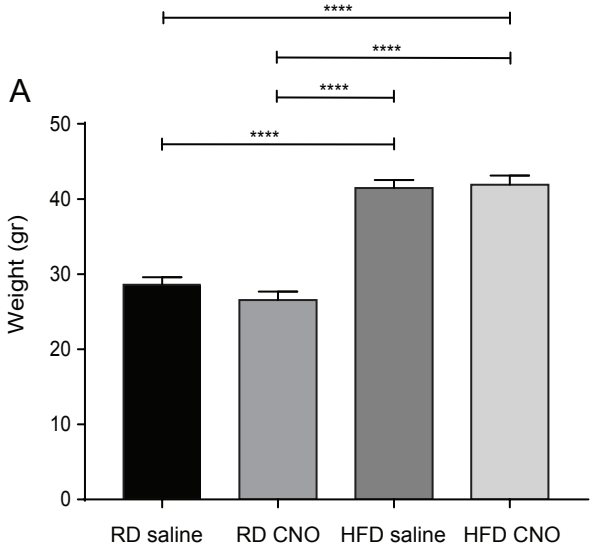

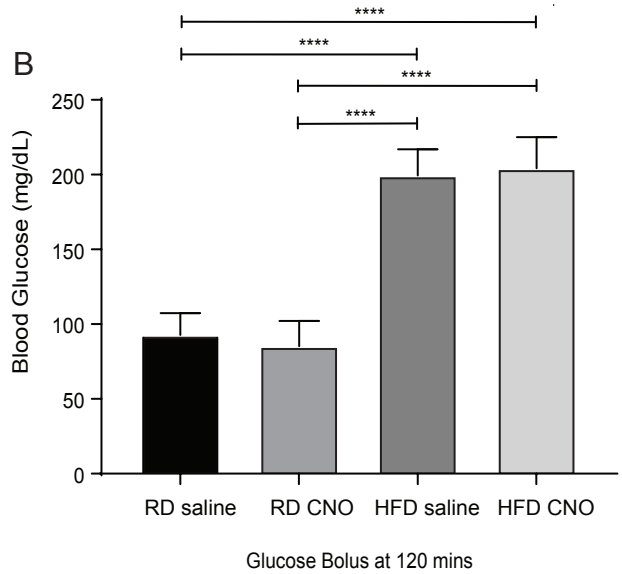

Na$_v$1.8-Cre;Ai9 mice

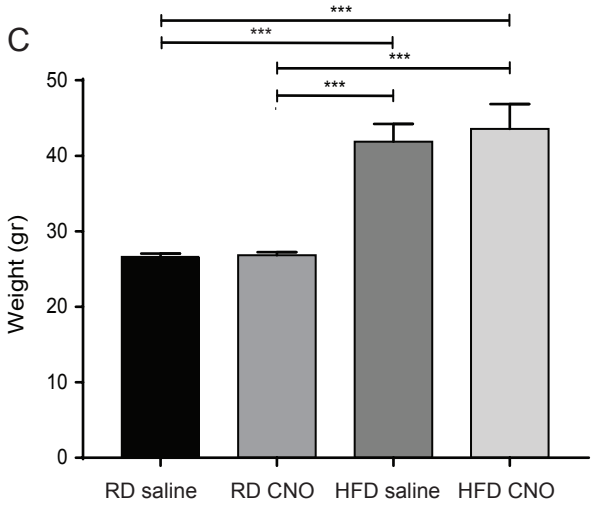

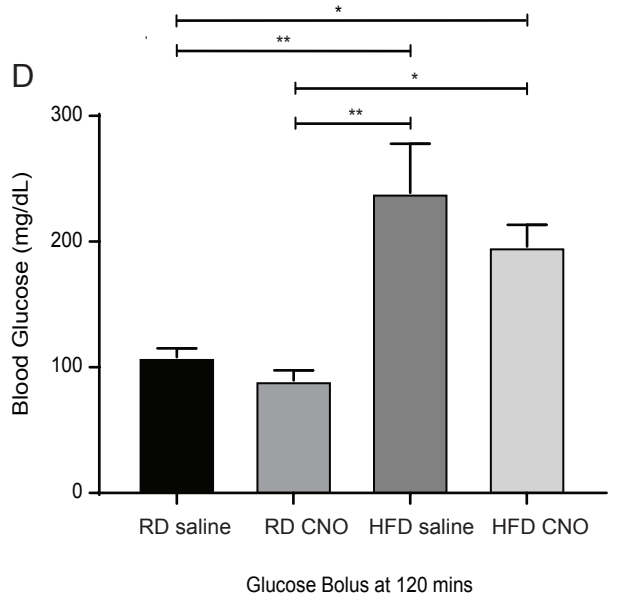

Supplemental Figure 8. Expression of inhibitory DREADD receptors, PDi in Na_v1.8-positive DRG neurons does not alter the metabolic profile in the HFD model. (**A**) Weight of Na_v1.8-Cre;RC::PDi mice in grams (gr) fed either RD or HFD for 10 weeks and injected with either CNO (10 mg/kg) or saline (****, $p<0.0001$) (n=6/group). (**B**) Blood glucose levels of the same mice 120 minutes after injection of glucose (45% D-glucose solution (2 mg glucose/1 g animal body weight)) (****, $p<0.0001$) (n=18/group). (**C**) Weight of Na_v1.8-Cre;Ai9 mice fed either RD or HFD and injected with either CNO (10 mg/kg) or saline (***, $p<0.001$) (n=6/group). (**D**) Blood glucose levels of the same mice 120 minutes after injection of glucose (*, $p<0.05$, **, $p<0.01$) (n=18/group). Values are expressed as mean ± S.E.M. p-values were calculated using one-way ANOVA, Bonferroni multiple comparison test.

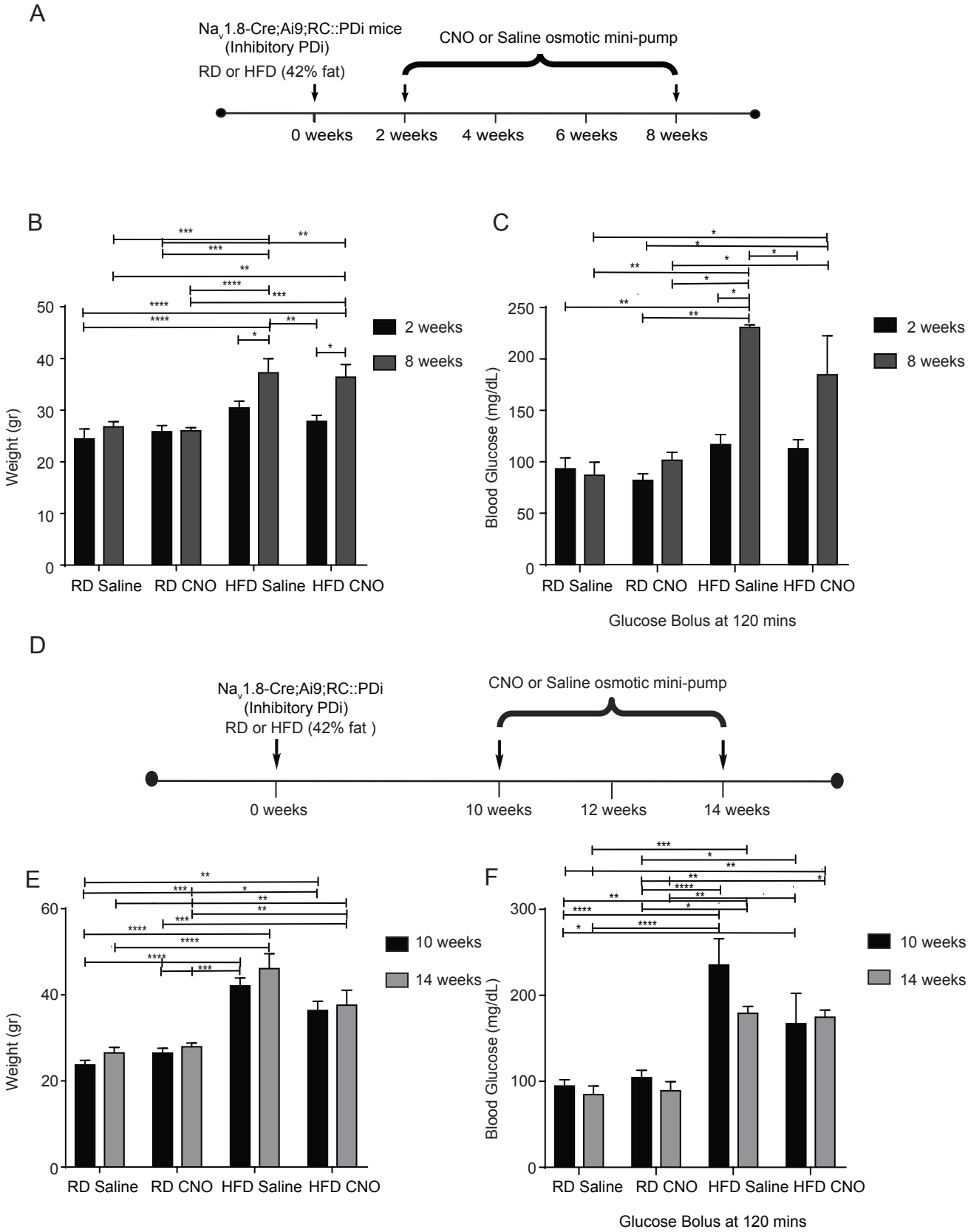
A
Nav1.8-Cre;Ai9;RC::PDi mice
(Inhibitory PDi)
RD or HFD (42% fat)
CNO or Saline osmotic mini-pump
0 weeks
2 weeks
4 weeks
6 weeks
8 weeks
B
Weight (gr)
2 weeks
8 weeks
RD Saline
RD CNO
HFD Saline
HFD CNO
C
Blood Glucose (mg/dL)
2 weeks
8 weeks
RD Saline
RD CNO
HFD Saline
HFD CNO
Glucose Bolus at 120 mins
D
Nav1.8-Cre;Ai9;RC::PDi
(Inhibitory PDi)
RD or HFD (42% fat)
CNO or Saline osmotic mini-pump
0 weeks
10 weeks
12 weeks
14 weeks
E
Weight (gr)
10 weeks
14 weeks
RD Saline
RD CNO
HFD Saline
HFD CNO
F
Blood Glucose (mg/dL)
10 weeks
14 weeks
RD Saline
RD CNO
HFD Saline
HFD CNO
Glucose Bolus at 120 mins

Supplemental Figure 9. Experimental plan, weights and blood glucose levels for prevention and reversal of PDN in mice that expressed inhibitory DREADD receptors, PDi. (**A**) Experimental timeline for the prevention set of experiments where Na_v1.8-Cre;Ai9;RC::PDi mice were administered CNO (10 mg/kg/day) or saline through an osmotic mini-pump concurrently with mice being fed either RD or HFD. Each arrow represents a time point when weight and blood glucose levels were measured. (**B**) Weights of these mice in grams (gr) after 2 or 8 weeks on the diet (*, $p<0.05$, **, $p<0.01$, ***, $p<0.001$, ****, $p<0.0001$) (n=6/group). (**C**) Blood glucose levels of these mice at 2 and 8 weeks on diet 120 minutes after injection of glucose (45% D-glucose solution (2mg glucose/1g animal body weight)) (*, $p<0.05$, **, $p<0.01$) (n=6/group). (**D**) Experimental timeline for the reversal set of experiments where Na_v1.8-Cre;Ai9;RC::PDi mice were administered CNO (10 mg/kg/day) or saline through an osmotic mini-pump after being fed on diet. Each arrow represents a time point when weight and blood glucose levels were measured. (**E**) Weights of these mice in grams (gr) after 10 or 14 weeks on RD or HFD (*, $p<0.05$, **, $p<0.01$, ***, $p<0.001$, ****, $p<0.0001$) (n=6/group). (**F**) Blood glucose levels of these mice at 10 and 14 weeks on diet (*, $p<0.05$, **, $p<0.01$, ***, $p<0.001$, ****, $p<0.0001$) (n=6/group). Values are expressed as mean $\pm$ S.E.M. p-values were calculated using two-way ANOVA, Bonferroni multiple comparison test.

A

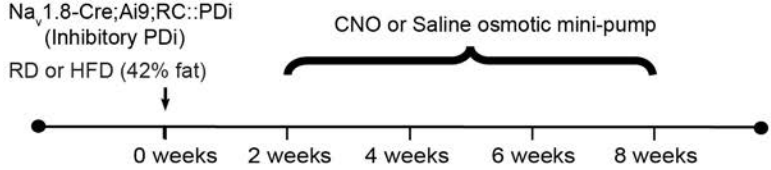
Na$_v$1.8-Cre;Ai9;RC::PDi
(Inhibitory PDi)
RD or HFD (42% fat)
CNO or Saline osmotic mini-pump
0 weeks
2 weeks
4 weeks
6 weeks
8 weeks

B

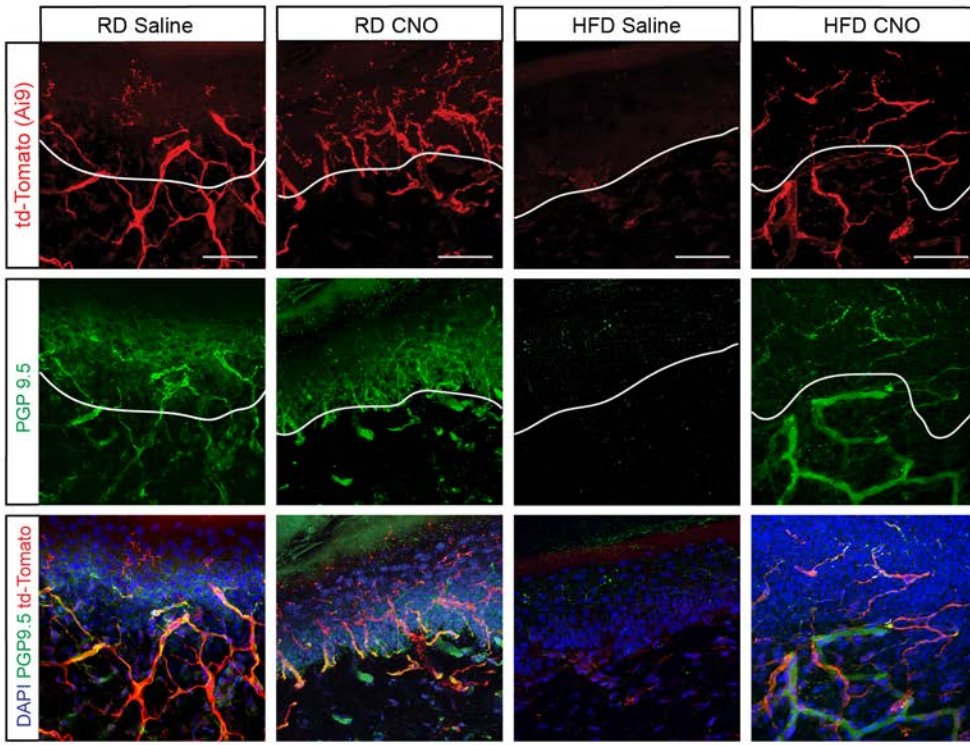
RD Saline
RD CNO
HFD Saline
HFD CNO
td-Tomato (Ai9)
PGP 9.5
DAPI PGP9.5 td-Tomato

C

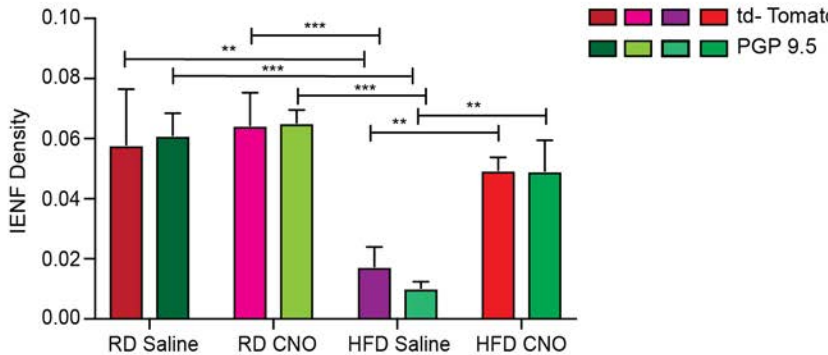
td- Tomato
PGP 9.5
IENF Density
0.10
0.08
0.06
0.04
0.02
0.00
**
***
***
***
**
**
RD Saline
RD CNO
HFD Saline
HFD CNO

Supplemental Figure 10. Chemogenetic inhibition of Na_v1.8-positive DRG neurons can prevent small-fiber degeneration visualized by either td-Tomato positive fibers or fibers stained with PGP 9.5. (**A**) Experimental setup: osmotic mini-pumps infusing either CNO (10mg/kg/day) or saline were implanted i.p. in Na_v1.8-Cre;Ai9;RC::PDi between 2 and 8 weeks of RD or HFD. (**B**) Confocal analysis of skin from these mice that express the inhibitory DREADD receptor, PDi, fed either RD or HFD showing td-Tomato (**red**) in Na_v1.8-positive fibers, immunolabeling with antibody against PGP 9.5 (**green**), and merged images with the nuclear marker DAPI (**blue**). Mice on RD given either saline or CNO showed normal skin innervation. In diabetic mice given saline there was a reduction in skin innervation, but it was reversed for mice on HFD given CNO. CNO infusion prevented small-fiber degeneration of mice on HFD. Magnification 60x (scale bar=50μm). (**C**) This effect was quantified using intra-epidermal nerve density (IENF density) which is expressed as the number of nerves crossing the epidermal-dermal junction (outlined in white) as a function of epidermal-dermal junction length. IENF densities were calculated using both td-Tomato labeled fibers (shades of red) and PGP 9.5 labeled fibers (shades of green) (**, $p<0.01$, ***, $p<0.01$) (n=7 for all groups with 3 non-contiguous sections analyzed per sample). Values are expressed as mean $\pm$ S.E.M. p-values were calculated using a two-way ANOVA with Dunnet Multiple comparison test.

A

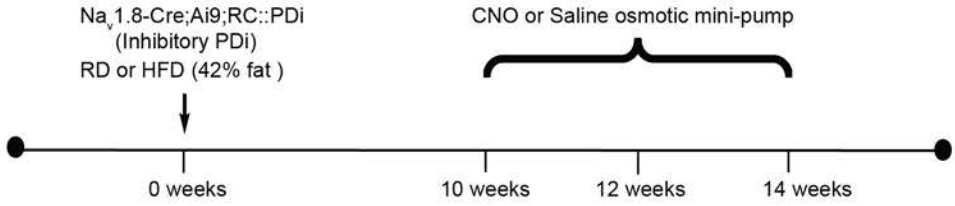
Nav1.8-Cre;Ai9;RC::PDi
(Inhibitory PDi)
RD or HFD (42% fat)
CNO or Saline osmotic mini-pump
0 weeks
10 weeks
12 weeks
14 weeks

B

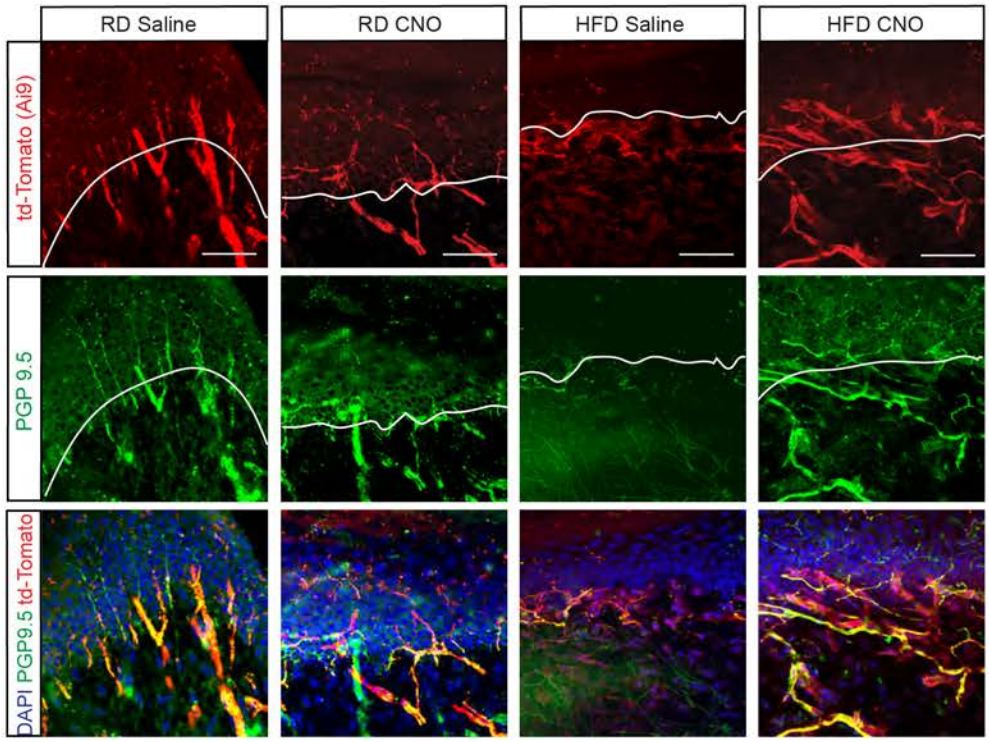
RD Saline
RD CNO
HFD Saline
HFD CNO
td-Tomato (Ai9)
PGP 9.5
DAPI PGP9.5 td-Tomato

C

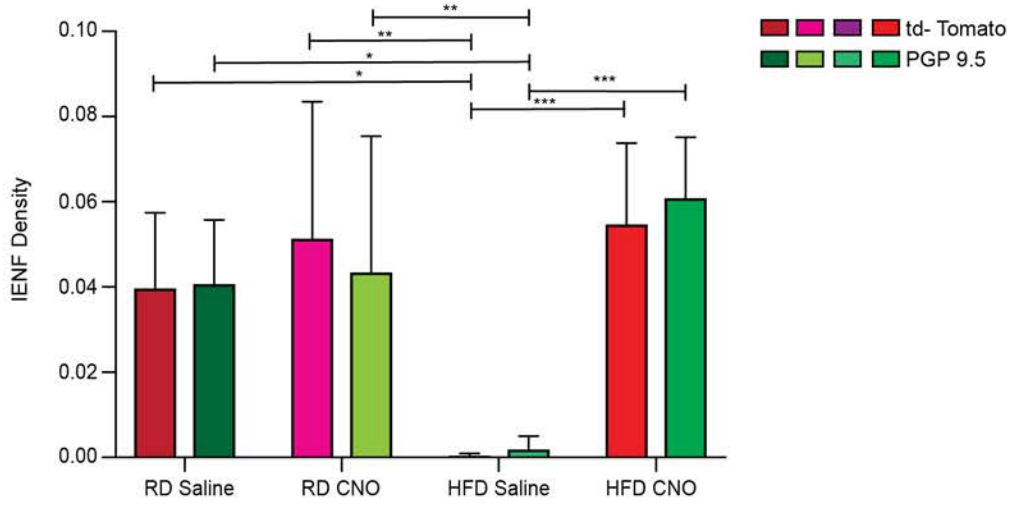
td- Tomato
PGP 9.5
IENF Density
0.10
0.08
0.06
0.04
0.02
0.00
RD Saline
RD CNO
HFD Saline
HFD CNO
**
**
*
*
***
***

Supplemental Figure 11. Chemogenetic inhibition of Na_v1.8-positive DRG neurons can reverse small-fiber degeneration visualized by either td-Tomato fibers or fibers stained with PGP 9.5. (**A**) Experimental setup for the reversal set of experiments. Na_v1.8-Cre;Ai9;RC::PDi were fitted with osmotic mini-pumps i.p. infusing either CNO (10mg/kg/day) or saline between 10-14 weeks of either RD or HFD. (**B**) Confocal analysis of skin from these mice that express the inhibitory DREADD receptor PDi fed either RD or HFD showing td-Tomato (**red**) in Na_v1.8-positive fibers, immunolabeling with antibody against the protein gene product 9.5 (PGP 9.5) (**green**), and merged images with the nuclear marker DAPI (**blue**). Control mice on a RD with saline or CNO pumps showed normal skin innervation. Diabetic mice on HFD implanted with a saline pump showed reduced skin innervation. However, diabetic mice on a HFD fitted with CNO pumps showed a significant improvement in skin innervation. (**C**) This effect was quantified using intra-epidermal nerve density (IENF density) which is expressed as the number of nerves crossing the epidermal-dermal junction (outlined in white) as a function of epidermal-dermal junction length. IENF densities were calculated using both td-Tomato fibers (shades of red) and with PGP 9.5 fibers (shades of green) (n=6 from each group with 3 non-contiguous sections analyzed per sample). (*, $p<0.05$, **, $p<0.01$, ***, $p<0.001$). Values are expressed as mean ± S.E.M. p-values were calculated using a two-way ANOVA with Dunnet Multiple comparison test.

A

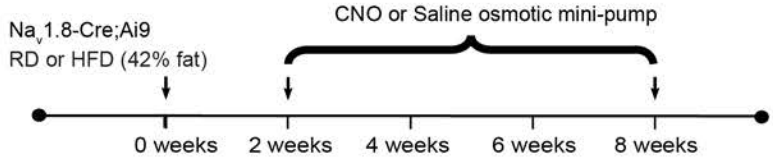
Na$_v$1.8-Cre;Ai9
RD or HFD (42% fat)
CNO or Saline osmotic mini-pump
0 weeks
2 weeks
4 weeks
6 weeks
8 weeks

B

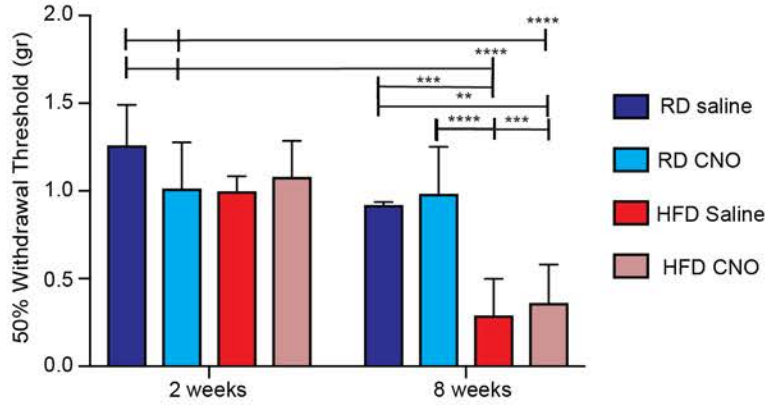
50% Withdrawal Threshold (gr)
2.0
1.5
1.0
0.5
0.0
2 weeks
8 weeks
****
***
**
RD saline
RD CNO
HFD Saline
HFD CNO

C

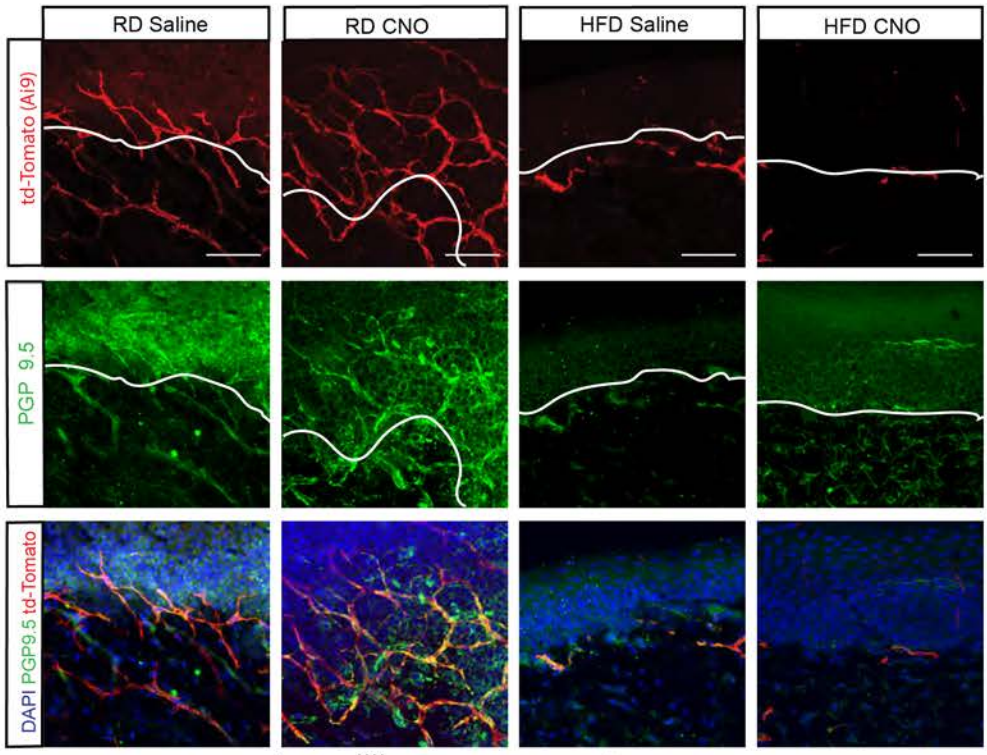
RD Saline
RD CNO
HFD Saline
HFD CNO
td-Tomato (Ai9)
PGP 9.5
DAPI PGP9.5 td-Tomato

D

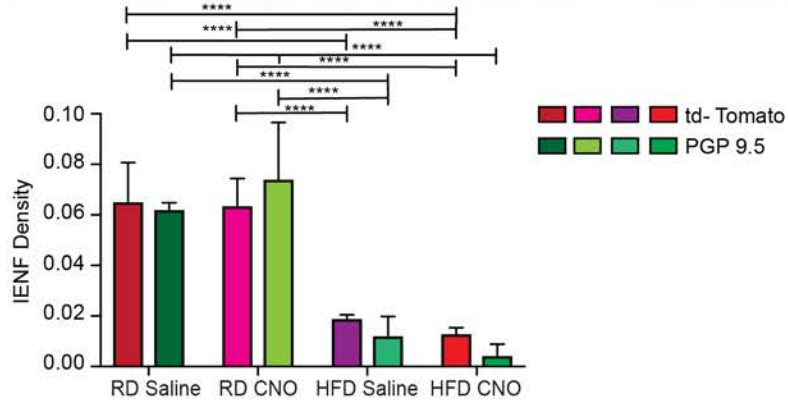
IENF Density
0.10
0.08
0.06
0.04
0.02
0.00
RD Saline
RD CNO
HFD Saline
HFD CNO
td- Tomato
PGP 9.5
****

Supplemental Figure 12. Long-term treatment with CNO to prevent PDN onset has no effect on mice that do not express DREADD receptors. (**A**) Experimental timeline for the prevention set of experiments where Na_v1.8-Cre;Ai9 mice, that do not express DREADD receptors, are administered CNO (10 mg/kg/day) or saline through an osmotic mini-pump implanted i.p. concurrently with being fed either RD or HFD. Each arrow represents a time point where pain behavior is assessed. (**B**) von Frey behavioral testing was done at 2 and 8 weeks showing that HFD mice show a decreased withdrawal threshold only after being on the diet for 8 weeks. Treatment with CNO pump did not change the decreased withdrawal threshold observed in HFD mice and also had no effect on RD mice (**, $p<0.01$, ***, $p<0.001$, ****, $p<0.0001$) (n=6/group). p-values were calculated using a two-way ANOVA with Bonferroni Multiple comparison test (**C**) Representative confocal micrographs taken from the skin of these animals showing the Na_v1.8-positive fibers labeled with td-Tomato (**red**), immunolabeling for PGP 9.5 (**green**) and merged images with the nuclear marker DAPI (**blue**). Mice on HFD given CNO showed no change in skin innervation. Magnification 60x (scale bar=50μm). (**D**) This effect was quantified using intra-epidermal nerve density (IENF density) which is expressed as the number of nerves crossing the epidermal-dermal junction (outlined in white) as a function of epidermal-dermal junction length. IENF densities were calculated using both td-Tomato fibers (shades of red) and with PGP 9.5 fibers (shades of green) (****, $p<0.0001$) (n=6/group with 3 non-contiguous sections analyzed per sample). Values are expressed as mean $\pm$ S.E.M. p-values were calculated using a two-way ANOVA with Dunnet Multiple comparison test.

A

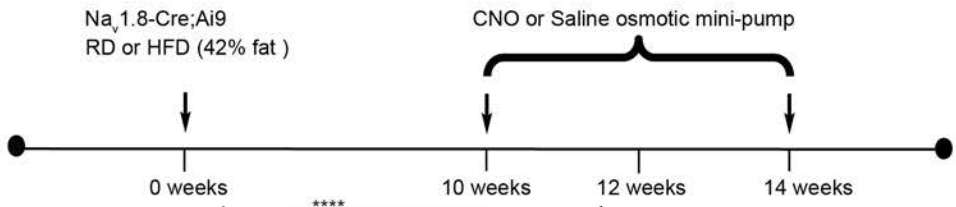
Na$_v$1.8-Cre;Ai9
RD or HFD (42% fat)
CNO or Saline osmotic mini-pump
0 weeks
10 weeks
12 weeks
14 weeks

B

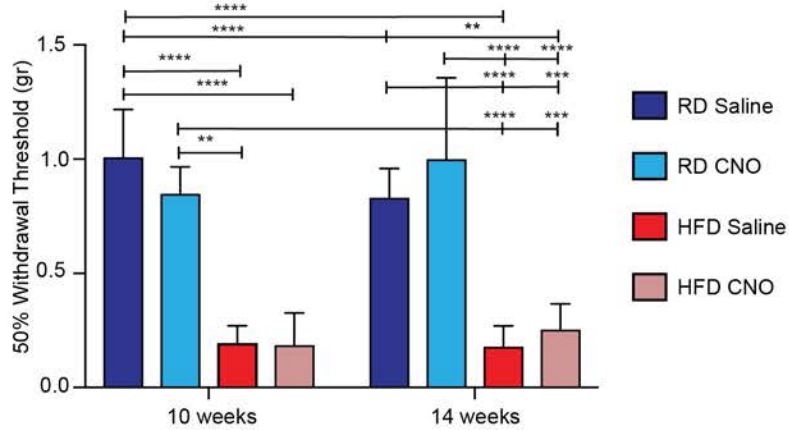
50% Withdrawal Threshold (gr)
1.5
1.0
0.5
0.0
10 weeks
14 weeks
RD Saline
RD CNO
HFD Saline
HFD CNO

C

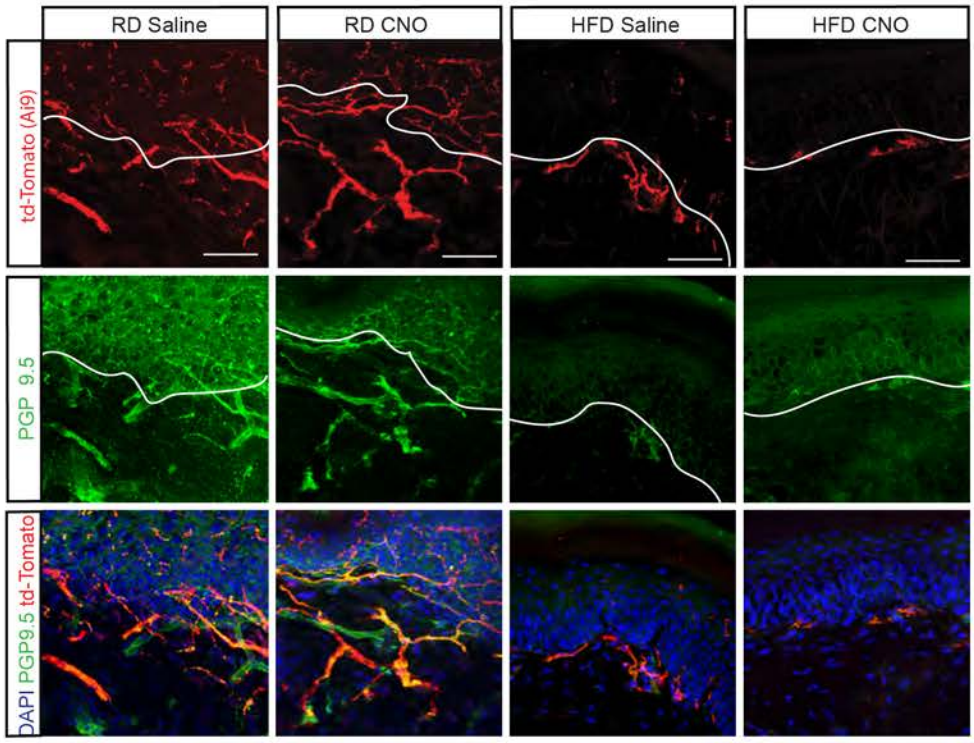
RD Saline
RD CNO
HFD Saline
HFD CNO
td-Tomato (Ai9)
PGP 9.5
DAPI PGP9.5 td-Tomato

D

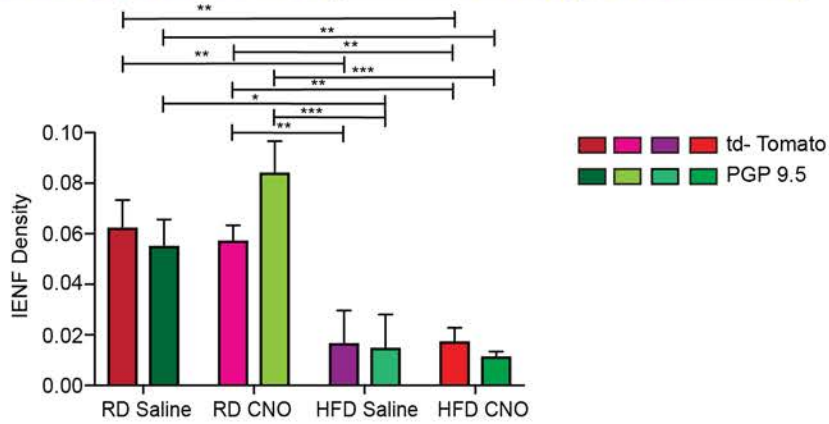
IENF Density
0.10
0.08
0.06
0.04
0.02
0.00
RD Saline
RD CNO
HFD Saline
HFD CNO
td- Tomato
PGP 9.5

Supplemental Figure 13. Long-term treatment to reverse PDN with CNO has no effect on mice that do not express DREADD receptors. (**A**) Experimental timeline for the reversal set of experiments where Na_v1.8-Cre;Ai9 mice are administered CNO (10 mg/kg/day) or saline through an osmotic mini-pump implanted i.p. following being fed either RD or HFD for 10 weeks. Each arrow represents a time point where pain behavior was assessed. (**B**) von Frey behavioral testing was done at 10 and 14 weeks showing that, as expected, mice on HFD given saline have a much lower withdrawal threshold compared to RD mice. When HFD mice were given CNO there is no change in the withdrawal threshold (**, $p<0.01$, ***, $p<0.001$, ****, $p<0.0001$) (n=6/group). p-values were calculated using a two-way ANOVA, Bonferroni Multiple comparison test (**C**) Representative confocal micrographs taken from the skin of these animals showing the Na_v1.8-positive fibers labeled with td-Tomato (**red**), immunolabeling for PGP 9.5 (**green**) and merged images with the nuclear marker DAPI (**blue**). Mice on HFD given CNO showed no improvement in skin innervation. Magnification 60x (scale bar=50μm). (**D**) This effect was quantified using intra-epidermal nerve density (IENF density) which is expressed as the number of nerves crossing the epidermal-dermal junction (outlined in white) as a function of epidermal-dermal junction length. IENF densities were calculated using both td-Tomato fibers (shades of red) and with PGP 9.5 fibers (shades of green) (*, $p<0.05$, **, $p<0.01$, ***, $p<0.001$) (n=6/group with 3 non-contiguous sections analyzed per sample). Values are expressed as mean $\pm$ S.E.M. p-values were calculated using a two-way ANOVA with Dunnet Multiple comparison test.

A

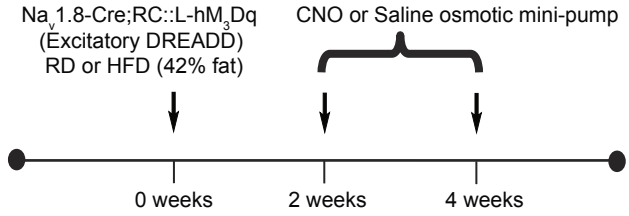
Na$_v$1.8-Cre;RC::L-hM$_3$Dq
(Excitatory DREADD)
RD or HFD (42% fat)
CNO or Saline osmotic mini-pump
0 weeks
2 weeks
4 weeks

B

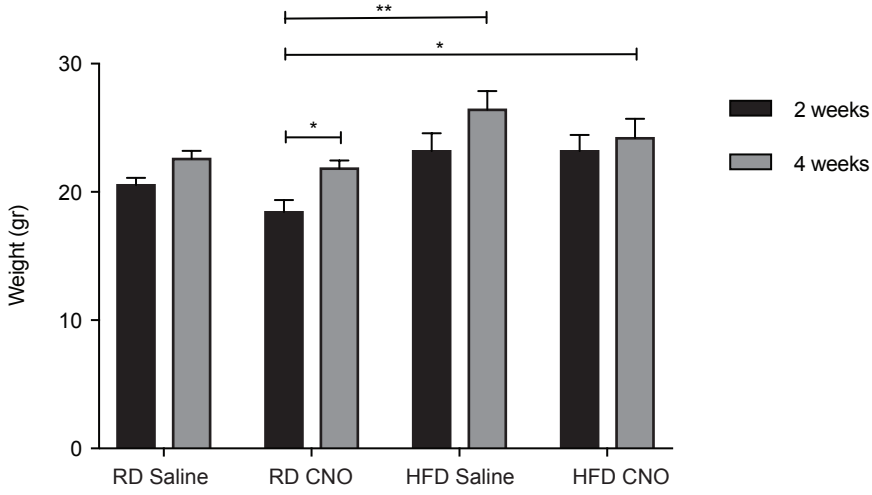
**
*
*
30
20
10
0
Weight (gr)
RD Saline
RD CNO
HFD Saline
HFD CNO
2 weeks
4 weeks

C

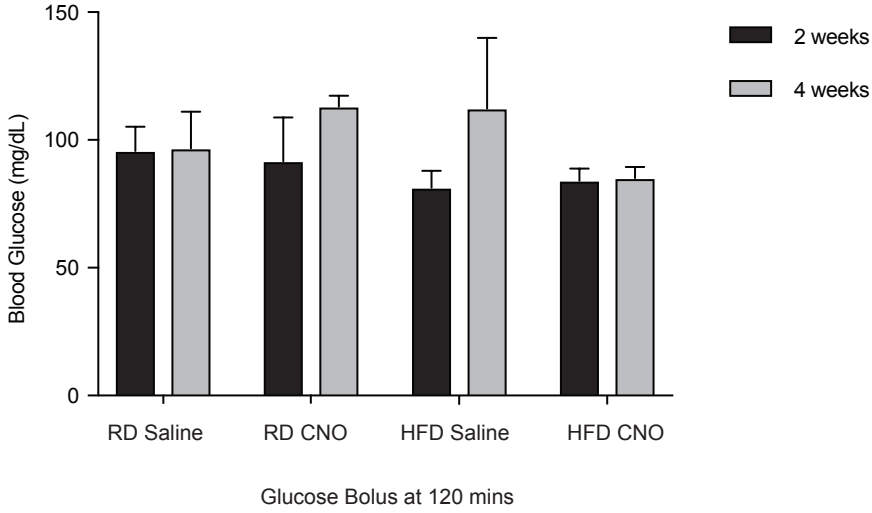
150
100
50
0
Blood Glucose (mg/dL)
RD Saline
RD CNO
HFD Saline
HFD CNO
2 weeks
4 weeks
Glucose Bolus at 120 mins

Supplemental Figure 14. Continuous CNO infusion did not alter the metabolic profile of mice expressing hM_3Dq excitatory DREADD receptors. (**A**) Experimental setup of osmotic mini-pump implantation in $Na_v1.8$-Cre;RC::L-hM_3Dq mice. $Na_v1.8$-Cre;RC::L-hM_3Dq mice that expressed excitatory hM_3Dq DREADD receptors were fed either RD or HFD and had a osmotic mini-pump implanted intraperitoneally, which administered either saline or CNO (10mg/kg/day) for the period from 2 to 4 weeks following the commencement of HFD or RD. (**B**) Weights of these mice in grams (gr) after 2 or 4 weeks on the diet (*, $p<0.05$, **, <0.01) (n=6/group). (**C**) Blood glucose levels of these mice at two and four weeks on RD or HFD 120 minutes after injection of glucose (45% D-glucose solution (2mg glucose/1g animal body weight)) (n=6/group). Values are expressed as mean ± S.E.M. p-values were calculated using two-way ANOVA with Bonferroni Multiple comparison test.

Supplemental Table 1: Electrophysiological parameters of neurons used for recordings of Figure 11. Cells were recorded at culture days 2 – 4. For this dataset only a few medium and large neurons were included in the data. Values are expressed as mean ± S.E.M.

Genotype (n)	Vm (mV)	capacitance (pF)	smallest (pF)	biggest (pF)	Rin (MΩ)	rheobase (pA)
$Na_v1.8$-Cre;Ai9 (16)	-61.3 ± 0.6	51.3 ± 11.7	20	196	501 ± 59	318.5 ± 108.25
$Na_v1.8$-Cre;RC::L-hM_3Dq (28)	-62.8 ± 0.8	29.9 ± 1.7	19	53	641 ± 47	136 ± 22.7

Supplemental Table 2: $[Ca^{2+}]i$ responses of parvalbumin-Cre::GCaMP6 explants to CXCL12 or to different concentration of potassium buffer after 8 weeks on either diet (RD, n=88 neurons , 6 explants; HFD n=118, 9 explants). Values are expressed as mean ± SEM. p-values were calculated using p- values were calculated using a Mann-Whitney test.

Parvalbumin-Cre::GCaMP6	CXCL12	HK10	HK25	HK50
RD	0	10.594±3.41	22.818±5.82	47.225±2.34
HFD	3.33±3.33	19.878±9.23	37.288±11.69	54.752±9.57